Characterization of the crosstalk between the ER and endocytic pathway in plant cells

Tatiana Filipa Fernandes Cardoso
Biologia Molecular e Celular
Departamento de Biologia
2021

Orientador
Cláudia Pereira, Investigadora Pos-doc e Professora auxiliar convidada, GreenUPorto, FCUP

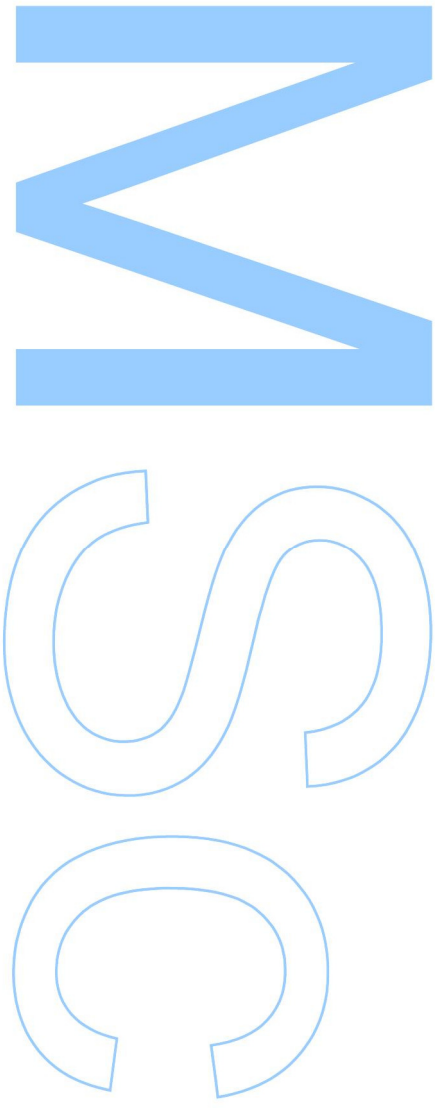
Coorientador
José Pissarra, Professor associado, GreenUporto, FCUP



Todas as correções determinadas pelo júri, e só essas, foram efetuadas.

O Presidente do Júri,

Porto, _____/_____/_____



ACKNOWLEDGEMENTS

“The most important thing is to never stop questioning.”

- Albert Einstein

These past two years I’ve spent doing this master’s course have been the most challenging and the most rewarding of my life, and now that this beautiful journey is coming to an end, I can only be grateful for all the people in my life who supported and helped me through it.

Firstly, I would like to say how thankful I am to have these supervisors always by my side and to be part of the PSI Lab team. So, to you, Dr. Cláudia Pereira, thank you for welcoming me to the team with open arms, for always having a kind word to give, and, mostly, thank you for the patience, the guidance, and the trust. I’m inspired everyday by your knowledge and skills and I’m grateful you share that with me. Secondly, to Professor José Pissarra, thank you for always being present, for your kindness and for taking care of the group’s best interests. To both of you, I can only be eternally grateful for allowing me to do what I love and love what I do. And, of course, to Professor Susana, thank you for all the help and support given without question.

To my dearest childhood friends Inês Sofia and Mariana and to my sister Francisca, thank you for the long years of friendship and sharing. Thank you for being there for me, no matter when, where or how far. Thank you for being in my life, always. Growing with you has been truly magical, and we’re not done yet!

To my BioHienas, thank you for brightening my faculty years. A special thanks to my Catarina, thank you for the unconditional support, for the laughs and tears, for the friendship since the first day. Only with you could I have lived the crazy things I have lived. You will always have a special place in my heart. To my Moutcha, thank you for always having a thoughtful advice to give and a bed to share. The best nights were the ones shared with you. Also, to Melo, to Marcus, to Carlos and to Torres, thank you for your kind friendship and for being part of my life. I’ll never forget all the memories.

To Maria, thank you for all the advices and for your unexpected friendship. Your caring soul and your decisive mind will always inspire to me.

To Carlota and Jorge, thank you for always being there and for growing with me. Thank you for sharing your craziness with me and for being an ever-present light in the dark.

To my friends, Rute, Bruno, Carlos, Diogo, Quintas and Barbosa, thank you for all the coffee dates to forget about life's worries and responsibilities.

To my master colleague Rute, thank you for the long conversations about everything and nothing. Your friendship was a truly good surprise.

Of course, I could not forget about my lab colleagues! Miguel, João Neves, Inês and Diana, thank you for keeping the lab work joyful and for all the coffee breaks. We're the best team!

To my family, thank you for putting up with my worst and for the eternal support. You made me the person I am today, and I cannot ever be thankful enough for that. Your belief in me will always take me further.

Lastly, but certainly not the least, to my love João. To you I'm deeply grateful. For your warm embrace, for your outstanding patience, for your kind and caring soul. It will always amaze me how much you believe in me. You changed my life the second you entered in it. I only hope to continue to share the everyday with you. Thank you, thank you, thank you!

To all of you, thank you for shining a light into my life and for pushing me to be better, to do better. I'm ready for what comes next if you are! Let's go!

RESUMO

A via secretora é a principal via de transporte do sistema endomembranar em células eucarióticas, envolvendo vários compartimentos membranares, como o Retículo Endoplasmático (ER), o Golgi e os Vacúolos. Uma vez que a partir daí proteínas recentemente sintetizadas são distribuídas a vários organelos celulares, o retículo é considerado como o centro da via secretora. A endocitose é outra via de transporte fundamental, ocorrendo na membrana citoplasmática e facilitando a reciclagem de membranas, canais iónicos e recetores da superfície celular. Recentemente, foi proposta a existência de um compartimento de natureza reticular que poderá ser identificado como um endossoma de reciclagem, mas que também participa no trânsito vacuolar. O nosso principal objetivo com este estudo foi identificar um compartimento celular que participaria tanto na via secretora como na via endocítica, representando uma ligação entre estas. Para tal, combinámos a utilização de mutantes de *Arabidopsis thaliana* com uma estrutura reticular alterada e a expressão de marcadores vacuolares conhecidos. Em primeiro lugar, foi analisada a ultra-estrutura destes mutantes e, através de Microscopia Eletrónica de Transmissão (TEM), foram observados enormes grânulos de amido bem definidos assim como cisternas do Golgi dilatadas. Adicionalmente, para avaliar se os defeitos reticulares das linhas de Arabidopsis mutantes interferiam com o direcionamento e/ou trânsito proteico, o domínio Plant Specific Insert das cardosinas A e B fundido com mCherry foram expressos de forma transitória nos mutantes. Através de Microscopia Confocal, o PSI A foi observado principalmente no vacúolo, enquanto o PSI B foi tanto secretado para a meio extracelular como acumulado no vacúolo. Estas plantas transformadas foram também sujeitas a um tratamento com Brefeldina A, onde ambos os PSI mantiveram o mesmo padrão de localização, contudo foram observadas menos células com padrão de secreção para o PSI B. Para confirmar que o PSI B estava realmente a ser acumulado no meio extracelular, foi realizado um ensaio de secreção, e o PSI B foi detetado com sucesso no conteúdo proteico extracelular das linhas de Arabidopsis mutadas. Finalmente, para escrutinar o cruzamento entre as vias secretora e endocítica nestes mutantes, foi analisada a co-localização entre os PSIs e o marcador do endossoma FM2-10, revelando alguma sobreposição destes dois marcadores na periferia da célula em algumas linhas mutantes. Embora promissores, os dados aqui apresentados requerem mais observações e análises para ser possível compreender plenamente o efeito destas mutações no transito vacuolar de proteínas e as suas implicações nas vias secretora e endocítica.

PALAVRAS-CHAVE

Via Secretora, Endocitose, Retículo Endoplasmático, Plant Specific Insert (PSI); Trânsito e direcionamento proteico, *Arabidopsis thaliana*, Microscopia

ABSTRACT

The secretory pathway is the main transport route of the endomembrane system in eukaryotic cells, involving several membranous compartments, as the Endoplasmic Reticulum (ER), the Golgi and Vacuoles. Since from there, newly synthesised proteins are distributed to several cellular organelles, the ER is regarded as the hub of the secretory pathway. Endocytosis is another fundamental transport route, occurring at the plasma membrane and facilitating the recycling of membranes, ion channels and cell surface receptors. It has been proposed the direct generation of a compartment from the ER that may be identified as a recycling endosome but also participates in vacuolar trafficking. Our main objective with this study was to identify a cell compartment that would participate in both secretory and endocytic trafficking routes, representing a link between these pathways. To do so, we combined the use of *Arabidopsis thaliana* mutants with altered ER structure and the expression of known vacuolar markers. Firstly, the ultrastructure of these mutants was analysed and, through Transmission Electron Microscopy (TEM), huge well-defined starch granules along with enlarged Golgi cisternae were revealed. Additionally, to assess if the ER defects of the mutated Arabidopsis lines interfered with protein sorting and/or trafficking, the Plant Specific Insert domains of the cardosins A and B fused with the mCherry tag were infiltrated in the mutants for transient expression. Through Confocal Microscopy, PSI A was observed mainly in the vacuole, while PSI B was both secreted and accumulated in the vacuole. Such transformed plants were also subjected to a Brefeldin A treatment, where both PSIs maintained the same pattern of localization, however, the number of cells observed where PSI B was secreted, decreased. To further confirm this PSI B localization at the extracellular space, a secretion assay was conducted, and PSI B was successfully detected in the extracellular protein content of the ER-defective Arabidopsis lines. Finally, to scrutinize the crosstalk between the secretory and endocytic pathways in these mutants, co-localization between the PSIs and the endosomal marker FM2-10 was analysed, revealing some overlap of the two markers at the cell periphery in some mutated lines. Although promising, the data here presented requires further observations and analysis to fully comprehend the effect of these mutations in protein vacuolar trafficking and their implications on the secretory and endocytic pathways.

KEYWORDS

Secretory pathway, Endocytosis, Endoplasmic Reticulum, Plant Specific Insert (PSI), Protein trafficking and sorting, *Arabidopsis thaliana*, Microscopy

TABLE OF CONTENTS

ACKNOWLEDGEMENTS V

RESUMO VII

ABSTRACT IX

TABLE OF CONTENTS XI

LIST OF TABLES XV

LIST OF FIGURES XVII

LIST OF ABREVIATIONS XIX

1. INTRODUCTION 1

1.1. The endomembrane system 1

1.1.1. The endoplasmic reticulum (ER) 3

1.1.2. The Golgi 6

1.1.3. The Vacuoles 8

1.1.4. The plasma membrane 9

1.2. Vacuolar trafficking and the pathways to the vacuoles 11

1.2.1. The conventional routes 12

1.2.2. The unconventional routes 15

1.2.3. The Plant specific insert (PSI) and PSI mediated routes 16

1.3. Endocytosis in plant cells 20

1.4. *Arabidopsis thaliana* as a model organism 24

1.5. Aims of the study 26

2. MATERIALS AND METHODS 27

2.1. Biological material – selection, germination, and growth conditions 27

2.2. Constructs generation through Molecular Biology Tools 27

2.2.1. DNA Amplification 28

2.2.2. Gibson Assembly Cloning 31

2.2.3. Preparation of electrocompetent *Escherichia coli* cells 31

2.2.4. Preparation of electrocompetent *Agrobacterium tumefaciens* cells 32

2.2.5. Bacteria transformation by electroporation 32

2.2.6. Screening of positive clones 33
2.3. Transmission Electron Microscopy 33
2.3.1. Chemical Fixation for Epoxy Resin Embedding 33
2.3.2. Block Sectioning 34
2.3.3. Post-Staining 34
2.3.4. Transmission Electron Microscopy observations 34
2.4. Vacuum infiltration for transient transformation of *Arabidopsis thaliana* seedlings 35
2.4.1. Seedlings' growth conditions 35
2.4.2. *Agrobacterium tumefaciens* culture preparation 35
2.4.3. Preparation of *A. tumefaciens* suspension for infiltration 35
2.4.4. Agroinfiltration of the *A. thaliana* seedlings 36
2.5. Agrobacterium-mediated Infiltration of *Arabidopsis thaliana* and *Nicotiana tabacum* Leaves 36
2.6. Cell imaging 37
2.6.1. Confocal Laser Scanning Microscopy Analysis 37
2.6.2. Drug Treatment Assays 37
2.6.3. FM2-10 staining 38
2.7. Secretion Assays 38
2.7.1. Extraction of extracellular proteins 38
2.7.2. TCA precipitation 38
2.7.3. Discontinuous denaturing Gel Electrophoresis 39
2.7.4. Western Blot 39
3. RESULTS 41
3.1. Characterization of *Arabidopsis thaliana* ER-defective plants 41
3.1.1. Developmental assays of ER-defective lines 41
3.1.2. TEM imaging 42
3.2. Definition of trafficking pathways in ER-defective plants 51
3.2.1. Selection of constructs for co-expression of PSIs and marker proteins 51
3.2.2. Expression of PSIs in ER-defective plants 52

3.2.3. Expression of PSIs in ER-defective plants treated with BFA 56
3.2.4. Co-localization with the endosomal marker FM2-10 60
3.2.5. Analysis of secreted proteins 62
4. DISCUSSION 64
4.1. Characterization of *Arabidopsis thaliana* ER-defective plants 64
4.2. Definition of trafficking pathways in ER-defective plants 68
4.2.1. Expression of the PSIs and the effect of BFA 68
4.2.2. Co-expression of the PSIs with FM2-10 70
4.2.3. Western blotting analysis of PSI B secretion 71
5. CONCLUSIONS 72
6. REFERENCES 73
7. APPENDIX 102

LIST OF TABLES

Table 2.1 – List of selected *Arabidopsis thaliana* lines used..... 27
Table 2.2 – List of cDNAs used..... 28
Table 2.3 – Primers used for Gibson Assembly and primers for sequencing..... 29
Table 2.4 – Component mix for PCR reactions using Phusion High-Fidelity PCR Master Mix with HF Buffer (Thermo Scientific™) and Platinum SuperFi PCR Master Mix (Invitrogen by Thermo Fisher Scientific)..... 30
Table 2.5 – Program for PCR reactions using Phusion High-Fidelity PCR Master Mix with HF Buffer (Thermo Scientific™) and Platinum SuperFi PCR Master Mix (Invitrogen by Thermo Fisher Scientific). 30
Table 2.6 – Gibson Assembly Reaction Mix..... 31
Table 2.7 – Reaction mixture of enzymatic restriction for screening of positive clones. 33
Table 3.1 – Summary of the ultrastructural features of the *Arabidopsis thaliana* ER-defective plants..... 48

LIST OF FIGURES

Figure 1.1 – Different routes for endomembrane trafficking and their organelles. 1
Figure 1.2 – Schematic representation of the several ER domains found in the cell that establish contact sites between the ER and other membranes. 5
Figure 1.3 – Conventional routes to the vacuoles. 14
Figure 1.4 – Unconventional routes to the vacuoles. 16
Figure 1.5 – Domain organization of Cardosin A and B and the sequential processing steps to acquire the mature form 18
Figure 1.6 – Endosomal trafficking and its different routes in plants. 21
Figure 2.1 – Schematic representation of Gibson Assembly reactions. 29
Figure 3.1 – Chronological progression indicating the main growth stages of *A. thaliana* mutated and wild-type lines. 41
Figure 3.2 – Ultrastructure of cells from *Arabidopsis thaliana* wild-type line, in seedling leaf (A) and mature leaf (B). 43
Figure 3.3 – Ultrastructure of cells from *Arabidopsis thaliana syp22-1 syp23* mutated line, in seedling leaf (A) and mature leaf (B). 44
Figure 3.4 – Ultrastructure of cells from *Arabidopsis thaliana sec24a-2* mutated line, in seedling leaf (A) and mature leaf (B). 45
Figure 3.5 – Ultrastructure of cells from *Arabidopsis thaliana nai GFP-h* mutated line, in seedling leaf (A) and mature leaf (B). 46
Figure 3.6 – Ultrastructure of cells from *Arabidopsis thaliana nai2-2* mutated line, in seedling leaf (A) and mature leaf (B). 47
Figure 3.7 – Ultrastructure of cells from *Arabidopsis thaliana leb-2 GFP-h* mutated line, in seedling leaf (A) and mature leaf (B). 48
Figure 3.8 – Perimeter of starch granules in chloroplasts *of Arabidopsis thaliana* cells from seedling-leaves (A) and mature-leaves (B) and perimeter of chloroplasts *of Arabidopsis thaliana* cells from seedling-leaves (C) and mature-leaves (D). 50
Figure 3.9 – Alignment of the sequencing results of pMDC83::SP::PSIA::mEos3.2. ... 51
Figure 3.10 – Alignment of the sequencing results of pMDC83::SP::PSIB::mEos3.2. . 51
Figure 3.11 – Subcellular localization of Cardosin PSI A fused with mCherry in cotyledon leaves of *Arabidopsis thaliana* wild-type and ER-defective seedlings. 53
Figure 3.12 – Additional observed subcellular localizations of Cardosin PSI A fused with mCherry in cotyledon leaves of *Arabidopsis thaliana* wild-type and ER-defective seedlings. 54

Figure 3.13 – Subcellular localization of Cardosin PSI B fused with mCherry in cotyledon leaves of *Arabidopsis thaliana* wild-type and ER-defective seedlings. 55
Figure 3.14 – Quantitative localization of Cardosin A and B PSI in cotyledon leaves of *Arabidopsis thaliana* wild-type and ER-defective seedlings. 56
Figure 3.15 – Subcellular localization of Cardosin PSI A fused with mCherry in cotyledon leaves of *Arabidopsis thaliana* wild-type and ER-defective seedlings treated with BFA. 57
Figure 3.16 – Subcellular localization of Cardosin PSI B fused with mCherry in cotyledon leaves of *Arabidopsis thaliana* wild-type and ER-defective seedlings treated with BFA. 58
Figure 3.17 – Quantitative localization of Cardosin A PSI in cotyledonary leaves of *Arabidopsis thaliana* wild-type and ER-defective seedlings untreated and treated with BFA. 59
Figure 3.18 – Quantitative localization of Cardosin B PSI in cotyledonary leaves of *Arabidopsis thaliana* wild-type and ER-defective seedlings untreated and treated with BFA. 59
Figure 3.19 – Subcellular co-localization of Cardosin PSI A fused with mCherry, and FM2-10 dye in cotyledonary leaves of *Arabidopsis thaliana* wild-type and ER-defective seedlings. 61
Figure 3.20 – Subcellular co-localization of Cardosin PSI B fused with mCherry, and FM2-10 dye in cotyledonary leaves of *Arabidopsis thaliana* wild-type and ER-defective seedlings. 62
Figure 3.21 – pMDC83::SP::PSICardB::mCherry expression and secretion in *Arabidopsis thaliana* wild-type and mutated lines. 63

Supplementary figure 7.1 – pMDC83 empty plasmid map. 102
Supplementary figure 7.2 – pMDC83 construct containing PSI A fused with mEos 3.2. 103
Supplementary figure 7.3 – pMDC83 construct containing PSI B fused with mEos 3.2. 103
Supplementary figure 7.4 – pMDC83 construct containing PSI A fused with mCherry. 104
Supplementary figure 7.5 – pMDC83 construct containing PSI B fused with mCherry. 104

LIST OF ABREVIATIONS

AP1	Adaptor protein 1
AP3	Adaptor protein 3
APs	Aspartic proteinases
ARF-GAPs	ARF GTPase-activating proteins
ARF-GEFs	ARF guanine exchange factors
ASG	Acyl steryl glycosides
BFA	Brefeldin A
bp	Base Pair
BR	Brassinosteroids
BRI1	Brassinosteroid insensitive 1
CCV	Clathrin-coated vesicles
CCPs	Clathrin-coated pits
CGN	*cis*-Golgi network
CIE	Clathrin-independent endocytosis
CME	Clathrin-mediated endocytosis
COPI	Coat protein complex I
COPII	Coat protein complex II
CLSM	Confocal Laser Scanning Microscopy
CtVSDs	C-terminal vacuolar sorting determinants
DVs	Dense vesicles
EE	Early endosome
ER	Endoplasmic Reticulum
ERAD	ER-associated protein degradation
ERES	ER-exit sites
ERGIC	ER–Golgi intermediate compartment
ESCRT	Endosomal sorting complex required for transport
Flot1	Flotillin1
Fw	Forward
GIPCs	Glycosyl inositol phosphorylceramides
GFP	Green Fluorescent Protein
ILVs	Intraluminal vesicles
LB	Luria Broth medium
LE	Late endosomes
LV	Lytic vacuole
MPR	Mannose 6-phosphate receptors
MVB	Multivesicular body
NASC	Nottingham Arabidopsis Stock Centre
NE	Nuclear envelop
NPIRL	Aspargine-proline-isoleucine-arginine-leucine
PACs	Precursor-accumulating compartments
PM	Plasma membrane
PRE	Presegment
PRO	Prosegment
PSI	Plant specific insert

psVSDs	VSDs dependent on the physical structure of proteins
PSV	Protein storage vacuole
PVC	Pre-vacuolar Compartment
Qa-SNAREs	Qa- of soluble N-ethylmaleimide-sensitive factor attachment protein receptor
RMR	Receptor membrane ring-H2
RT	Room temperature
Rv	Reverse
SA	Salicylic acid
SDS-PAGE	Sodium Dodecyl Sulphate–Polyacrylamide Gel Electrophoresis
SG	Steryl glycosides
ssVSDs	Sequence-specific VSDs
TAIR	The Arabidopsis Information Resource
TEM	Transmission Electron Microscopy
TGN	*trans* Golgi Network
VSDs	Vacuolar sorting determinants
VSRs	Vacuolar sorting receptors
v/v	Volume Per Volume
WT	Wild-type
w/v	Weight Per Volume

1. INTRODUCTION

1.1. The endomembrane system

The endomembrane trafficking system of eukaryotic cells is vital for important cellular functions, upholding cellular homeostasis and proliferation, as well as specific requirements characteristic of multicellular organisms (Morita and Shimada 2014; Cevher-Keskin 2020). It consists of a perplexing network of membrane compartments responsible for the synthesis, modification, transport and delivery of numerous proteins, polysaccharides, and metabolites to their final destination. This delivery of cargo molecules is especially complex and well-coordinated in plant cells, occurring along several compartmentalized organelles: the Endoplasmic Reticulum (ER), the Golgi, the Trans Golgi Network (TGN), the Pre-vacuolar Compartment (PVC), the Vacuole, secretory vesicles, and endosomes (Frigerio and Hawes 2008; Stefano et al. 2014a; Wang et al. 2017, 2020).

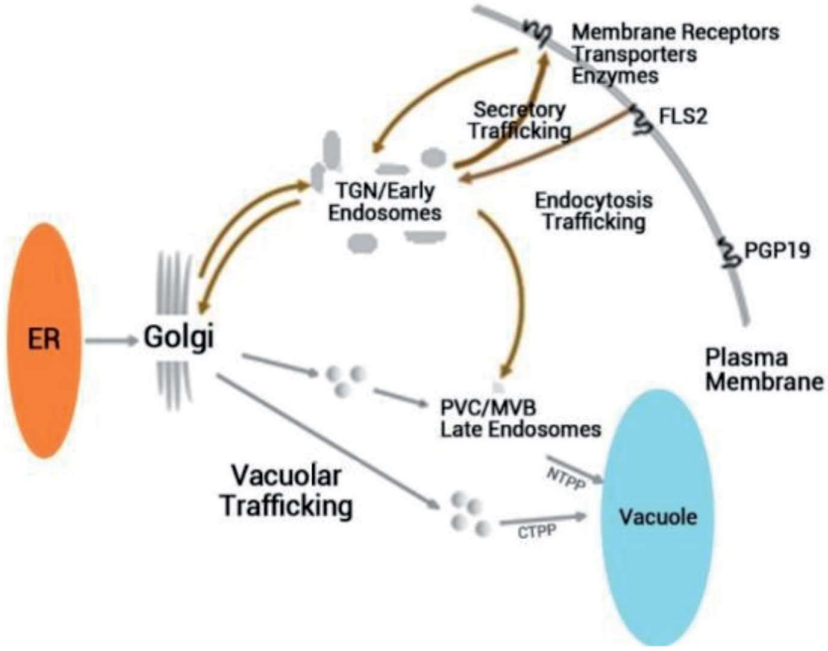


Figure 1.1 – Different routes for endomembrane trafficking and their organelles. The three key endomembrane trafficking pathways include the secretory, the endocytic and the vacuolar pathways. Proteins begin their journey through the endomembrane system at the ER, before moving to the Golgi and TGN, where the final post-translational modifications needed for proper functioning occur. Finally, proteins enter a vesicle carrier, like PVC, for example, for subsequent fusion with the vacuole. Abbreviations: ER, endoplasmic reticulum; MVB, multivesicular body; PVC, pre-vacuolar compartment; TGN, trans Golgi network. Retrieved from Cevher-Keskin (2020).

In plant cells, endomembrane trafficking may be divided into three major pathways (Figure 1.1): (i) the biosynthetic secretory pathway, where newly synthesised proteins are transported from the ER to their needed location, being the plasma membrane (PM), the apoplast and/or extracellular space; (ii) the endocytic pathway, that mediates the recycling of membranes, ion channels and surface cell receptors, as well as being essential in controlling the lipid and protein composition of the PM (Stefano et al. 2015); and (iii) the vacuolar transport pathway, comprising the delivery of various molecules, such as proteins, to the vacuoles (Inada and Ueda 2014; Cevher-Keskin 2020). The traffic between the endomembrane system organelles works in two directions: the anterograde transports begins at the ER and flows towards the final destination, and the retrograde transport represents the transport occurring in the opposite direction (Cevher-Keskin 2020). A similar process of transport occurs in the different pathways, and it is dependent on vesicle exchange, which comprehends budding, directional transport and targeting, tethering, membrane recognition and fusion of vesicle transporters, and recycling of the transport machinery elements (Rojo and Denecke 2008; Cevher-Keskin 2020). In fact, as it is for most of the eukaryotes, various vesicles are involved in cargo trafficking: clathrin-coated vesicles (CCV), caveolin vesicles, coat protein complex I (COPI) vesicles, coat protein complex II (COPII) vesicles and dense vesicles (DVs). These different carriers are ubiquitously present and possess the proper budding machineries for the correct function of the vesicle trafficking mechanism (Jürgens 2004; Xiang et al. 2013). Moreover, some of these vesicle carriers are specific for transport between organelles (such as the COP vesicles that operate between the ER and Golgi), and their molecule composition is also specific to each membrane type.

Higher plants have developed some unique mechanisms, while conserving the dynamic activities of the endomembrane system as all eukaryotes (Jürgens 2004). The secretory and biosynthetic pathway of the plant cell are implicated in several crucial mechanisms that include gravitropism, autophagy, hormone transport, cytokinesis, and abiotic/biotic stress responses (Surpin and Raikhel 2004; Carter et al. 2004), in addition to ion secretion by salt glands, nectar production, and the secretion of viscin, which is the elastic, mucilaginous and sticky tissue that attaches falling parasitic mistletoe seeds to branches (Echeverría 2000). By using different systems and approaches, the understanding of plant protein and membrane trafficking underwent astonishing progress (Rojo and Denecke 2008; Marcos Lousa et al. 2012). The secretory pathway of plant cells has its gateway in the ER, an adaptable and versatile organelle that forms a three-dimensional network of continuous tubules and cisterns contacting with several organelles in the cell, such as the PM, the Golgi, endosomes, lysosomes, mitochondria,

and peroxisomes, and coordinating with multiple membrane compartments along both the secretory and endocytic pathways (Staehelin 1997; Stefan et al. 2013; Stefano et al. 2015). Here, proteins are synthesized, modified and correctly folded for delivery to the Golgi (Vitale and Denecke 1999).

1.1.1. The endoplasmic reticulum (ER)

Given its unique features, dynamics and complex morphology, the Endoplasmic Reticulum (ER) is a key organelle that participates and contributes actively to the life of the eukaryotic cell. It forms a vast and continuous membrane mesh of tubules and cisternae broadly dispersed across the cytoplasm, making it the organelle with the largest membrane surface area in the cell (Staehelin 1997; Vitale and Denecke 1999; Nakano et al. 2009; Stefano et al. 2014a; Viotti 2014; Afrin et al. 2020). As it is exceedingly dynamic, the ER exhibits considerable movement, and its network may sustain extensive alterations during cellular growth (Stefano et al. 2014a, b), maintaining, however, its overall structure (English and Voeltz 2013). Morphologically speaking, the ER comprises the nuclear envelop (NE), the peripheral ER cisternae, and an interconnected tubular network (English and Voeltz 2013). The NE is the part of the ER closest to the cell nucleus surrounding it and acting as a double membrane bilayer, that includes the inner and outer nuclear membranes with the internuclear membrane space between them (Hetzer 2010). This barrier allows the selective control of the molecules directed to and extracted from the nucleus (English and Voeltz 2013). The peripheral ER extends from the outer nuclear membrane and branches out into interconnections of cisternae, that tend to be nearer the NE, and tubules that are more noticeable in the periphery and are constantly rearranging through tubule growth, retraction, and homotypic fusion with adjacent ER membranes (Terasaki et al. 1986; Puhka et al. 2007). The ER cisternae have also been categorized as rough ER (ribosome-bound), as ribosomes tend to be more concentrated here than in tubules and cisternae have a higher luminal volume to surface area, making them preferable for typical luminal processes, such as protein folding (Shibata et al. 2010; West et al. 2011; Puhka et al. 2012). On the other hand, ER tubules have been considered the smooth ER (ribosome-free), since they possess smaller luminal volume to surface area compared to cisternae, which would make them prone to accumulate integral membrane proteins and for processes associated with lipid synthesis (West et al. 2011). However, ER tubules are not always ribosome excluded, as there are many examples of ribosome bound tubules (West et al. 2011; Puhka et al. 2012; English and Voeltz 2013).

The ER represents the starting point of the secretory pathway, as it is responsible for synthesis, folding, assembly, posttranslational modifications, and quality control of

membrane proteins, soluble cargoes, and lipids (Vitale and Denecke 1999; Matheson et al. 2006; Schröder 2008; Liu et al. 2012; Viotti 2014). The mechanisms of quality control guarantee that only correctly folded and matured proteins leave the ER for transport through the secretory pathway to their final destination (Schröder 2008; Viotti 2014). When proteins are slowly folding and/or remain unfolded, they are targeted for proteasomal degradation through the ER-associated protein degradation (ERAD) (Meusser et al. 2005). On the other hand, when proteins are found to be correctly folded and ready to continue their journey, they may exit the ER via COPII-mediated transport. This is the best characterized mechanism in all eukaryotes for exiting the ER and it is known that the assembly of the coat protein complex II (COPII) takes place at specific points in the ER membrane, called ER-exit sites (ERES), and the vesicles may be freed from these locations (Viotti 2014). More recently, novel theories on ER-Golgi export have emerged, suggesting the existence of physical connections between these organelles, which may play an important role in the ER to Golgi transport (Vieira et al. 2020). Additionally, the ER has a central role in the Ca^{2+} homeostasis, as it is here that Ca^{2+} is stored in the cell (Staehelin 1997; Galili 2004; Heiland and Erdmann 2005; Bernales et al. 2006). This interesting organelle is also involved in essential cellular processes that include direct biogenesis of other cell structures, such as peroxisomes, oil bodies, and autophagic bodies, acting as a membrane source for such compartments (Galili 2004; Heiland and Erdmann 2005; Bernales et al. 2006; Stefano et al. 2014a). Finally, the ER is used as the framework for various membrane-binding signalling proteins, including essential membrane-tethered transcription factors, which evoke fast transcriptional responses upon stress and growth clues, and works as a sensor for numerous cellular stresses (Chen et al. 2008).

As sessile beings, plants are forced to adapt faster and in different ways than other eukaryotes. The plant ER distribution and functions reflect this fast adaptation and how different plant cells can be from the other eukaryotic cells, as it underscores that eukaryotes must have developed specific mechanisms to suit the ER structure and function to the cell's specific features acquired during evolution (Stefano et al. 2014a). In plants, unlike what we see in yeast and animal cells, the ER is confined to a small space of cytoplasm between the PM and the vacuolar membrane, while being extensively distributed and showing considerable movement in the cell (Quader and Schnepf 1986; Nakano et al. 2009). Moreover, this organelle serves as a repository of plant-specific hormones (Chen et al. 2002; Dhonukshe et al. 2007), is the membrane origin for the lytic vacuole in meristematic cells through a Golgi-independent pathway (Viotti et al. 2013), operates as a protein storage compartment during growth and defence in many tissues

(Yamada et al. 2011; Ibl and Stoger 2012) and mediates functional interactions with chloroplasts essential for lipids synthesis (Benning 2009). Some organisms may even develop characteristic ER-derived structures, as the ER bodies, that are cylindrical compartments for the accumulation of large amounts of β-glucosidase (PYK10), which may be involved in plant defence, and are found in Brassicaceae plants and some related species (Matsushima et al. 2003a; Hara-Nishimura et al. 2004). Another unique feature of the plant ER is its elaborate arrangement in the phragmoplast, which originates the cell plate upon cell division and, simultaneously, forms the plasmodesmata (Gupton et al. 2006).

Being spread throughout the cell, the ER connects with several other organelles (Figure 1.2), including plasma membrane (PM), Golgi, mitochondria, peroxisomes, chloroplasts, endosomes, lysosomes, and lipid droplets, coordinating with multiple compartments along the secretory and endocytic pathway (Staehelin 1997; English and Voeltz 2013; Stefan et al. 2013; Stefano et al. 2014a). These domains are both abundant and dispersed through the cytoplasm and they may contribute to the ER's complex organization, enhancing its dynamics and shaping its distribution, as well as possibly contributing to the movement of the other organelles (English and Voeltz 2013).

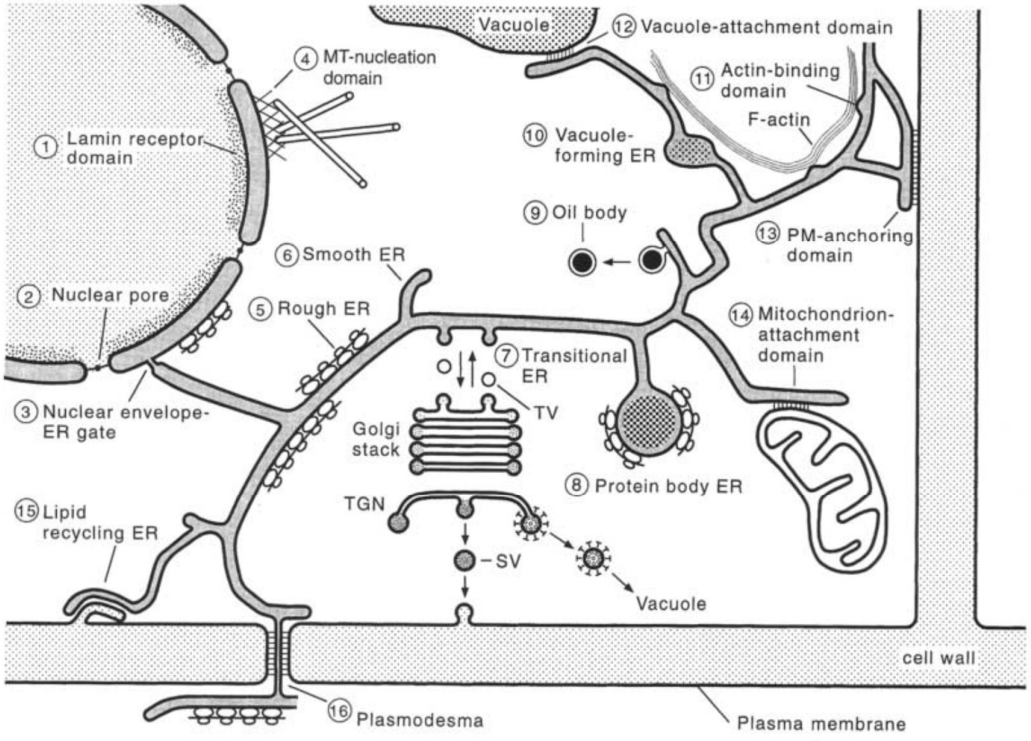


Figure 1.2 – Schematic representation of the several ER domains found in the cell that establish contact sites between the ER and other membranes. Abbreviations: PM, plasma membrane; TV, transport vesicle; SV, secretory vesicle; TGN, trans Golgi network. Retrieved from Staehelin (1997).

The ER-PM contact sites facilitate the crosstalk between both compartments, important to balance changes in PM composition with ER metabolism. These junction points have well-established roles in both calcium and lipid transport and additional roles in controlling the shape and morphology of organelles, cell stress responses and signalling networks, and membrane trafficking pathways. Furthermore, inter-organelle communication signalling through ER contact sites may facilitate the exchange of information between different organelles and thus strengthen cellular responses to various stimuli and synergize the functions of specialized organelles (Stefan et al. 2013). More recently, it has been established that the plant ER is in close association with endosomes and the integrity of the reticular network is a requirement for the positioning and dynamics of the endosomes and for endocytosis, denoting a conservation of the association of the ER with post-Golgi organelles in eukaryotes (Stefano et al. 2015).

1.1.2. The Golgi

Although the starting point of the secretory pathway is the ER (Staehelin 1997), the Golgi represents an important step in this pathway. In most eukaryotes, this intriguing membrane bound organelle consists of a series of flattened cisternae layered on top of each other to form the Golgi stack (Glick and Nakano 2009; Lowe 2011). These stacks are polarised, in a *cis* to *trans* direction, based on glycosylation enzyme composition within each compartment (Dunphy and Rothman 1985; Kleene and Berger 1993), and functionally divided into three distinct compartments: the *cis*-cisternae, forming the *cis*-Golgi network (CGN) that are the gateway for secretory cargo into the Golgi and, therefore, facing the ER from where cargo is exported; the median-cisternae, the trans-cisternae; and the trans Golgi network (TGN), a tubular-fenestrated structure formed as a product of the trans-cisternae and an important sorting site (Robinson 2020). However, there are some particularities to the Golgi's structural organization. In mammalian cells, the Golgi stacks appear laterally connected near the centrosome in a single copy structure named the Golgi ribbon that is immobile (Rambourg and Clermont 1990; Lowe 2011). Another example of a different organization is the Golgi of the budding yeast *Saccharomyces cerevisiae*, which comprises individual cisternae spread throughout the cytoplasm (Preuss et al. 1992). In the case of plant cells, the functional Golgi unit consists of the Golgi stack, its associated TGN and the Golgi matrix surrounding these structures (Staehelin and Moore 1995; Glick and Nakano 2009). This unit is found closely associated with actin (Boevink et al. 1998) and varies in number of stacks and their distribution throughput the cytoplasm, depending on the cell type, the plant, the stage of development of the cell, and the types and amounts of molecules produced by the endomembrane system (Staehelin and Moore 1995; Dupree and Sherrier 1998). Another

differentiating feature among eukaryotes is that animal cells present an ER–Golgi intermediate compartment (ERGIC), which is a mobile microtubule-dependent structure crossing at the interface between ERES and the *cis*-Golgi (Appenzeller-Herzog and Hauri 2006), whereas plants lack the ERGIC and ERES and the *cis*-Golgi may be a few hundred nanometers away (Hawes 2012). Yet, more recently, throught flourescently labbled plant COPII homologous, ERES have been identified in plants (Robinson 2020).

The structural organization of the Golgi apparatus is a reflection of its functional role inside the cell. This organelle serves as carbohydrate synthesis station to process oligosaccharide side chains on newly synthesized glycoproteins and glycolipids (Mellman and Simons 1992) and as a sorting and dispatching site for proteins exiting the ER for further protein processing before being sent to other locations (Alberts et al. 2002). As proteins travel along the Golgi stacks in a *cis* to *trans* manner, they acquire the necessary post-translational modifications (such as glycosylation, sulfation and phosphorylation) mainly through transmembrane processing enzymes. Once modified, proteins follow to the TGN where they can be sorted into a variety of vesicles and carried to their destinated locations (Alberts et al. 2002; Glick and Nakano 2009). Additionally, the Golgi acts as a membrane frame for adhesion of varied signalling, sorting and cytoskeleton proteins (Donaldson and Lippincott-Schwartz 2000; Matteis and Morrow 2000; Altan-Bonnet et al. 2003). Finally, the Golgi apparatus is responsible for the synthesis of many of the cell's polysaccharides, which include the hemicellulose and pectin present in the cell wall and most of the glycosaminoglycans found in the extracellular space in animals (Alberts et al. 2002). Regarding specifically the TGN, this is where the separation between the secreted and vacuolar protein transport occurs and, in plants, it acts as an endocytic compartment, functioning as the early endosome (EE) (Viotti et al. 2010).

Although much has been discovered about endomembrane trafficking, how cargo travels within the Golgi apparatus is still controversial, but three models remain in the spotlight: cisternal maturation (Glick and Malhotra 1998), vesicular transport between stable compartments (Rothman and Wieland 1996) and the rapid partitioning model (Patterson et al. 2008). According to the cisternal maturation model, cisternae are viewed as transient carriers from the ER that assemble at the *cis* face of the stack and progressively mature through the Golgi, while transporting cargo forward, culminating at the TGN. This maturation is driven by the retrograde recycling of resident Golgi proteins, involving COPI vesicles within the stacks and may also include clathrin-mediated recycling from a maturing TGN compartment (Glick and Nakano 2009; Boncompain and Weigel 2018). Conversely, in the vesicular transport model, the *cis*-, *medial*- and *trans*-

Golgi cisternae and the TGN are viewed as stable compartments where a unique set of resident Golgi proteins are retained and cargoes move from compartment to compartment in an assembly-line manner via anterograde COPII vesicles (Rothman and Wieland 1996). This advantageous model offers an explanation to the polarity of the Golgi as it considers its stacks as distinct suborganelles, each of which with its own set of specific resident proteins (Dunphy and Rothman 1985; Farquhar 1985). Moreover, the observation of abundant COPI transport vesicles around the Golgi is also accounted for, apparently forming and fusing at the cisternal rims (Farquhar 1985; Orci et al. 1986). Biochemical evidence for this model arose from the implication of COPI vesicles and the vesicle fusion machinery in intra-Golgi transport in a cell-free reconstitution system (Rothman and Wieland 1996). Nevertheless, the stable compartments model came across some obstacles. In many organisms, the Golgi stack transport cargoes are too large to fit in conventional COPI vesicles, with examples that include scales in algae (Becker and Melkonian 1996) and procollagen in mammalian fibroblasts (Bonfanti et al. 1998). Besides, the evidence for anterograde COPII-dependent transport is less solid then that accounting for retrograde COPI-dependent transport (Rabouille and Klumperman 2005). Such problems are solved by the cisternal maturation model, as accumulating data has oriented the field towards this model. However, it fails to explain how differente cargoes traffic at variable rates and mono-exponential export kinetics from the Golgi apparatus (Boncompain and Weigel 2018). The observation of such kinetics enabled the development of the rapid partitioning model (Patterson et al. 2008). Here, the Golgi is viewed as a single interconnected compartment containing processing and export domains, based on a lipid gradient. As cargo arrives from the ER, it quickly partitions between two domains, then stochastically leaving from every level of the stacks to its final destination. The observations of different export kinetics from different cargoes are explained by the residence time in processing domains, the diffusion properties of the cargo and the site of Golgi exit.

1.1.3. The Vacuoles

The vacuole is a cellular organelle that belongs to the endomembrane system (Jürgens 2004) and is the largest membranous compartment of the mature plant cell, occupying up to 80-90 % of the cell volume (Marty 1999; Bassham et al. 2008; Eisenach et al. 2015). This multifunctional compartment actively participates in maintaining cell homeostasis contributing to growth and development, through maintenance of the turgor pressure, as well as in cellular responses to abiotic and biotic cues (Marty 1999; Martinoia et al. 2007; Bassham et al. 2008). Generally, the vacuoles are responsible for the storage of water, nutrients, ions, hormones, secondary metabolites, and proteins

(Bassham et al. 2008), along with toxic cell residues, waste products and excess solutes (Jiang et al. 2000; Martinoia et al. 2000; Bethke and Jones 2000; Hatsugai et al. 2004), and also take part in the programmed death of the cell (Hara-Nishimura and Hatsugai 2011). Plant vacuoles not only vary in function, but also in shape, size, and content (Marty 1999). In plant cells, two major types of vacuoles may be defined: the protein storage vacuoles (PSV) and the lytic vacuole (LV). Since they have higher pH and lower hydrolytic activity than LVs, PSVs are the eligible site for protein accumulation and they are typically found not only in storage tissues, such as cotyledons, endosperm and tubers, but also in the vegetative tissues of mature plants, like bark, leaves or pods (Müntz 1998; Vitale and Hinz 2005; Zouhar et al. 2010). Conversely, given their lower pH and higher hydrolytic activity, LVs serve as a degradative station of multiple macromolecules and other compounds (Rogers 2008; Frigerio et al. 2008), helping in the detoxification of damaging products (Eisenach et al. 2015), in addition to their role in senescence and programmed cell death (Bassham et al. 2008; Shimada et al. 2018). Being the equivalent to animal lysosomes or yeast vacuoles, LVs also function as deposit and storage sites for waste compounds (Jürgens 2004), and they mostly occur in vegetative tissues (Shimada et al. 2018). These different vacuoles have been distinguished through intrinsic proteins found in the tonoplast, the delimiting membrane of the vacuole (Bassham et al. 2008; Hara-Nishimura and Hatsugai 2011). Interestingly, studies done in root tip cells of barley and pea seedlings have revealed the co-existence of both PSV and LV in the same cell, contrary to what one might expect (Paris et al. 1996; Olbrich et al. 2007). Such occurrence entails that plants cells must distinguish trafficking pathways and mechanisms for different proteins and the presence of both vacuole types might confer flexibility to the cell to better deal with altering environmental conditions (Jürgens 2004; Vitale and Hinz 2005; Pereira et al. 2014). Moreover, plants are capable of developing specialized vacuoles, which contain particular materials. For instance, in *Brassicaceae*, myrosinases (ß-thioglucoside glucohydrolases), used for chemical defence against herbivores, are accumulated in the vacuoles of myrosin cells along leaf veins (Shimada et al. 2018).

1.1.4. The plasma membrane

Delimiting the cell, the plasma membrane (PM) is the key cell structure for cell protection, regulation of nutrient exchanges and control of signal perception (Cassim et al. 2019). By docking the suitable signalling cascades that permit adaptive responses, the PM guarantees cell functions, crucial for cell survival in an everchanging environment. To do so, it must combine stability and robustness without neglecting its dynamics, which is possible due to its diverse molecular organization (Cassim et al.

2019). Eukaryotic PMs are composed mainly of three classes of lipids: glycerolipids, sphingolipids, and sterols (Yetukuri et al. 2008; Shevchenko and Simons 2010). In general, the same molecular moieties of all glycerolipids are shared by plants, animals, and fungi, contrasting with sterols and sphingolipids, which are kingdom specific. For plant cells, characterization of the lipidic content of the PM (Samarakoon et al. 2012; Yu et al. 2018) includes phospholipids (Grison et al. 2015), phosphoinositides (Doignon et al. 2016), sphingolipids (Markham et al. 2006; Markham and Jaworski 2007) and sterols (Wewer et al. 2011; Schrick et al. 2012). Among the sterols found in plant PM, β-sitosterol, stigmasterol, and campesterol are the most prevalent (Furt et al. 2011). Additionally, approximately 15 % of the *Nicotiana tabacum* PM consists of conjugated phytosterols, forming steryl glycosides (SG) and acyl steryl glycosides (ASG) (Furt et al. 2011). Phytosterols are regarded as the major component that contributes to plant PM rigidity (Roche et al. 2008, 2010; Gerbeau-Pissot et al. 2014). Considering the sphingolipids, the major phosphosphingolipid of animals (sphingomyelin) is not found in plants. Conversely, glycosyl inositol phosphorylceramides (GIPCs), which are absent in animals, represent the major class of sphingolipids of plants. These molecules represent up to 40 mol % of the total PM lipids of tobacco (*Nicotiana tabacum*) plants and are enriched in the outer leaflet of the PM, with 60% to 80% of total outer leaflet lipids (Cacas et al. 2016). GIPCs are immensely relevant in plant PM with a vast array of contributions to PM correct functioning. They are involved in raft formation in both PM leaflets (Raffaele et al. 2009; Furt et al. 2010; Mongrand et al. 2010), participate in the early stages of symbiosis (Hernandez et al. 1995), in Golgi and ER integrity (Chen et al. 2008), in growth, and in the hypersensitive response through salicylic acid production (Mortimer et al. 2013). Moreover, plant GIPCs may also be determinant contributors in cell signalling, cell-to-cell communication, plant defence, and the sorting of proteins, similar to what is depicted for complex sphingolipids in animal development (Worrall et al. 2003), as well as showing an aptitude to increase the lipid packing of the PM, through a sterol-dependent manner (Grosjean et al. 2015).

Besides limiting the cell and sensing environmental cues, the PM functions as the targeted station of cargo, being it intended for secretion or for incorporation into the membrane. As a result, secreted proteins and extracellular components leave the cell to the apoplast so they might either turn into incorporated components of the extracellular matrix or diffuse away. Membrane proteins are integrated into the PM leaflets to perform imperative tasks as ion channels, membrane transporters, ligand receptors, signalling complexes or physical contact points between the intracellular cytoskeleton network and the extracellular matrix (Bassham et al. 2008). The combination of the variety of lipids

and proteins and their interactions at the PM adds up to its complex organization, and interactions between lipids and lipids and proteins are believed to be fundamental to the organization of the plant PM (Cassim et al. 2019). Therefore, this structure must be viewed as a mosaic that is both fluid and yet highly compartmentalized, wherein numerous membrane domains co-exist, although they are different in composition and biophysical properties (Ott 2017; Gronnier et al. 2018). As seen in other eukaryotes, such domains are highly enriched in certain types of lipids, and work as concentrators of certain types of proteins, such as receptor/signalling complexes, cytoskeleton attachment points, and endocytic machinery. Moreover, the plant PM is likely to have polarity regarding the location of such domains in the lipidic bilayer. Such is crucial for cell functioning and signalling and is achieved by specific targeting to a particular domain, by specific retrieval through endocytosis, and by peculiar characteristics of the lipid patches found in the domains (Bassham et al. 2008).

In plant cells, the PM and the ER intimately crosstalk at ER–PM contact sites that facilitate the balance of the ER metabolism with the changes in PM composition (Stefan et al. 2013). These membrane junctions are abundant structures and differ on architecture, depending on the cell type (Carrasco and Meyer 2011). Furthermore, ER–PM contacts are well-known to control calcium dynamics, are involved in non-vesicular sterol lipid transport (Lev 2010; Toulmay and Prinz 2011), and there is growing evidence that these are sites for signal transmission (Stefan et al. 2013). Another specific and relevant feature of plant PM is its close association with the cell wall (Kohorn 2000). As turgor pressure firmly presses the PM against the cell wall, this structure helps regulate protein lateral mobility, through this intimate connection, affecting not only the outer leaflet but also the inner one (Martinière et al. 2012).

1.2. Vacuolar trafficking and the pathways to the vacuoles

The endomembrane system is an intricate network of membranous compartments and dynamic trafficking routes, among which the most significant are the secretory (involving biosynthesis and sorting) and the endocytic pathways. In the past years, astonishing results have been obtained to help us further understand how protein sorting is processed and its underlying mechanisms. Given its relevance in plant cell homeostasis, the study of vacuolar targeted proteins, the pathways they follow and how they are sorted has been exceptionally highlighted and the knowledge acquired so far is fairly thorough, with many signals and protein effectors already described. Yet, more recently collected data on the subject is suggestive of alternative routes that might challenge the classical view of protein delivery to the vacuole (di Sansebastiano et al. 2018; Vieira et al. 2019). Upon synthesis, proteins and other cargoes are designed to

take a certain sorting pathway to reach their final destination. A protein is taken on a particular path in the cell, depending on the interactions between sorting motifs present in its sequence and the motif-recognizing machinery of the cell. The sorting motifs are also known as vacuolar sorting determinants (VSDs) and are divided into three types: sequence-specific VSDs (ssVSDs), C-terminal VSDs (Ct-VSDs) and VSDs dependent on the physical structure of proteins (psVSDs) (Vitale and Hinz 2005; Pereira et al. 2014). They are normally recognized when proteins reach the late or post-Golgi level and redirect proteins away from the secretory pathway, leading them to the vacuole. Several of such motifs have been found conserved in yeast and humans (Marcos Lousa et al. 2012). Typically, the secretory pathway of proteins starts at the ER, travels through the Golgi complex and reaches its final stop at the vacuole, other compartments or the cell surface (Rojo and Denecke 2008; Marcos Lousa et al. 2012).

1.2.1. The conventional routes

Eukaryotic cells have their different organelles scattered across the cytoplasm in a functionally and interconnected manner, through multiple transport routes that form the secretory pathway. The conventional trafficking through the secretory pathway takes proteins from the ER and leads them through the Golgi apparatus until their final destination, which might be the vacuole, other compartments, or the plasma membrane (Rojo and Denecke 2008; Marcos Lousa et al. 2012). As plant cells have two different types of vacuoles (PSVs and LVs) and both may co-exist within the same cell (Paris et al. 1996; Olbrich et al. 2007), it is important to understand the mechanisms and regulation behind vacuolar trafficking, as vacuoles play a central role in plant cell homeostasis. The storage proteins may arrive at the PSV through a Golgi-dependent route and this path is determined by vesicular cargo type and the plant developmental stage (Robinson et al. 2005; Rojo and Denecke 2008). The carriers responsible for this transport are dense vesicles (DVs), which are small and uniform vesicles that are uniquely found in plants (Vitale and Chrispeels 1992; Hinz et al. 1997; Vitale and Hinz 2005; Maruyama et al. 2006) and hold intrinsic membrane proteins leading them towards the PSV. After being firstly detected in common bean (Chrispeels 1983), DVs have since been discovered in other plant species, including wheat (Kim et al. 1988), pea (Hinz et al. 1999) and Arabidopsis (Hinz et al. 2007). These carriers begin to form within the *cis*-Golgi, given the accumulation and condensation of storage proteins, and from here they are directed to the TGN. Simultaneously with this transfer, DVs increase in density so they can be freed from the TGN (Hinz et al. 2007; Hwang 2008). The mature DVs are not coated vesicles, which facilitates their fusion with multivesicular bodies (MVBs) before reaching the PSV or directly with PSV, expelling their contents (Hohl et al. 1996;

Jiang et al. 2000, 2001; Tse et al. 2004; Hinz et al. 2007; Hwang 2008; Pereira et al. 2014; Peixoto et al. 2018; di Sansebastiano et al. 2018). Present in all eukaryotes and characterized by their internal vesicles, MVBs participate in several post-Golgi processes of the biosynthetic trafficking pathway and, upon fusion, DVs release their contents to this compartment (Tse et al. 2004). Finally, the PSV receives the MVB along with their cargoes. Thus, the conventional route to the PSV via a Golgi-dependent pathway is defined by the following compartments: ER - Golgi - DV - MVBs - PSV (Figure 1.3). Although receptor-mediated sorting might also be involved, protein trafficking to the PSV is mostly processed through aggregation (Molina et al. 2006). In receptor-mediated sorting, the vacuolar sorting receptors (VSRs) implicated are BP80 homologues (like PV72, AtELP1) and receptor membrane ring-H2 (RMRs) (Vitale and Hinz 2005; Jolliffe et al. 2005; Li et al. 2006; Fuji et al. 2007; Hwang 2008). VSRs are type I membrane proteins, containing a cytosolic motif and a large lumenal domain. Such membrane proteins are commonly considered to mediate protein sorting to LV and are capable of recognizing aspargine-proline-isoleucine-arginine-leucine (NPIRL) and NPIRL-like consensus motifs in cargo proteins (mostly present at the N-terminus in cargo) and also are susceptible to being recognized themselves by adaptor protein 1 (AP1) via its tyrosine consensus motif at the C-terminus that promote packing into the CCV (Happel et al. 2004; Jürgens 2004). On the other hand, proteins directed to the PSV usually contain a Ct-VSD, such as in the case of tobacco (*Nicotiana tabacum*) chitinase A (Neuhaus et al. 1994). Several reports have mentioned proteins sorted to the PSV in a DV manner, including legumin, vicilin and sucrose-binding-protein homologue (Wenzel et al. 2005; Molina et al. 2006).

Contrasting to what has been observed for the PSV, protein trafficking to the LVs/lysosomes is mediated by CCVs rather than DVs (Chrispeels 1983; Hohl et al. 1996), in a pathway seemingly conserved among all eukaryotes. The TGN membrane receptors recognise the specific sorting motifs to be condensed into CCVs so they can be directed to the PVC and, finally, to the LVs (Robinson et al. 1998; Rouillé et al. 2000). The mannose 6-phosphate receptors (MPR) enable acid hydrolases sorting to the lysosome in animal cells (Ghosh et al. 2003). Through a process facilitated by Golgi-localized, γ-adaptin ear-containing, ARF-binding proteins and by the AP1 complex interacting with MPRs tyrosine (YXXΦ) and dileucine (LL) motifs at the cytosolic tail, the recruitment of MPR-ligand complexes into CCVs occurs at the TGN (Doray et al. 2002; Ghosh et al. 2003). A similar sorting and delivery to the LV take place in yeast (Deloche et al. 2001; Costaguta et al. 2001). Trafficking to plant LVs is believed to happen through this delivery mechanism, even though proteins targeted to the LV interact with VSRs,

which do not show homology to MPRs (Kirchhausen 2000). In plant cells, sequence-specific VSDs, as NPIRL-like consensus motifs, present in proteins targeted to the LV (e.g., barley aleurain), are recognized by VSRs (Matsuoka and Neuhaus 1999; Paris and Neuhaus 2002), which, in turn, interact with AP1 through a tyrosine-based sorting motif. This interaction differs from that of yeast and animals, where it involves a dileucine motif (Happel et al. 2004). Once cargo-VSR is assembled into CCVs, these carriers are released from the TGN and taken to the PVC, where CCVs are emptied upon fusion (Hinz et al. 1999; Tse et al. 2004). Given the lower pH of the PVC, ligands are disconnected from the respective receptor, so the receptor may be recycled back to the Golgi (Raiborg et al. 2003; Maxfield and McGraw 2004; Seaman 2005).

In addition to this pathway, other routes to the LV have been reported: an MPR-independent pathway in animal cells, and a VPS10-independent lysosome sorting pathway in yeast (Iwaki et al. 2006; Reczek et al. 2007). In this pathway, it is AP3 that seems to serve a pivotal part, instead of AP1. This adaptor protein recognizes both dileucine and tyrosine motifs in animals, while in yeast it is only capable of recognizing dileucine signals (Bonifacino and Traub 2003; Braulke and Bonifacino 2009). As demonstrated by recent data on sorting of tonoplast transporters in Arabidopsis mesophyll protoplasts, it is suggested that plants may have a similar route (Figure 1.3) (Wolfenstetter et al. 2012). Moreover, AP3 subunits are hypothesized to have a role in the biogenesis, morphology and function of the PVC and vacuoles in plant cells (Niihama et al. 2009; Feraru et al. 2010; Zwiewka et al. 2011).

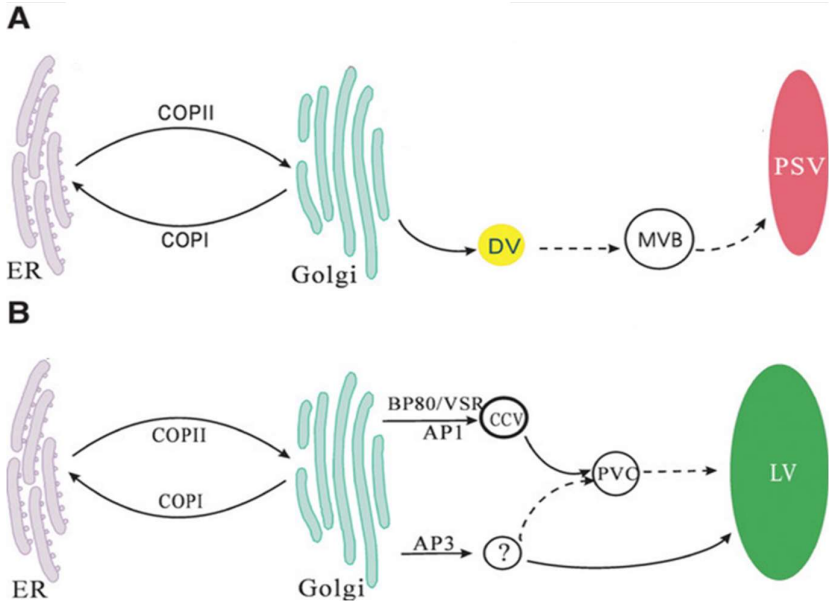


Figure 1.3 – Conventional routes to the vacuoles. (A) Proteins targeted to the PSV begin their path in the cell at the ER and may follow a Golgi-dependent pathway. Through this pathway, proteins leave the ER via COPII vesicles to the

Golgi, where they are aggregated and develop into the cargo of DVs, proceeding their journey to multivesicular bodies and finally fusing into the PSV. (B) Similar, LV resident proteins, after synthesis at the ER, are taken by COPII to the Golgi, where they are recognized BP80/VSR to become the cargo of CCV that are shipped to the PVC, before reaching the LV. Alternatively, proteins destined to the LV can follow a putative AP3-mediated pathway. Abbreviations: AP1, adaptor protein 1; AP3, adaptor protein 3; BP80, vacuolar sorting receptor; CCV, clathrin coated vesicle; COPI, coat protein complex I; COPII, coat protein complex II; DV, dense vesicles; ER, endoplasmic reticulum; MVB, multivesicular body; PSV, protein storage vacuole; PVC, pre-vacuolar compartment; LV, lytic vacuole; PV72/ RMR, vacuole sorting receptor; VSR, vacuolar sorting receptor. Adapted from Xiang et al. (2013).

1.2.2. The unconventional routes

The transport of proteins in the cell can occur through different routes and engage different intermediates and, as more studies accumulate on this topic, novel pathways are defying the classical view of protein sorting and trafficking. Alongside the conventional transport route previously described, proteins targeted to the PSV can follow an alternative route bypassing the Golgi (Figure 1.4). This appears to be the case of globulins, which are major vacuolar storage proteins in pumpkins. These storage proteins have been suggested to be transported to the PSV directly from the ER through precursor-accumulating compartments (PACs), which are bigger carriers than DVs (Hara-Nishimura et al. 1998; Toyooka et al. 2000). Similar observations have been done with cysteine proteinases (Toyooka et al. 2000; Mitsuhashi et al. 2001). As they derive directly from the ER, PACs are filled with non-glycosylated precursors of storage proteins and mediate the sorting by protein aggregation. However, PACs are susceptible to uptake glycosylated proteins derived from the Golgi as they are transported to the PSV (Hara-Nishimura et al. 1998; Jolliffe et al. 2005). Finally, as PACs reach the PSV, their cargo is integrated into the PSV lumen either by fusion of the PAC itself with the PSV through autophagy (Van der Wilden et al. 1980; Robinson et al. 1995) or the membranes of the PAC and the PSV fuse directly (Shimada et al. 1994; Robinson et al. 1995). These carriers have been found in pumpkin, castor beans and wheat (Hara-Nishimura et al. 1998; Mori et al. 2004; Takahashi et al. 2005).

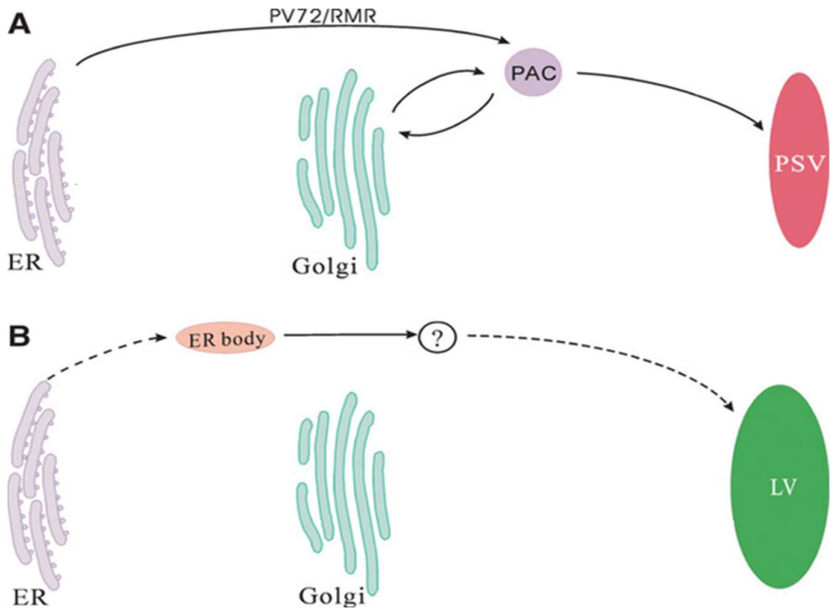


Figure 1.4 – Unconventional routes to the vacuoles. (A) Storage proteins may arrive at the PSV in a Golgi-independent manner, as they leave the ER and are recognized by RMRs or VSRs (PV72 in the figure), leading to their package into precursor accumulating vesicles that take them to the PSV, without passing through the Golgi apparatus. (B) Similarly, LV resident proteins can reach this compartment in ER bodies, bypassing the Golgi. Abbreviations: ER, endoplasmic reticulum; LV, lytic vacuole; PAC, precursor-accumulating compartments; PSV, protein storage vacuole; PV72/ RMR, vacuole sorting receptor. Adapted from Xiang et al. (2013).

Similarly, proteins that are targeted for the LV may also travel through alternative routes. In a process exclusive to plants, proteins destined to the LV might be transported directly from the ER and bypass the Golgi, with the intermediate compartments being ER bodies (Hara-Nishimura et al. 2004). Therefore, the plasticity of the ER to form subcellular structures appears to be a distinguishing feature of plants. These structures are either stably accumulated in the ER or conveyed to the LV and they are mostly spherical with a dense core composed of a self-assembling or aggregating protein, oil or rubber, delimited by a membrane originated from the ER (Matsushima et al. 2003a; Herman 2008). There is some evidence regarding unconventional ER trafficking involving a bypass of the Golgi to the lysosome of animal cells (Teckman and Perlmutter 2000). Bearing this in mind, a similar route is proposed to be taken by ER bodies in plants, where these subcellular structures are directed to the LV in a Golgi-independent manner, fusing directly with the LV, in accordance with what happens under stress conditions (Hayashi et al. 2001; Herman and Schmidt 2004).

1.2.3. The Plant specific insert (PSI) and PSI mediated routes

Aspartic proteinases (APs) have been extensively studied throughout the years and our laboratory has been especially interested in their biogenesis and sorting mechanisms, having collected a rich amount of data on the subject (Vieira et al. 2001;

Pissarra et al. 2007; Pereira et al. 2008, 2013; Duarte et al. 2008; Oliveira et al. 2010; da Costa et al. 2010, 2011; Vieira et al. 2019). Since different APs are able to accumulate in different cellular compartments and the same protein is susceptible to secretion to the apoplast or directed to the vacuole depending on the cell type and developmental stage (Ramalho-Santos et al. 1998; Oliveira et al. 2010; da Costa et al. 2010), it has been hypothesized that different APs present different sorting motifs, providing some flexibility depending on the conditions influencing the cell. Our laboratory has been using as working models cardosin A and cardosin B, which are well-characterized APs found in *Cynara cardunculus* (Ramalho-Santos et al. 1998; Vieira et al. 2001). Despite being highly similar regarding protein sequence, these enzymes may accumulate in different cell compartments during plant development (Ramalho-Santos et al. 1997; Vieira et al. 2001). Cardosin A has been shown to accumulate in PSVs or LVs and its final destination in the cell is dependent on development stage and specific cellular needs (Ramalho-Santos et al. 1997; Pissarra et al. 2007; Pereira et al. 2008; Oliveira et al. 2010), whereas cardosin B appeared extracellularly (Vieira et al. 2001). Moreover, when expressed in *Arabidopsis thaliana* and *Nicotiana tabacum*, cardosin A was accumulated in both vacuoles (PSV and LV) (Duarte et al. 2008; Pereira et al. 2013) and cardosin B, in the same heterologous systems, was found to accumulate in LVs (da Costa et al. 2010). Such characteristics make cardosins intriguing and provide solid evidence for their utility as reporters for the study of vacuolar trafficking and VSDs in plants. Both cardosins (A and B) are synthesized in the cell as pre-proenzymes, reaching their mature form as they undergo multiple cleavages along their route in the endomembrane system. A presegment (PRE), a prosegment (PRO), heavy and light chains and a PSI constitute the precursor form of the cardosins. The cardosins' maturation process involves the cleavage of the PRO sequence and the PSI, leaving the enzyme with a heavy and a light chain (Ramalho-Santos et al. 1997) (Figure 1.5).

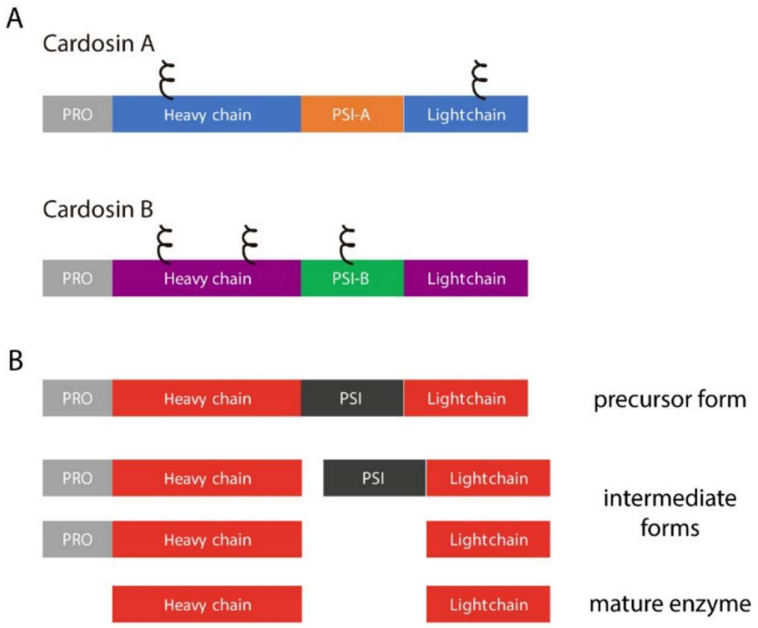


Figure 1.5 – Domain organization of Cardosin A and B and the sequential processing steps to acquire the mature form. (A) In both cardosins, a presegment and a prosegment are observed, as well as the PSI separating the heavy (31 and 34 kDa, respectively) and light (15 and 14 kDa, respectively) chains of the mature form of the enzymes. The *N*-glycosylation sites are also illustrated (ξ). (B) Processing steps cardosins undergo along the endomembrane system to acquire their mature form, composed of heavy and light chains. Abbreviations: PRO, prosegment; PSI, plant specific insert domain. Retrieved from Vieira et al. (2019).

Similarly to what is observed in some plant APs, both Cardosin A and B possess specific sequences designated Plant Specific Inserts (PSIs), that consist of unique protein domains of about 100 amino acids (Simões and Faro 2004; Soares et al. 2019). The PSI is frequently designated “an enzyme within an enzyme”, since, when isolated and *in vitro*, it presents several function such as: acting as a detergent, mediating lipid membrane interactions, presents putative antimicrobial activity and is able to induce membrane permeabilization, along with membrane modulation (Egas et al. 2000; Terauchi et al. 2006; Muñoz et al. 2010, 2014; Curto et al. 2014; De Moura et al. 2014; Frey et al. 2018). Although its functions in cells still need to be clarified, some reports have associated the PSI with vacuolar targeting of the APs (Egas et al. 2000; Törmäkangas et al. 2001; Terauchi et al. 2006; Pereira et al. 2013).

As novel unconventional routes for vacuolar sorting where proteins are directly sorted to the LV, bypassing the Golgi (de Caroli et al. 2011; Stigliano et al. 2013; De Marchis et al. 2013; Pereira et al. 2013; di Sansebastiano et al. 2018), are being revealed, it is necessary to understand where the PSI fits in the complex network of vacuolar protein trafficking. In a process that remains to be fully understood, PSI domain of cardosin A and B have been demonstrated to be capable of redirecting secreted

proteins to the vacuole following different routes. Intriguingly, cardosin A contains two different sorting signals: a classic VSD, the C-terminal peptide (Ct-VSD), and a more atypical VSD, the PSI, as it cannot be placed in any known VSD category (Pereira et al. 2013). Each VSD was demonstrated to take a different route to reach the protein's final destination: The PSI mediates a direct ER-to-vacuole route, while the C-terminal peptide follows a classic ER-Golgi-PVC route to the vacuole, thus establishing a poly-sorting mechanism for cardosin A (Pereira et al. 2013). Moreover, the presence of either of these VSDs was sufficient and necessary for the protein to reach the vacuole. These two vacuolar sorting motifs of cardosin A appear to strengthen the cell with some metabolic flexibility, since their activation depends on the developmental stage and the environmental conditions (Pereira et al. 2008, 2013). In the case of cardosin B, both the C-terminal and PSI domains also act as vacuolar sorting domains, however, this latter PSI domain does not mediate a Golgi bypass (Pereira et al. 2013).

Even if both the cardosin A PSI (PSI A) and the cardosin B PSI (PSI B) are capable of leading the AP to the vacuole, how each PSI does it is very different. The transport from the ER to the Golgi in PSI B-mediated sorting is COPII-dependent, whereas PSI A-mediated sorting is COPII-independent. As such findings were more explored, co-expression with $Sar1^{H74L}$ (a dominant negative mutant that blocks COPII-mediated transport) demonstrated that proteins still reached the vacuole through PSI A-mediated sorting, whereas, in this scenario, PSI B-mediated sorting was blocked and, subsequently, proteins accumulated in the ER (Vieira et al. 2019). Such results corroborated the Golgi-bypass of the PSI A-mediated route, but its mechanisms were still unknown. To further understand the differences between the routes mediated by the PSI A and PSI B, both sequences were investigated and compared. Differences in the glycosylation status of the PSIs were found: a N-linked glycosylation site that appeared in PSI B was missing in PSI A (Figure 1.5) (Vieira et al. 2019). Such findings could have repercussions on the route followed by cardosins. In fact, it was observed that altering these glycosylation patterns also alters the route taken by the protein: when co-expressed with $Sar1^{H74L}$, the insertion of a glycosylation site in PSI A lead to a protein accumulation in the ER, while non-glycosylated PSI B bypassed ER-to-Golgi blockage and accumulated in the vacuole, and this remained true when considering the full-length cardosin (Vieira et al. 2019). However, the results for PSI B were not as clear as those of PSI A, as some PSI B was still retained in the ER in addition that located in the vacuole. One possible explanation for this could be the existence of other post-transcriptional modifications in the PSI B sequence that are yet to be elucidated and require further research.

Since the conventional ER - Golgi - PVC - Vacuole pathway has been extensively researched, investigators are becoming increasingly interested in unravelling how vacuolar sorting signals such as the PSIs and Chitinase A are capable of bypassing the Golgi on their way to the vacuole (Stigliano et al. 2013; Occhialini et al. 2016; Pompa et al. 2017). Still, the underlying mechanisms potentializing unconventional sorting pathways remain ambiguous.

1.3. Endocytosis in plant cells

Occurring at the plasma membrane of eukaryotic cells, endocytosis is a fundamental process characterized by the uptake of extracellular materials and cell surface proteins and their transport to the proper compartment in the cell (Fan et al. 2015) and mediates the recycling of membranes, ion channels and surface cell receptors as well as being essential in controlling the lipid and protein composition of the plasma membrane (Stefano et al. 2015). Additionally, this transport step contributes to the perception of extracellular cues, through the regulation of recycling or degradation of plasma membrane receptors (Dhonukshe et al. 2007; Taylor 2011; Stefano et al. 2015). Cargo endocytosis is believed to be mediated by vesicles, leading to a class of organelles roughly defined as endosomes, which are membranous compartments that function as critical sorting stations for membrane trafficking, protein targeting and maturation (Stefano et al. 2015). In plant cells, endocytosis and endosomes are vital for auxin-mediated intercellular communication, gravitropic responses, stomatal movements, and cell wall morphogenesis (Šamaj et al. 2005), as well as hormonal signalling and communication with the environment including nutrient delivery, toxin avoidance, and pathogen defence (Chen et al. 2011). Moreover, endosomes are also important in the biosynthetic pathway by leading proteins to the vacuole and recycling vacuolar cargo receptors (Reyes et al. 2011).

After the initial internalization process, a series of mainly vesicle-mediated transfer steps follows, which convey the cargo molecules through endosomal compartments (Figure 1.6). Once inside the cell, endocytic cargo can take one of two routes, being either recycled to the PM or transported for degradation in the lytic compartment (Robinson et al. 2008). The nature of the cargo molecules and the targeted organelle define the internalization and the following route of endocytic vesicles (Aguilar and Wendland 2005) and this process encompasses several subcellular compartments that include the early endosome (EE), trans Golgi network (TGN), multivesicular body (MVB)/pre-vacuolar compartment (PVC), and the lysosome/vacuole (Onelli et al. 2008). Additionally, it has been recognized that the endocytic and secretory pathways intersect at these organelles (Ghedin et al. 2001) and that this is true for animal (Henkel et al.

1996; Ang et al. 2004) and plant cells (Šamaj et al. 2005; Lam et al. 2007), indicating that intracellular vesicular transport occurs in many directions and the different systems involved are highly interconnected (Etxeberria et al. 2009).

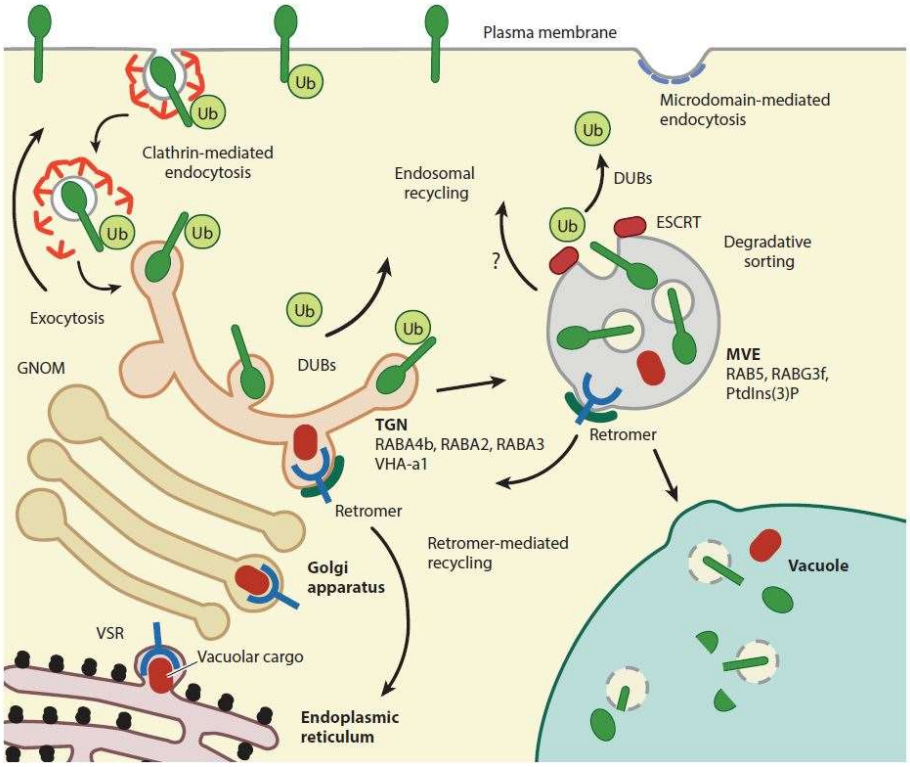


Figure 1.6 – Endosomal trafficking and its different routes in plants. Abbreviations: DUB, deubiquitinating enzyme; ESCRT, endosomal sorting complex required for transport; MVE, multivesicular endosomes PtdIns(3)P, phosphatidylinositol 3-phosphate; TGN, trans Golgi network; Ub, ubiquitin; VHA, vacuolar H^+-ATPase; VSR, vacuolar sorting receptor. Retrieved from Paez Valencia et al. (2016).

The early endosomes (EE) are the first compartments to receive the internalized cargo (Šamaj et al. 2005; Viotti et al. 2010) and in plants, the TGN is regarded as the EE equivalent, since it is where endocytic cargo accumulates first (Stefano et al. 2015). Thus, the EE and the TGN are believed to be a merge point of the secretory and endocytic pathways (Stefano et al. 2015). When cargo is targeted for degradation, it passes through the late endosomes (LE) that are identical to multivesicular bodies (MVB) and/or pre-vacuolar compartments (PVC), characterised by containing small internal vesicles in their lumen (Tse et al. 2004; Šamaj et al. 2005; Marcos Lousa et al. 2012). Functionally equivalent to mammalian lysosomes and yeast vacuoles, the lytic vacuoles in plants are the specialized compartments for the degradation and turnover of cargo (Šamaj et al. 2005). The identification of the different endocytic compartments can be defined by the functional accumulation of molecular markers that include Rab GTPases,

SNAREs, ARF, ARF-GEF, vacuolar sorting receptors and PtdIns(3)P-binding FYVE-domain (Šamaj et al. 2005).

Generally, cargo macromolecules must concentrate in a patch of the donor membrane to allow sorting and packaging of such cargo in vesicles for transfer from donor to acceptor compartments. A protein coat facilitates the local deformation of the membrane into a pit and is recruited either directly by the cargo itself or through adaptors. These adaptor proteins, as well as binding cargo, are able to directly bind specific phosphoinositides on membranes and other accessory proteins (Paczkowski et al. 2015). Membrane scission finally releases the newly formed vesicle from the donor compartment. This carrier eventually loses its coat upon fusion with the acceptor compartment in a process that involves membrane fusion factors such as SNAREs and small GTPases (Paez Valencia et al. 2016). In eukaryotes, there are different endocytic pathways that include clathrin-dependent and clathrin-independent mechanisms, with the most prominent in both plants and animals being mediated by clathrin (Paez Valencia et al. 2016). Clathrin-mediated endocytosis (CME) occurs in all known eukaryotic cells and is initiated by the invagination of the membrane, forming clathrin-coated pits (CCPs) (Chen et al. 2011). There is emerging evidence that, in line with what is observed in animals, plant cells present alternative endocytic pathways beyond CME. For instance, the membrane microdomain-associated flotillin1 (Flot1) participates in clathrin-independent endocytosis in Arabidopsis (Li et al. 2012). Moreover, several pathways of clathrin-independent endocytosis (CIE) in plants have been unveiled, which include membrane microdomain-associated endocytosis, fluid phase endocytosis, and phagocytosis-like uptake of rhizobia (Son et al. 2003; Baluška et al. 2004; Chen et al. 2011; Malinsky et al. 2013). One distinguishing factor between both pathways is the size of the endocytic vesicles (Li et al. 2012). Since CIE-derived vesicles are bigger, they are likely to require a higher energy expenditure to overcome the turgor pressure characteristic of the plant cell, which may explain why CIE is less prominent in plants (Zwiewka et al. 2015). In plants, both CME and CIE cooperatively control membrane protein activity, and this control seems to be highly influenced by the physiological status and/or environmental stimuli (Zhang et al. 2019).

The sorting motifs present in the cytosolic domains of PM proteins dictate the direction such cargo must engage in the cell, and they can be generally grouped into three classes: linear amino acid motifs, conformational motifs, and post-translational modifications, such as phosphorylation and ubiquitination (Traub and Bonifacino 2013). Cargo recognition may involve more than one sorting signal for the same cargo protein, and other sorting complexes found in organelles along the endocytic and secretory

pathways, such as the TGN and endosomes, which are able to recognize similar motifs (Paez Valencia et al. 2016). Cargo proteins that are sorted for recycling back to the PM rely on small GTPases of the ARF family: ARF GTPase-activating proteins (ARF-GAPs) that stimulate GTPase hydrolytic activity, and ARF guanine exchange factors (ARF-GEFs) that facilitate GDP–GTP exchange (Reyes et al. 2011). Another structure is also involved in endosomal recycling. The Retromer is a phylogenetically conserved pentameric protein complex localized at EE that sorts transmembrane proteins back from the TGN (Reyes et al. 2011). It is responsible for the recycling of biosynthetic receptors, including the Vps10p vacuolar hydrolase receptors in yeast, cation-independent mannose 6-phosphate receptors in mammals (McGough and Cullen 2011), and vacuolar sorting receptors (VSRs) in Arabidopsis (Shimada et al. 2006; Yamazaki et al. 2008; Niemes et al. 2010). On the other hand, ubiquitination of PM proteins signals their internalization and degradation (Reyes et al. 2011), and such proteins are sorted into endosomal vesicles by the endosomal sorting complex required for transport (ESCRT) machinery for degradation in the vacuole/lysosome (Paez Valencia et al. 2016). Ubiquitin is a highly conserved 76-amino acid polypeptide that covalently binds to targeted proteins, regulating the internalization of PM proteins in mammalian and plant cells (MacGurn et al. 2012). ESCRTs complexes act at the endosomal membranes, mediating the concentration of ubiquitinated cargo into intraluminal vesicles (ILVs) within the endosome, which are responsible for the degradative sorting of monoubiquitinated membrane proteins (Reyes et al. 2011; Fan et al. 2015). It is suggested that the ESCRT sorting machinery has a relatively conserved role across kingdoms, since three ESCRT complexes (I, II, and III) are found in plants, with the exception of ESCRT-0 (Fan et al. 2015). The degradative sorting of many PM proteins is also affected by their phosphorylation state (Reyes et al. 2011).

There are other aspects that influence the regulation of endocytosis in cells. Since endocytosis has repercussions on the abundance and distribution of molecules present in the cell surface, such as signalling receptors and transporters, it becomes subject of regulation by multiple abiotic and biotic factors, which include phytohormones, such as auxin, cytokinins, strigolactone, and salicylic acid (Paez Valencia et al. 2016). It is suggested that auxin regulates the endocytic cycling of its own efflux carriers (the PIN proteins) by modulating the endocytic machinery (Fan et al. 2015). Interacting with the auxin pathways, primarily at the transcriptional regulation level, cytokinin is also an important regulator of plant endocytosis (Zhao et al. 2010). Moreover, the major plant brassinosteroids (BR) receptor, the brassinosteroid insensitive 1 (BRI1), was found to mainly localize to the PM and EE compartments in Arabidopsis root cells (Russinova et

al. 2004), and a recent study discovered that salicylic acid (SA) treatment interferes with endocytic cycling of PM-localized proteins (Du et al. 2013). In eukaryotes, several receptors are endocytosed as a consequence of the binding of their ligands, which may trigger conformational and post-translational changes that induce receptor-ligand endocytosis (Paez Valencia et al. 2016). The high concentrations of metal ions can promote the endocytosis and subsequent degradation of some plant metal ion transporters, constituting a significant feedback loop regulating ion homeostasis in plants (Paez Valencia et al. 2016). Finally, the cytoskeleton also influences endocytosis and membrane remodelling (Šamaj et al. 2006) and collected data on PIN protein polarity establishment allowed the identification of gravity as another plant-specific regulator of endocytosis (Fan et al. 2015).

1.4. *Arabidopsis thaliana* as a model organism

Belonging to the *Brassicaceae* family, which encompasses numerous crops of economic and agronomic importance, *Arabidopsis thaliana* is a small weed native to Europe and Asia (Hoffmann 2002; Woodward and Bartel 2018; Diaz 2019). This plant has proven to be so useful for modern science that, over the past decade, the number of publications using Arabidopsis as a working model has overcome not only those of model plants, like maize and rice, but also the classic genetic model organism *Drosophila melanogaster* (Woodward and Bartel 2018). Furthermore, by 2015, there were over 50,000 publications of Arabidopsis articles (Provart et al. 2016; Woodward and Bartel 2018). In fact, many discoveries in plant biology were firstly made in Arabidopsis and even when progress was made in other species, research in Arabidopsis often elucidated their fundamental workings (Provart et al. 2016).

When we take a closer look at this small weed, we find several features that could explain the interest of the scientific community. *A. thaliana* plants can grow from seed to a fully developed plants with mature seeds in about 6 weeks, depending on growth conditions (Woodward and Bartel 2018). Additionally, Arabidopsis seeds and seedlings are small and able to numerously germinate in Petri dishes, requiring very little space even when fully developed, as well as being able to grow indoors under fluorescent lights, which may be unsuitable for other plants (Woodward and Bartel 2018; Diaz 2019). Contrary to what happens for other eukaryotic models, it is not necessary to have extensive specialized training to maintain Arabidopsis plants nor do they require much regulatory oversight (Diaz 2019). They also do not need any coculture with other species, enabling growth in aseptic conditions and maximum variable control (Woodward and Bartel 2018).

Being a multicellular differentiated and autotrophic organism, Arabidopsis provides immense chemical and enzymatic diversity, which is susceptible to research, although its genome is small (~132 Mbp), containing ~38,000 loci that include 20,000 protein-coding genes distributed among five nuclear chromosomes (Kaul et al. 2000; Cheng et al. 2017; Woodward and Bartel 2018). Moreover, Arabidopsis can tolerate a high degree of homozygosity, a feature that cannot be found in many genetic models. This is a self-fertile plant, with flowers containing both stamens and carpel. Also, the most typical features and specialized cell types of seed plants are modelled in Arabidopsis, allowing the results of research in this plant to be extended and generalised to other plants (Woodward and Bartel 2018).

Another appealing factor for Arabidopsis research, beyond the long list of available tools and techniques, is the existence of abundant bioinformatics resources and helpful curated community collections that provide mutated lines for various projects, as the Arabidopsis Biological Resource Center (https://abrc.osu.edu/), where we can find full length complementary DNAs for most genes (Yamada et al. 2003; Woodward and Bartel 2018; Diaz 2019); or the Nottingham Arabidopsis Stock Centre (http://www.arabidopsis.info), that keep sequence indexed collections of >30,000 homozygous T-DNA insertional lines (O'Malley and Ecker 2010) from numerous insertion events (Alonso et al. 2003; Woodward and Bartel 2018). For overexpression, localization, and interaction studies, there are also available collections of Arabidopsis expression vectors (Curtis and Grossniklaus 2003; Earley et al. 2006) and yeast two-hybrid vectors (Trigg et al. 2017; Woodward and Bartel 2018). Moreover, we may find a wealth of shared data available regarding Arabidopsis, that includes The Arabidopsis Information Resource (TAIR; www.arabidopsis.org), Araport (www.araport.org), and ePlant (Waese et al. 2017), as well as numerous other informational resources (Schwacke et al. 2003; Schmid et al. 2005; Kilian et al. 2007; Winter et al. 2007; Baerenfaller et al. 2008; Kim et al. 2013; Trigg et al. 2017; Hooper et al. 2017; Woodward and Bartel 2018).

However, the use of Arabidopsis as a model organism has also some disadvantages. It is not possible to embody the characteristics of all plants in one single species, although it may allow the analysis of many features for different areas of research. Arabidopsis plants do not possess all genes found in other plants nor enable the occurrence of some interesting research problems typical of other plants. Its relatively small mass per individual plant can restrain research on biochemicals that may be spars and difficult to extract or even non-existent altogether (Woodward and Bartel 2018).

1.5. Aims of the study

As a working hypothesis, this dissertation considers the possibility that the Endoplasmic Reticulum (ER) directly generates a compartment that can be identified as a recycling endosome, but which can also be placed in the vacuolar route. Therefore, our main objective is to identify a cell compartment common to both secretory and endocytic trafficking routes that would represent a link between the two pathways. Our first approach was to evaluate if defects at the ER level lead to any alterations in protein sorting. To do so, using the Nottingham Arabidopsis Stock Centre (NASC) database, we searched and selected *Arabidopsis thaliana* lines with mutations in genes leading to alterations in ER morphology. Such plants were then used for an ultrastructural characterization and for co-expression with reporter and marker proteins, such as PSI A and PSI B, to evaluate how the sorting of these proteins is affected. Both PSIs were also fused with the photoconvertible fluorescent tag mEos 3.2 to allow the dissection of the pathways previously mentioned. Lastly, the use of endosomal markers/dyes, such as FM2-10, was performed to complement the previous localization approaches. Ultimately, we expected to provide deeper knowledge on the interactions taking place among the different organelles of the endomembrane system and how protein trafficking and sorting occur within plant cells.

2. MATERIALS AND METHODS

2.1. Biological material – selection, germination, and growth conditions

Resorting to the Nottingham Arabidopsis Stock Centre (NASC), five *Arabidopsis thaliana* lines described as having defects in ER morphology or mutations in ER-resident proteins were selected for the present study (Table 2.1). Seeds from those lines, as well as a wild-type line (WT; *col0*), were sown and germinated in plates containing MS (Mourashige and Skooge, Duchefa) medium [2,2 g/L MS, 1,5 % (w/v) sucrose, 0,7 % (w/v) Bacto-agar and pH 5.7]. Before plating, seeds were sterilized in 70 % (v/v) ethanol for 5 min in agitation and left to dry onto a filter paper in the flow hood. When justified, due to contamination, another step of sterilization was added: after sterilization with 70 % (v/v) ethanol, 1 mL of a bleach solution was added to the seeds [1 % (v/v) SDS and 10 % (v/v) sodium hypochlorite]. The seeds were kept in agitation on this bleach solution for 10 min, then the solution was removed, and the seeds washed with 0.5 – 1 mL of sterile water for 3 – 4 times. About 100 µL of sterile water containing the seeds were placed directly onto the plates. Plates were then sealed with gas-permeable surgical tape. Plants were kept for 48 h at 4 °C and, after stratification, were grown under the following conditions: at 22 °C with 60 % humidity and 16h light over 8h dark photoperiod (OSRAM L 36W/77 e OSRAM L 36W/840) at the intensity of 110 µmol m^{-2} s.

After approximately 12-15 days, seedlings were transferred to individual pots with fertilized substrate (Universal substrate, SYRO PLANT) and grown under continuous light at 22 °C with 50-60 % relative humidity and light intensity at 180 µmole m^{-2} s. Upon transfer, the pots were covered for 3-5 days with plastic wrap for acclimatization. To evaluate plant development, seven stages of the chronological progression of the plants' growth were defined according to Boyes et al. (2001).

Table 2.1 – List of selected *Arabidopsis thaliana* lines used.

NASC code	Name	Obtained from
N68719	*syp22-1 syp23 or vam3-1 plp*	(Shirakawa et al. 2010)
N68909	*sec24a-2*	(Qu et al. 2014)
N69075	*nai GFP-h*	(Matsushima et al. 2004)
N69077	*nai2-2*	(Yamada et al. 2008)
N69081	*leb-2 GFP-h*	Unpublished

2.2. Constructs generation through Molecular Biology Tools

In the literature, the available data regarding our selected Arabidopsis lines do not focus on how protein sorting is affected by the defects in ER morphology. Thus, such

plants were used for co-expression of constructs harbouring fusions of PSI A and PSI B to mEos 3.2. These constructs were obtained by cloning the corresponding genes in a suitable vector (pMDC83), through PCR and Gibson Assembly techniques. The mEos 3.2 tag, an improved version of EosFP, is a photoconvertible protein that emits strong green fluorescence (516 nm) that changes to red (581 nm) upon near-UV irradiation at ~390 nm (Wiedenmann et al. 2004; Zhang et al. 2012), allowing the *in vivo* visualization of the PSIs localization along with their route by following the protein produced *de novo*.

2.2.1. DNA Amplification

Plasmids [pMDC83 (Supplementary figure 7.1)] and cDNAs (Table 2.2) to be used were available at the laboratory and maintained in *Escherichia coli* DH5α glycerol stocks. Plasmids were extracted from *E. coli* using the *Illustra plasmidPrep Mini Spin Kit* (GE Healthcare Life Sciences), following the manufacturer's instruction, except for the final elution volume that was 30 µL.

Table 2.2 – List of cDNAs used.

cDNAs used	Obtained from
pMDC83::SP::PSICardA::mCherry	Unpublished
pMDC83::SP::PSICardB::mCherry	Unpublished
mEos3.2-N1	Adgene

The strategy was to replace the fluorescent protein mCherry with mEos3.2 in both cDNAs containing the PSIs (Table 2.2) and to combine the new constructs using Gibson Assembly technique (Gibson et al. 2009). To do so, pMDC83::SP::PSICardA::mCherry, pMDC83::SP::PSICardB::mCherry and mEos3.2 were amplified with specific primer pairs (Table 2.3) harbouring adapters with overlaps in both N- and C-terminal sequences, allowing cloning by Gibson Assembly. By using such primers, three fragments from each cDNA (pMDC83::SP::PSICardA::mCherry and pMDC83::SP::PSICardB::mCherry) were obtained for Gibson Assembly (Figure 2.1).

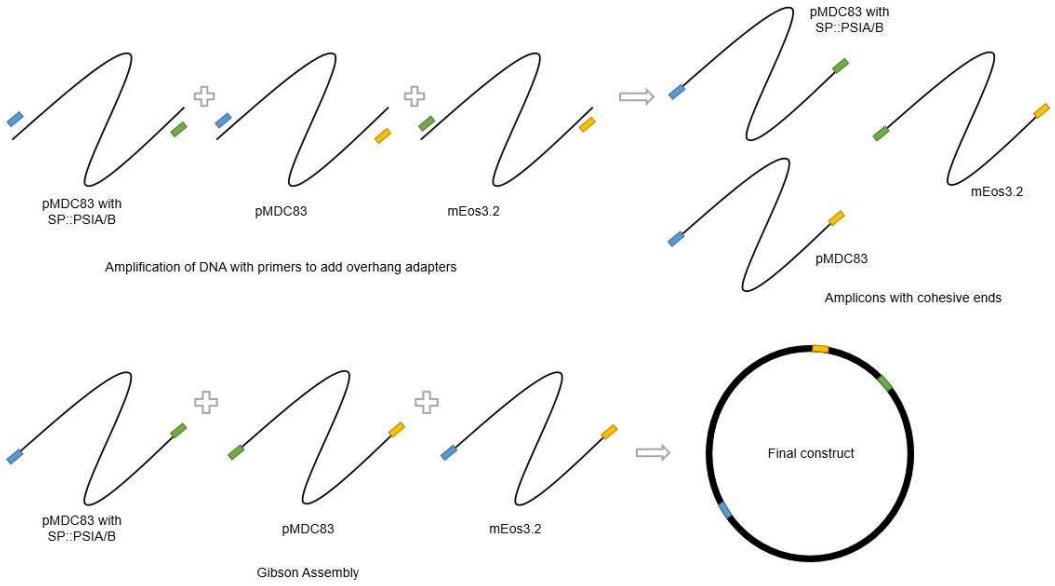


Figure 2.1 – Schematic representation of Gibson Assembly reactions. DNA sequences represented in blue, yellow, and green facilitate recombination of amplicons with the result being a complete plasmid, through the action of the enzymes DNA ligase, DNA polymerase and exonuclease.

Table 2.3 – Primers used for Gibson Assembly and primers for sequencing.

Fragment	Primer	Sequence (5' - 3')	Product size
mEos 3.2	mEos overlap with PSI fw	TGGTGCGTCGACAATGAGTGCGATTAAGCCAG	706 bp
	mEos overlap with pMDC rv	CTGAGCTCGGATCCTTATCGTCTGGCATTGTCAG	
pMDC83 SP PSIA	pMDC overlap with mEos fw	ATCGCACTCATTGTCGACGCACCACCTGCA	6972 bp
	pMDC kan rv	CAAAGCCCTGAAAAGATTATCGAGCTGTATGCG	
pMDC83 mCh A	pMDC kan fw	CGCATACAGCTCGATAATCTTTTCAGGGCTTTG	3461 bp
	pMDC overlap with mEos rv	GCCAGACGATAAGGATCCGAGCTC	
pMDC83 SP PSIB	pMDC overlap with mEos fw	ATCGCACTCATTGTCGACGCACCACCTGCA	6972 bp
	pMDC kan rv	CAAAGCCCTGAAAAGATTATCGAGCTGTATGCG	
pMDC83 mCh B	pMDC kan fw	CGCATACAGCTCGATAATCTTTTCAGGGCTTTG	3461 bp
	pMDC overlap with mEos rv	GCCAGACGATAAGGATCCGAGCTC	
	M13 rv	CAGGAAACAGCTATGAC	
	PSIA rv	GGATAAGTGTTCACACAACTC	
	PSIB rv	TTCTGCACTTGAAGTGGGTA	

For amplification, *Phusion High-Fidelity PCR Master Mix with HF Buffer* (Thermo Scientific™) and *Platinum SuperFi PCR Master Mix* (Invitrogen by Thermo Fisher Scientific) were used following the PCR reaction mix and PCR program described in Table 2.4 and Table 2.5, respectively.

Table 2.4 – Component mix for PCR reactions using Phusion High-Fidelity PCR Master Mix with HF Buffer (Thermo Scientific™) and Platinum SuperFi PCR Master Mix (Invitrogen by Thermo Fisher Scientific).

Enzyme	Components	Concentrations	Volume
Phusion High-Fidelity	H_2O	-	21.5 µL
	Phusion Master Mix	1x	25 µL
	Primer Forward	0.5 µM	1.25 µL
	Primer Reverse	0.5 µM	1.25 µL
	DNA template	10 ng	1 µL
	Final Volume	-	50 µL
Platinum SuperFi	H_2O	-	3.6 µL
	SuperFi Master Mix	1x	10 µL
	Primer Forward	0.5 µM	1 µL
	Primer Reverse	0.5 µM	1 µL
	DNA template	10 ng	0.4 µL
	DMSO	20%	4 µL
	Final Volume	-	20 µL

Table 2.5 – Program for PCR reactions using Phusion High-Fidelity PCR Master Mix with HF Buffer (Thermo Scientific™) and Platinum SuperFi PCR Master Mix (Invitrogen by Thermo Fisher Scientific).

Enzyme	Steps		Temperature	Time
Phusion High-Fidelity	Initial denaturation		98 °C	30 seconds
	35x	Denaturation	98 °C	10 seconds
		Annealing	56°C	30 seconds
		Extension	72 °C	30 seconds/kb
	Final extension		72 °C	10 minutes
	Hold		6 °C	∞
Platinum SuperFi	Initial denaturation		95 °C	5 minutes
	35x	Denaturation	95 °C	30 seconds
		Annealing	56 °C	30 seconds
		Extension	72 °C	30 seconds/kb
	Final extension		72 °C	10 minutes
	Hold		6 °C	∞

After amplification, the PCR products were verified by separation in a 1 % (w/v) agarose gel prepared in 1x TAE (4.84 g Trizma Base (Sigma), 1.14 mL de acetic acid (Merck) and 20 mL EDTA 0,5M (Pharmacia biotech) for 1 L of distilled water) with GreenSafe Premium (NZYTech). Before loading in gel, DNA Gel Loading Dye (6X) (Thermo Scientific™) was added to each sample and GeneRuler DNA Ladder Mix (Thermo Scientific™) was used as a molecular weight marker. Separation of amplified DNA fragments was done through electrophoresis in a horizontal electrophoresis system (Horizon 58, Life Technologies) at 100 V for 25-35 min, in 1x TAE. Then, PCR products were purified using the *GeneJET Gel Extraction and DNA Cleanup Micro Kit* (Thermo

Scientific™) in accordance with the manufacturer's guidelines and quantified using 1 µL of DNA in a DS-11 Spectrophotometer/Fluorometer (DeNovix).

2.2.2. Gibson Assembly Cloning

To combine the PSIs with mEos3.2, amplified fragments were cloned as represented in Figure 2.1 through Gibson Assembly. The reaction components were mixed as outlined in Table 2.6 and the reaction tube was transferred to a 50 °C preheated thermocycler block and incubated for 1 h (Gibson et al. 2009).

Table 2.6 – Gibson Assembly Reaction Mix. The 5x IRB is composed of 25% (w/v) PEG-8000, 500 mM Tris·HCl pH 7.5, 50 mM $MgCl_2$, 50 mM DTT, 1 mM each of the four dNTPs and 5 mM NAD.

Components	Volume
DNA to assemble	Equimolar volume based on quantification
5x IRB	4 µL
Taq DNA Ligase (NEB)	2 µL
Phusion HF DNA Polymerase (Thermo Fisher)	0.25 µL
T5 Exonuclease (NEB)	0.25 µL (prediluted 1:30 in 1x IRB)
H_2O	Make up to a total volume of 20 µL

2.2.3. Preparation of electrocompetent *Escherichia coli* cells

For this study, the bacterial strain *Escherichia coli* DH5α was used as a cloning strain. To prepare electrocompetent cells, E. coli colonies were grown in a plate of Luria Broth medium (LB) 1.5 % (w/v) agar at 37 °C over night, without agitation. Then, in 50 mL falcons, two pre-cultures of 5 mL of liquid LB medium were inoculated each with one colony and allowed to grow at 37 °C for another 16-18 h, with agitation. These pre-cultures were transferred to 500 mL flasks for inoculation of 200 mL of liquid LB medium and incubated for about 3-4 h at 37 °C, with agitation, until an OD600 of 0.5-0.7 was reached. Meanwhile, 0.5 L and 5 mL of 10 % (v/v) glycerol were placed on ice for at least 1 h. The 200 mL cultures were divided into four 50 mL falcons each and centrifuged for 10 min at 2500 x g at 6 °C. The supernatant was discarded, and each pellet was resuspended in 25 mL ice-cold 10 % (v/v) glycerol by pipetting up and down, keeping the tube on ice. The cultures were then combined into two tubes, for a total of four tubes of 50 mL. A centrifuge was performed as before (10 min at 2500 x g at 6 °C), the supernatant was discarded, and the pellets were resuspended in 50 mL ice-cold 10 % (v/v) glycerol. One more centrifugation was done (10 min at 2500 x g at 6 °C), the supernatant was discarded, and the pellets were resuspended in 25 mL ice-cold 10 % (v/v) glycerol. Finally, the cell suspension was centrifuged for 10 min at 2500 x g at 6 °C. The supernatant was discarded, and the pellets were resuspended in 1 mL ice-cold 10 % (v/v) glycerol. Once resuspended, the pellets were aliquoted into 50 µL in the iced-cold Eppendorf tubes and stored at -80 °C.

2.2.4. Preparation of electrocompetent *Agrobacterium tumefaciens* cells

In this study, the bacterial strain *Agrobacterium tumefaciens* GV3101 was used for plant transformation. One aliquot of *A. tumefaciens* was inoculated in 5 mL of liquid LB medium with Gentamicin (50 µg/mL) and allowed to grow up to saturation at 28 °C, with agitation. Once grown, the pre-culture was transferred to 200 mL of liquid LB medium with Gentamicin (50 µg/mL) and this culture was grown until the OD600 of 0.5-0.6 at 28 °C, with agitation. When the OD600 was reached, the culture was cooled on ice for 30 min to 1 h. Meanwhile, 200 mL of 1 mM HEPES buffer were prepared, as well as 10 mL of 1 mM HEPES buffer with 10 % (v/v) glycerol and both solutions were left to cool on ice. From this point forward, all solutions were kept on ice as much as possible. The 200 mL culture was divided into four 50 mL falcon tubes and centrifuged for 10 min at 2500 x g at 4 °C. The supernatant was discarded, each pellet was resuspended in 25 mL of ice-cold 1 mM HEPES buffer by gently pipetting up and down, and the cultures were combined into two tubes. One more centrifugation was performed as before (10 min at 2500 x g at 4 °C). Again, the supernatant was discarded, and each pellet was resuspended in 25 mL of ice-cold 1 mM HEPES buffer. Another centrifugation was done as before (10 min at 2500 x g at 4 °C), the supernatant was poured off, and each pellet was resuspended in 20 mL of ice-cold 1 mM HEPES buffer with 10 % (v/v) glycerol. One final centrifugation was done (10 min at 4800 rpm at 4 °C), the supernatant was discarded, and each pellet was resuspended in 500 µL of ice-cold 1 mM HEPES buffer with 10 % (v/v) glycerol. At this point, the cells were ready to be aliquoted into 50 µL in ice-cold Eppendorf tubes and stored at -80 °C.

2.2.5. Bacteria transformation by electroporation

Both constructs (pMDC83::SP::PSIA::mEos3.2 and pMDC83::SP::PSIB::mEos3.2) were transformed into electrocompetent *E. coli* before being used to transform electrocompetent *A. tumefaciens*.

To transform *E. coli*, 50 µL of competent cells were gently mixed with 5 µL of each product of the Gibson Assembly reaction, after being on ice for about 5 min. This mixture was then transferred to an electroporation cuvette that was placed in the MicroPulser ™ electroporator (BioRad) where an electrical shock was delivered to the cells. Then, 1 mL of liquid LB medium was immediately added, and cells were transferred to a 1.5 mL centrifuge tube and incubated for 45 min at 37 °C, without agitation, for cell recovery. After this, the tubes were centrifuged for 2 min at 3,500 x g and 100 µL of transformed cells were spread onto LB 1.5 % (w/v) agar plates with the appropriate antibiotics

[Kanamycin (50 µg/mL)]. For the transformation of the *A. tumefaciens*, the steps were taken as described above, apart from the cell recovery that lasted for 4 h at 28 °C and the final plating step, where the cells were spread onto in LB 1.5 % (w/v) agar plates with Kanamycin (50 µg/mL) and Gentamicin (50 µg/mL).

2.2.6. Screening of positive clones

After transformation of *E. coli* cells, positive colonies were screened through enzymatic restriction. For this, 1 isolated colony was inoculated in 10 mL of liquid SOB medium [20 g/L tryptone, 5 g/L yeast extract, 0.5 g/L NaCl and, after autoclaving, 10 mL/L $MgCl_2$ 1M and 10 mL/L $MgSO_4$ 1M] with the appropriate antibiotics [Kanamycin (50 µg/mL)] in 50 mL falcons, for better aeration of the culture. These cultures were incubated overnight at 37 °C with agitation (200 rpm). Extraction from liquid cultures of bacterial plasmid DNA was performed using the *PlasmidPrep Mini Spin Kit* (GE Healthcare Life Sciences) following the manufacturer's instructions, except for the final elution volume (30 µL). The obtained plasmid DNA was then quantified resorting to DS-11 Spectrophotometer/Fluorometer (DeNovix). Positive clones were firstly screened through enzymatic restriction with EcoRI (Anza ThermoFisher). The reaction mixture was assembled as described in Table 2.7 and the reaction occurred at 37 °C for 20 min. Separation of obtained DNA fragments was done through electrophoresis in a horizontal electrophoresis system (Horizon 58, Life Technologies) at 100 V for 25-35 min, in 1x TAE. The constructs were also confirmed by DNA sequencing (Eurofins Genomics, Germany) and the sequencing data were analysed using SnapGene software (https://www.snapgene.com/). The confirmed positive cultures were aliquoted and stored in 25 % (w/v) glycerol (Sigma-Aldrich) at -80 °C.

Table 2.7 – Reaction mixture of enzymatic restriction for screening of positive clones.

Components	Volume
Enzyme	1 µL
Reaction Buffer	2 µL
DNA template	5 µL
H_2O	Make up to a total volume of 20 µL

2.3. Transmission Electron Microscopy

2.3.1. Chemical Fixation for Epoxy Resin Embedding

For this procedure, leaves from seedlings (12-15 days old) and mature plants of *A. thaliana* ER-defective lines and wild-type control were grown as described in section 2.1. Each leaf was cut into smaller pieces of approximately 1-2 mm and fixated in Na-PIPES 1.25 % (p/v) pH 7.2 and Glutaraldehyde 2.5 % (v/v) for 1 h at room temperature (RT).

Then, the samples were washed three times for 10 min each with Na-PIPES 2.5 % (p/v) pH 7.2, after which they were post-fixated with OsO_4 4 % (p/v) solution, previously prepared in Na-PIPES 2.5 % (p/v) pH 7.2 in a proportion of 1:1, for 1 h at RT. Post-fixation was followed by three washes with Na-PIPES 2.5 % (p/v) pH 7.2 for 10 min each. After these washes, proceeded the dehydration steps in an ethanol graded series at room temperature as follows: 10 % (v/v) for 10 minutes; 20 % (v/v), 30 % (v/v) and 50 % (v/v) for 15 minutes; and 70 % (v/v) and 100 % (v/v) for 20 minutes. Finally, the biological material was incubated in propylene oxide for 20 min.

For embedding, 100 mL of EPON resin (Agar Scientific) was prepared, for which 48 mL of the resin were mixed with 52 mL of MNA (Agar Scientific) and kept in agitation for 20 min. Then, 2 mL of DMP-30 (Agar Scientific) were added, and the mixture was kept in agitation for another 20 min. Once the EPON resin was ready to be used, 10 % resin and 90 % propylene oxide were mixed and added to the biological material and incubated for 15 min. Subsequently, drops of resin were added over time until the proportion of resin:propylene oxide was 50:50. The samples were incubated in such mixture overnight. On the following day, the mixture of resin and propylene oxide was removed and substituted by pure resin until the next day. After the embedding, the samples were transferred to orientated moulds covered in EPON resin. The moulds were polymerized at 60 °C overnight.

2.3.2. Block Sectioning

The sectioning of the EPON resin blocks was performed using a diamond knife (Diatome) in an Ultracut UC6 (Leica) ultramicrotome. Ultrathin sections of about 60-80 nm were obtained and placed in 400 mesh copper grids. Before placing the ultrathin sections, the grids were treated with acetone and let dry on a filter paper.

2.3.3. Post-Staining

Ultrathin sections on grids were post-stained with Uranyless EM Stain (Uranyless) for 5 min and washed by immersing them in distilled water several times, followed by Reynolds Lead citrate 3 % (Uranyless) for 5 min and washed again as before. Finally, the grids were dried on a filter paper before observation.

2.3.4. Transmission Electron Microscopy observations

After contrast, the grids containing ultrathin sections of leaves from seedlings and mature plants of *A. thaliana* ER-defective lines were observed using a Transmission Electron Microscope (TEM – Jeol JEM 1400) and the images were acquired by an Orius® SC200D camera. Image analysis and processing were done using ImageJ®/Fiji software.

2.4. Vacuum infiltration for transient transformation of *Arabidopsis thaliana* seedlings

For transient transformation of our *A. thaliana* ER-defective lines (Table 2.1) by vacuum infiltration, we adapted the protocol established by (Bernat-Silvestre et al. 2021). The constructs used were the following: two constructs harbouring fusions of both PSI A and B to mCherry; one construct harbouring the endoplasmic reticulum marker GFP::HDEL; and two more with both PSIs fused to mEos 3.2.

2.4.1. Seedlings' growth conditions

Seeds from *A. thaliana* mutated lines and wild-type line were sown and germinated in six well plates containing MS medium [2,2 g/L MS, 1,5 % (w/v) sucrose, 0,7 % Bacto-agar (w/v) and pH 5.7]. A small circle of sterilized 100 µm nylon mesh was placed over the solidified medium the help separate the seedlings upon germination. Before plating, seeds were sterilized in 70 % (v/v) ethanol for 5 min in agitation and left to dry onto a filter paper in the flow hood. When this sterilization was not enough and there was some contamination on the plates, after this first step, the ethanol was removed and a bleach solution (10 % (v/v) sodium hypochlorite and 0.25 % (w/v) SDS) was added to the seeds. The seeds were kept in this solution for 10 min in agitation. Then, the bleach solution was removed, and the seeds were washed 3-6 times in sterile water. Afterwards, the seeds were suspended in 0.5-1 mL of sterile water and poured onto the plates. Once the seeds were sowed, plates were then sealed with gas-permeable surgical tape and kept in for 48 h at 4 °C. After stratification, plants were grown for 5 days under the following conditions: at 22 °C with 60 % humidity and 16h light over 8h dark photoperiod (OSRAM L 36W/77 e OSRAM L 36W/840) at the intensity of 110 µmol m^{-2} s.

2.4.2. *Agrobacterium tumefaciens* culture preparation

One aliquot of *A. tumefaciens* harbouring each construct of our interest was inoculated in 10 mL of LB medium with the appropriate antibiotics [Kanamycin (50 µg/mL) and Gentamicin (50 µg/mL)] and incubated for 24 h in agitation at 28 °C. This allowed the culture to reach an OD600 of 2.2, approximately.

2.4.3. Preparation of *A. tumefaciens* suspension for infiltration

After checking that the OD600 of the *A. tumefaciens* culture was about 2.2, the remaining culture was centrifuged for 15 min at 6,000 x g at room temperature. The supernatant was removed, and the pellet resuspended in liquid MS medium [2,2 g/L MS, 1,5 % (w/v) sucrose and pH 5.7]. Then, the OD600 of this bacterial suspension was measured in a 1:20 dilution. The bacterial suspension was diluted with infiltration buffer

(liquid MS medium at RT with 0.005 % (v/v) Tween and 200 µM acetosyringone) to an OD600 of 2.2 to improve the transfection efficiency. This last suspension was kept at room temperature for 30-45 min, so the acetosyringone was assimilated by the bacteria and its virulence genes were activated.

2.4.4. Agroinfiltration of the *A. thaliana* seedlings

For the infiltration, the *A. tumefaciens* suspension in infiltration buffer was poured onto the six well plates with the *A. thaliana* seedlings (4 mL per well), so all the seedlings were completely covered. The plates were placed individually and opened into the vacuum desiccator and vacuum was applied at 300 mbar for 1 min. After this, the pressure was slowly increased to 400 mbar and vacuum applied for another minute. Once this was done, all bacterial suspension was removed carefully to avoid any contamination. The plates were reclosed with gas-permeable surgical tape and covered with aluminium foil for 45 min to 1 h to improve agroinfection. The aluminium foil was then removed, and the plates were kept for 3 days under the previously mentioned growth conditions before observation and image acquisition with a Confocal Laser Scanning Microscope.

2.5. Agrobacterium-mediated Infiltration of *Arabidopsis thaliana* and *Nicotiana tabacum* Leaves

Before infiltrating *A. thaliana* seedlings by vacuum with the constructs of our interest, these constructs were tested in both *A. thaliana* and *N. tabacum* leaves. For this assay, *A. thaliana* plants were grown as described in 2.1. *N. tabacum* plants were sown directly on fertilized substrate (Universal substrate, SYRO PLANT) and grown under continuous light at 22 °C with 50-60 % relative humidity and light intensity at 180 µmole m^{-2} s.

The bacterial cultures were previously prepared as described in section 2.4.2. Once ready, 1mL of each culture was transferred to a sterile 1.5 mL centrifuge tube and spun for 1 min at maximum speed. The supernatant was discarded. Then, 1 mL of 1x infiltration buffer was used to resuspend the pellet. The infiltration buffer had been previously prepared as follows: for 40 mL of 10x buffer, 4.26 g MES, 2.0 g glucose and 0.304 g $Na_3PO_4.12H_2O$ pH 5.6 (with 10 M NaOH) and divided into 5 mL aliquots stored at -20 °C. After the resuspension in the buffer, the samples were recentrifuged as before and the supernatant discarded. At this point, 100 µM acetosyringone was added to the 1x infiltration buffer, to increase the *A. tumefaciens* virulence, and 1 mL of this was used to resuspend the pellet. In an appropriate cuvette, a dilution 1:5 of the cell suspension from each sample was prepared and the OD600 was measured. After this, the mixtures for infiltration were prepared using the following equation: (desired OD600 / dilution

OD600) x 1000 = required volume (µL) of the dilution to prepare 1 mL of infiltration mixture. The OD600 used was 0.3. Once the mixtures were prepared, infiltration was performed: resorting to a 1 mL capacity syringe without needle, and adjusting the pressure applied with the syringe on the lower epidermis, a tobacco or Arabidopsis leaf was infiltrated until the liquid entered through the stomata and infiltrated in the intercellular spaces. The plants were kept under the previously mentioned growing conditions for 3 days, before observation and image acquisition with a Confocal Laser Scanning Microscope.

2.6. Cell imaging

2.6.1. Confocal Laser Scanning Microscopy Analysis

After infiltrating the *A. thaliana* seedlings by vacuum (section 2.4.) and the *A. thaliana* and *N. tabacum* leaves (2.5.), cells expressing our constructs of interest [fusions of PSI-A and PSI-B with mEos 3.2 and mCherry as well as an ER marker (GFP-HDEL)] were observed and analysed using a Confocal Laser Scanning Microscope (CLSM, Leica STELLARIS 8). Cotyledons from *A. thaliana* seedlings or a small section of the infiltrated leaf of *A. thaliana* and *N. tabacum* were prepared for observation by placing the biological material on a slide with a drop of sterile water covered by a cover slip. In all situations the lower epidermis was observed. For mCherry, using 561 nm excitation, the emission was detected between 580-630 nm. In the case of GFP, the excitation used was 488nm and the emission was detected between 500-528 nm. Analysis of the obtained images was performed using the ImageJ®/Fiji software.

2.6.2. Drug Treatment Assays

After infiltrating *A. thaliana* seedlings with *A. tumefaciens* expressing our constructs of interest as described in section 2.4. and before imaging with CLSM, the seedlings were re-infiltrated with Brefeldin A (BFA), that suppresses the recruitment of COPI coat proteins onto Golgi membranes resulting in a fusion of most Golgi cisternae directly to the ER culminating in the formation of an ER-Golgi hybrid compartment (Nebenführ et al. 2002).

Similarly, to what was done with the *A. tumefaciens*, a BFA solution (50 µg/mL) was prepared in MS liquid medium and 4 mL per well were poured over the infiltrated seedlings, so they were completely covered. Vacuum was applied as previously described (2.4.4.). Seedlings were kept in the BFA solution for about 16-18 h and the cells were imaged through CLSM. The BFA solution was applied to the seedlings one day after the *A. tumefaciens* infiltration.

2.6.3. FM2-10 staining

Two days after infiltrating the *A. thaliana* mutated lines with the PSIs, such seedlings were re-infiltrated with the endosomal marker FM2-10. A solution of FM2-10 dye (1 μM) was prepared in MS liquid medium and the *A. thaliana* seedlings expressing our constructs of interest were kept in this solution 2-3 h before imaging the cells through CLSM. As performed for the A. tumefaciens infiltration, 4 mL of the dye solution was poured over the seedlings and vacuum was applied as described in section 2.4.4. In this assay, the lines N69075 (*nai GFP-h*) and N69081 (*leb-2 GFP-h*) were not used since they stably express a GFP marker that would make the detection of the FM dye impossible.

2.7. Secretion Assays

2.7.1. Extraction of extracellular proteins

Extracellular proteins samples were obtained after growing the *A. thaliana* seedlings and infiltrating them as described in section 2.4., for this assay, the same seedlings were infiltrated with BFA 2 days after *A. tumefaciens* infiltration and kept in BFA solution for 16-18h. Control and BFA-infiltrated seedlings were cut into thin strips, placed into small Petri dishes, and incubated in 10x extraction buffer (1M NaCl, 40 mM HEPES pH 7.0, 5 mM DTT and 2 mM EDTA) in agitation (120 rpm) for 6 h at room temperature in the dark. It was used 1 mL of buffer per 100 mg of seeding tissue. After incubation, the buffer was collected with a disposable pipette and filtered to a new plate with a 100 μM nylon mesh. Then, this medium containing the secreted proteins was distributed to sterile 1.5 mL centrifuge tubes (1 mL of medium per tube) and centrifuged at 13,000 x g for 10-15min at 4 °C. The supernatant was collected to new centrifuge tubes and kept at -20 °C until further TCA precipitation.

2.7.2. TCA precipitation

The centrifuge tubes containing the secreted proteins were defrosted, 1 mL of 20 % (w/v) Tri-chloroacetic acid (TCA) was added per mL of medium and the tubes were vortexed for 15 sec. These were kept on ice for 15 min before being centrifuged at 13,000 x g for 15 min at 4 °C. The supernatant was pipetted off and discarded. Then, 1 mL of ice-cold acetone was added, and the tubes were centrifuged as before. This wash with acetone was repeated once more and the pellet was left to air-dry. When fully dried, the pellet was resuspended 40 μL of extraction buffer (section 2.7.1.) and the samples were quantified using 2 μL of sample in a DS-11 Spectrophotometer/Fluorometer (DeNovix). Once quantified, 5x SDS-PAGE sample loading buffer (Nzytech) was added to the

samples and boiled at 95 °C for 5 min. After this, the protein extracts were centrifuged for 2 min at top speed and then stored at -20 °C until use.

2.7.3. Discontinuous denaturing Gel Electrophoresis

For the analysis of extracellular proteins samples, a vertical electrophoresis on a discontinuous polyacrylamide gel under denaturing conditions was conducted. To do so, after the electrophoresis apparatus (BioRad) was assembled, a 12 % acrylamide running gel was prepared [2.1 mL distilled deionized water, 1.5 mL of polyacrylamide (40 % acrylamide/bisacrilamide solution - BioRad), 1.3 mL 1.5 M Tris pH 8.8, 50 µL 10 % (w/v) SDS, 50µL 10 % (w/v) APS and 2 µL of TEMED (N, N, N', N'-Tetramethylethylenediamine - Sigma)]. This gel mixture was transferred into the gap between the glass and the plate, avoiding the formation of bubbles. Isopropanol was added on top of the running gel to allow polymerization and to help with levelling of the gel surface. Once the gel was polymerized, the isopropanol was removed, and the gel surface was washed with distilled and deionized water. Then, a 4 % acrylamide stacking gel was prepared [2.472 mL distilled deionized water, 375 µL of polyacrylamide (40 % acrylamide/Bis Solution - BioRad), 130 µL 0.5 M Tris pH 6.8, 10 µL 10 % (w/v) SDS, 10 µL 10 % (w/v) APS and 3 µL mL of TEMED (N, N, N', N'-Tetramethylethylenediamine - BioRad)]. Immediately after removing the isopropanol solution and washing the gel surface with distilled water, the stacking gel was pipetted carefully onto the running gel and the comb placed so the stacking gel could polymerize. The comb was removed after placing the gel in running buffer for SDS-PAGE [165 mM Trizma base, 128 mM glycine and 1 % (w/v) SDS].

Protein samples were prepared as previously described in section 2.7.2. After being defrosted, the samples were incubated at 65 °C for 5 min and centrifuged at maximum speed for 2 min immediately before being applied to gel. As protein weight marker the PageRuler Plus Prestained Protein Ladder (Thermo Fisher) was used. Electrophoresis was conducted in running buffer for SDS-PAGE at 100-150 V until the blue colour of the SDS-PAGE ran out of the gel.

2.7.4. Western Blot

For band visualisation western blots were performed. Once the electrophoresis was finished, the gel was taken from the support, the stacking gel cut off and the remaining was incubated in transfer buffer [25 mM Tris, 192 mM Glycine, 20 % (v/v) methanol]. The nitrocellulose membrane (Protran nitrocellulose Hybridization Transfer Membrane, 0.2 mM - Schleicher and Schuell) and two portions of 3MM paper were cut with the dimensions of the gel and soaked in transfer buffer. The transfer unit (Omnipage mini,

Cleaver Scientific) was assembled for the blotting following the manufacturer's instructions. The unit was filled with transfer buffer until the membrane-gel cassette was completely covered. Transfer was performed at 100 V for 1 h, with refrigeration and constant stirring, so the buffer's temperature could be kept evenly cold. After the transfer, the membrane was rinsed for 2 min in TBS-T [50 mM Tris, 200 mM NaCl, 0.1 % (v/v) Tween 20], so any trance of methanol was washed. Then, the membrane was transferred to the blocking solution [5 % (w/v) skim milk and 0.5 % (v/v) Tween-20 in TBS-T] and incubated for 30 min at room temperature in agitation. The primary antibodies Polyclonal Anti-mCherry Antibody (Merk Millipore) and H3 Histone 3 core Monoclonal Antibody (Agrisera) were diluted (1:1000 and 1:5000, respectively) in blocking solution and the incubation was performed at 4 °C overnight with agitation. After this, the membrane was washed in TBS-T for 10 min and two more times also in TBS-T for 5 min. The incubation with the secondary antibodies Goat Anti-Rabbit IgG Antibody (H+L) HRP Conjugate and Goat Anti-Mouse IgG (H+L) HRP Conjugate (BioRad), diluted in TBS-T (1:2500 and 1:500, respectively), occurred at room temperature for 1 h in agitation. Then, the membrane was washed three times, as previously described. One final wash in water was performed. The visualization of the bands was carried out using the Clarity ECL Western Blotting Substrate Kit (BioRad), following the manufacture's instruction, and the imaging was done through digital visualization with ChemiDoc XRS+ System (BioRad). The analysis of the collected images was performed using the ImageJ® software.

3. RESULTS

3.1. Characterization of *Arabidopsis thaliana* ER-defective plants

3.1.1. Developmental assays of ER-defective lines

As we started our work with the selected *A. thaliana* mutated lines (Table 2.1) by growing the plants, we noticed some developmental differences between the mutated lines and the control (WT line). Therefore, a developmental assay was conducted and seven stages of the chronological progression of the plants' growth were evaluated. All plants were grown under the same conditions, after sustaining 48 h of seed inhibition. As it is demonstrated in Figure 3.1, the *nai2-2*, *seca24a-2*, *nai GFP-h* and *leb-2 GFP-h* mutated lines accompanied the WT growth, with little differences in timing observed. However, the delay in growth relative to the WT line was more pronounced in the *syp22-1 syp23* mutant, as this was the last line to present the first siliques, and this delay started at the emergence of the first flower buds (Figure 3.1, stage 5, dark orange lines).

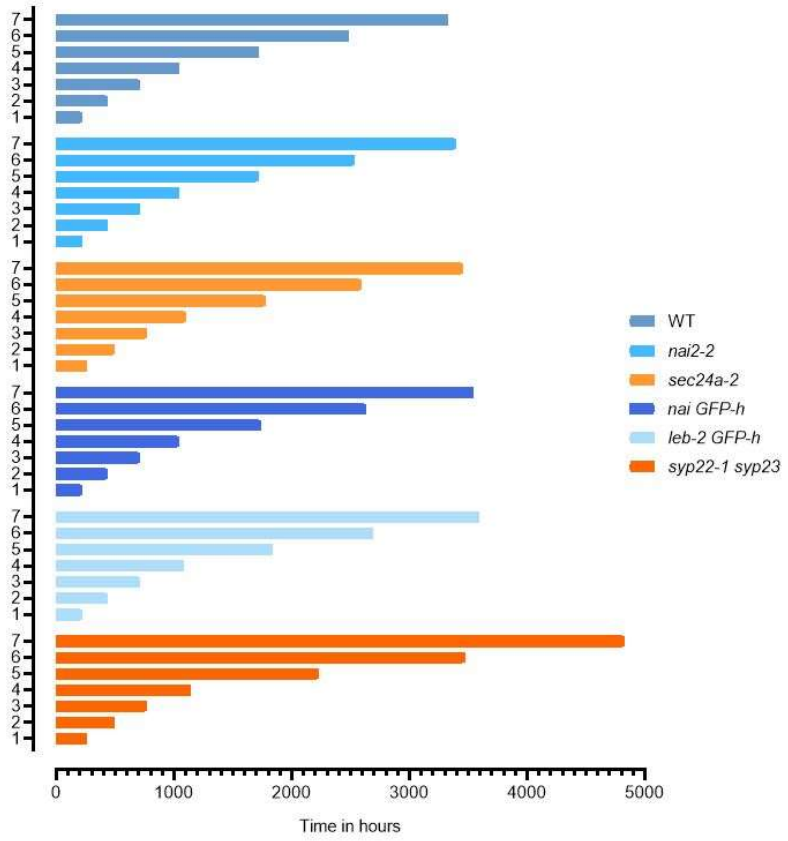


Figure 3.1 – Chronological progression indicating the main growth stages of *A. thaliana* mutated and wild-type lines. Time of growth was measured in hours. (1) Cotyledons fully opened; (2) Two rosette leaves; (3) Three rosette leaves; (4) Four rosette leaves; (5) First flower buds visible; (6) First flower open; (7) Presence of first siliques.

3.1.2. TEM imaging

To further characterize and understand the changes in the endomembrane system of the mutated lines, the ultrastructure of the cells was assessed through TEM, as described in section 2.3., allowing a deeper knowledge on the effects of these mutations in Arabidopsis. Special focus was given to the ER and associated vesicles, and to the Golgi, to detect subtle phenotypes in these organelles, as well as any other distinguishing phenotypic trait, since the provided description of the mutated lines did not include the ultrastructure. The wild-type line was used as the control and represents the normal organization of the cell. Two different tissues were analysed (seedling and mature leaves) to give a perspective of development, as one (seedling leaves) is of an early stage of growth of the plant and the other (mature leaves) represents the later stages. The images obtained may be found in Figure 3.2, Figure 3.3, Figure 3.4, Figure 3.5, Figure 3.6 and Figure 3.7.

As expected, the wild-type line presented a normal organization of the cell organelles, with organized chloroplasts in both analysed tissues, some vesicles present in the cytoplasm and normal ER tubules (Figure 3.2, red arrows). Generally, normal chloroplast shape and thylakoid formation, with the proper thylakoid ultrastructure organization in grana stacks and stroma lamellae and abundant starch granules in the stroma, were observed. Moreover, the cell's cytoplasm was rich in ribosomes and/or polyribosomes and vesicles were found in the chloroplasts in seedling leaves, as well as cytoplasmic invagination (Figure 3.2, orange arrows).

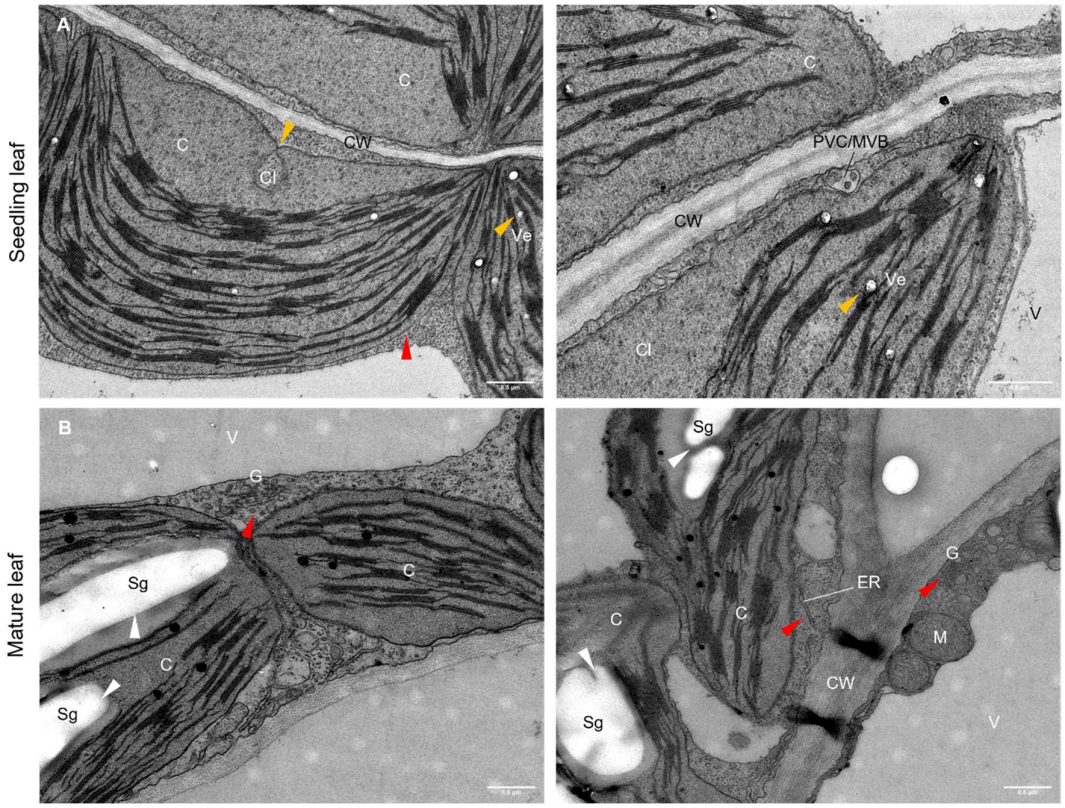


Figure 3.2 – Ultrastructure of cells from *Arabidopsis thaliana* wild-type line, in seedling leaf (A) and mature leaf (B). The most relevant organelles are evidenced and labelled. Red arrows indicate important organelles, white arrows indicate the starch granules and orange arrows indicate other relevant details of the cell's ultrastructure. Scale bars: 0.5 µm or 100 nm. Images were analyzed and processed using ImageJ/Fiji software. Abbreviations: C, chloroplasts; CI, cytoplasmic invagination; CW, cell wall; ER, endoplasmic reticulum; M, mitochondria; PVC/MVB, pre-vacuolar compartment/multivesicular body; Sg, starch granules; V, vacuole; Ve, vesicles.

In the *syp22-1 syp23* mutant, similarly to what was observed for the wild-type line, the starch granules were only observed in the mature leaf tissue (Figure 3.3, white arrows). However, the chloroplasts in the seedling leaves of this mutant were still at an early stage of development, compared to those of the wild-type with the same age, as their grana were still disorganized (Figure 3.3-A, red arrows). In the mature leaves of this line, the chloroplasts were more organized (Figure 3.3-B). One intriguing feature of this line was the enlarged cisternae of the Golgi apparatus in both seedling and mature leaves (Figure 3.3, red arrow). Moreover, several vesicles were observed in the cytoplasm and, apparently, in an unusual amount, as well as very close to the chloroplast (Figure 3.3, orange arrows). Another interesting aspect of this mutant is the density of the cell's cytoplasm in seedlings (Figure 3.3-A, orange arrows). Additionally, clusters of vesicles close to the envelope may be observed in mature leaves (Figure 3.3-B, orange arrows).

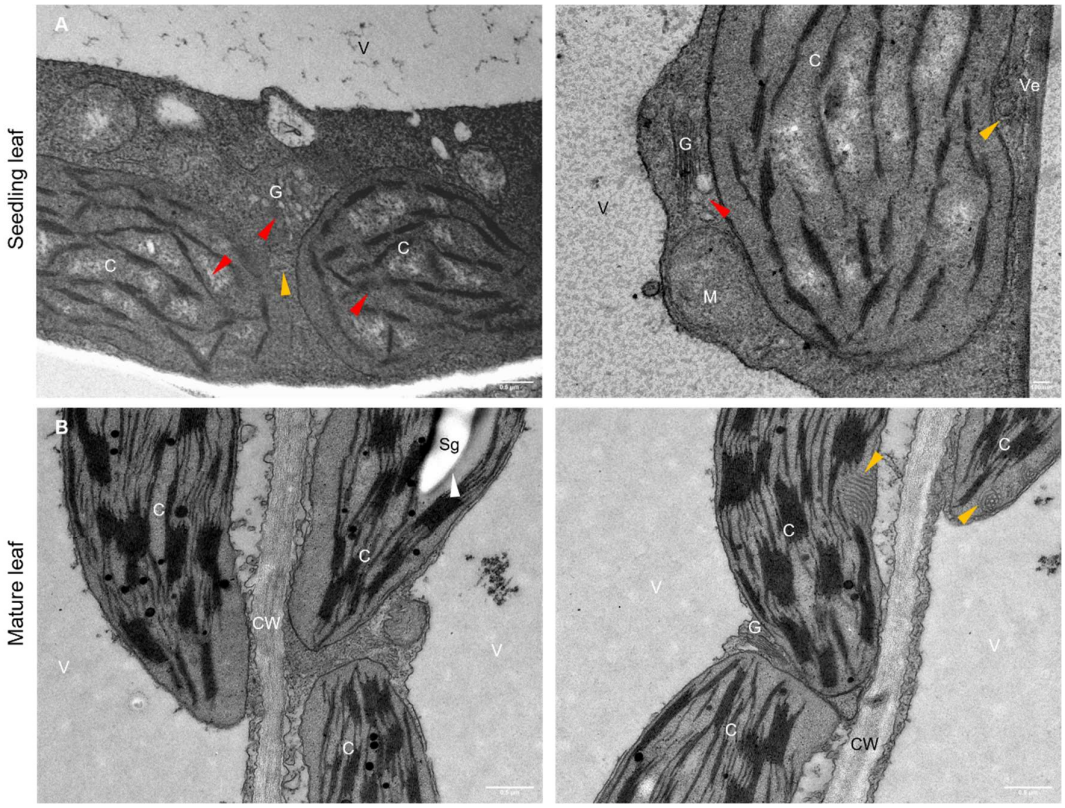


Figure 3.3 – Ultrastructure of cells from *Arabidopsis thaliana syp22-1 syp23* mutated line, in seedling leaf (A) and mature leaf (B). The most relevant organelles are evidenced and labelled. Red arrows indicate important organelles, white arrows indicate the starch granules and orange arrows indicate other relevant details of the cell's ultrastructure. Scale bars: 0.5 µm or 100 nm. Images were analyzed and processed using ImageJ/Fiji software. Abbreviations: C, chloroplasts; CW, cell wall; ER, endoplasmic reticulum; G, Golgi apparatus; M, mitochondria; Sg, starch granules; V, vacuole; Ve, vesicles.

In the *sec24a-2* mutant, the only ultrastructural difference observed from the wild-type line was the presence of huge well-defined starch granules in the chloroplasts of seedling leaves (Figure 3.4-A, white arrows). In both tissues analysed, the morphology of organelles, such as the ER and the Golgi, presented normal morphology (Figure 3.4, red arrows). Moreover, this mutant exhibited some chloroplast protrusion in both tissues and cytoplasmic invagination was observed in mature leaves (Figure 3.4, orange arrows).

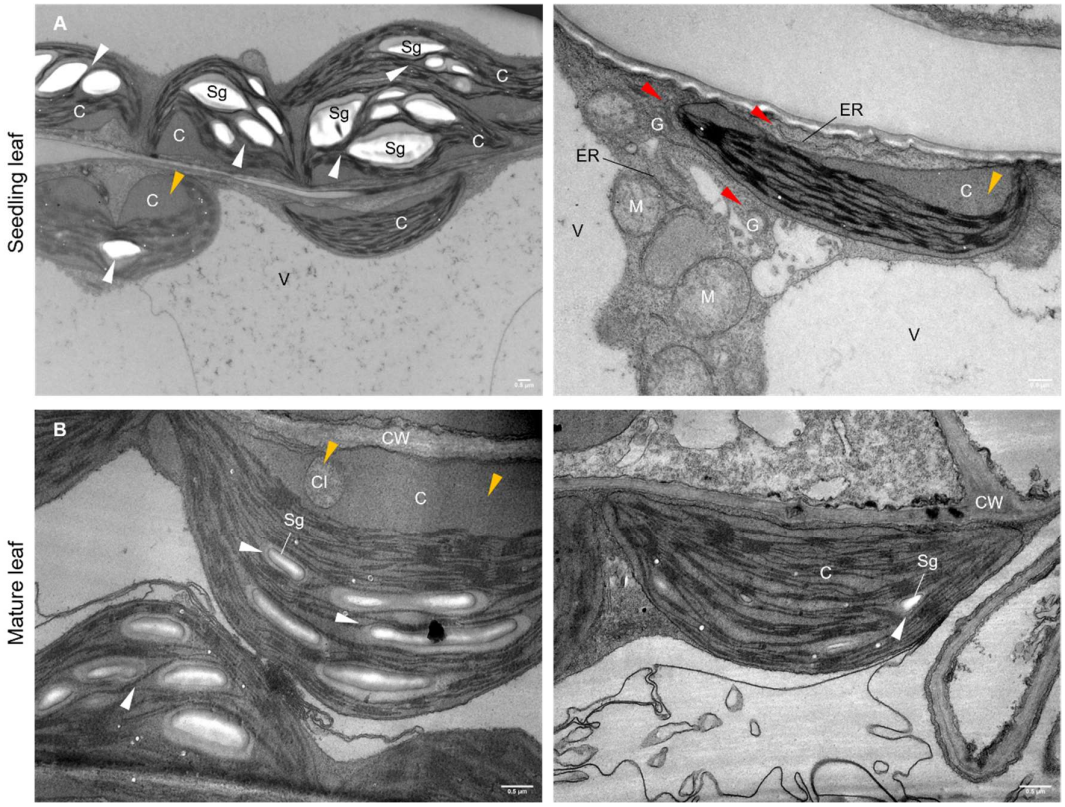


Figure 3.4 – Ultrastructure of cells from *Arabidopsis thaliana sec24a-2* mutated line, in seedling leaf (A) and mature leaf (B). The most relevant organelles are evidenced and labelled. Red arrows indicate important organelles, white arrows indicate the starch granules and orange arrows indicate other relevant details of the cell's ultrastructure. Scale bars: 0.5 µm or 100 nm. Images were analyzed and processed using ImageJ/Fiji software. Abbreviations: C, chloroplasts; CI, cytoplasmic invagination; CW, cell wall; ER, endoplasmic reticulum; G, Golgi apparatus; M, mitochondria; Sg, starch granules; V, vacuole.

In the *nai GFP-h* mutant, again, huge starch granules were observed in the chloroplasts of the seedling leaves (Figure 3.5-A, white arrows). However, such inclusions were not observed in the mature leaves (Figure 3.5-B). In this line, the ER tubules appeared normal, but the Golgi apparatus presented enlarged cisternae in the mature leaves (Figure 3.5-B, red arrows). Once more, the vesiculation observed in the cytoplasm appeared to be of abnormal amount. This mutant also exhibited chloroplast protrusion and cytoplasmic invagination in seedling leaves (Figure 3.5, orange arrows).

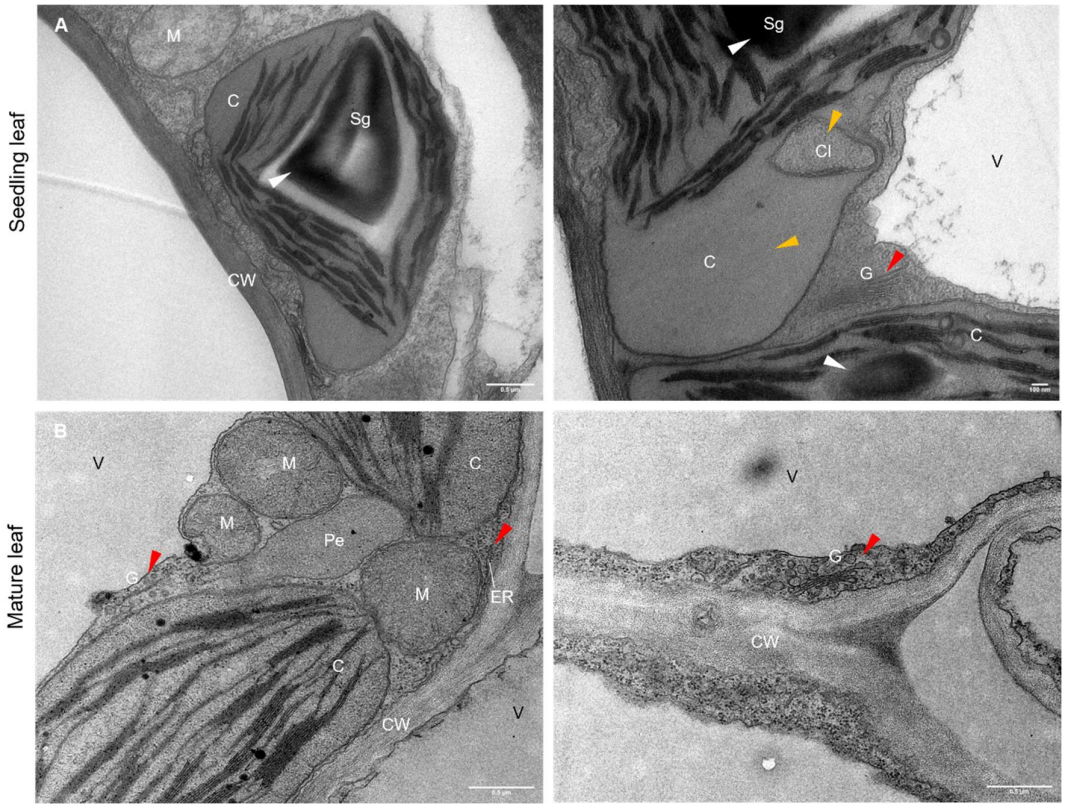


Figure 3.5 – Ultrastructure of cells from *Arabidopsis thaliana nai GFP-h* mutated line, in seedling leaf (A) and mature leaf (B). The most relevant organelles are evidenced and labelled. Red arrows indicate important organelles, white arrows indicate the starch granules and orange arrows indicate other relevant details of the cell's ultrastructure. Scale bars: 0.5 µm or 100 nm. Images were analyzed and processed using ImageJ/Fiji software. Abbreviations: C, chloroplasts; CI, cytoplasmic invagination; CW, cell wall; ER, endoplasmic reticulum; G, Golgi apparatus; M, mitochondria; Pe, peroxisome; Sg, starch granules; V, vacuole.

In the *nai2-2* mutated line, the huge well-defined starch granules were observed in both tissues along with the extensive vesiculation in the cytoplasm (Figure 3.6, white arrows). Contrarily to the other lines, in this mutant, the ER tubules are more prominent and present in higher amount in the mature leaves, whereas in the seedling leaves the Golgi, also with enlarged cisternae, predominate (Figure 3.6, red arrows). In the seedling leaves, an intriguing structure was observed and thought to be chloroplast with concentric inner membrane structures (Figure 3.6-A, orange arrow). In mature leaves, numerous vesicles may be observed (Figure 3.6-B, orange arrows).

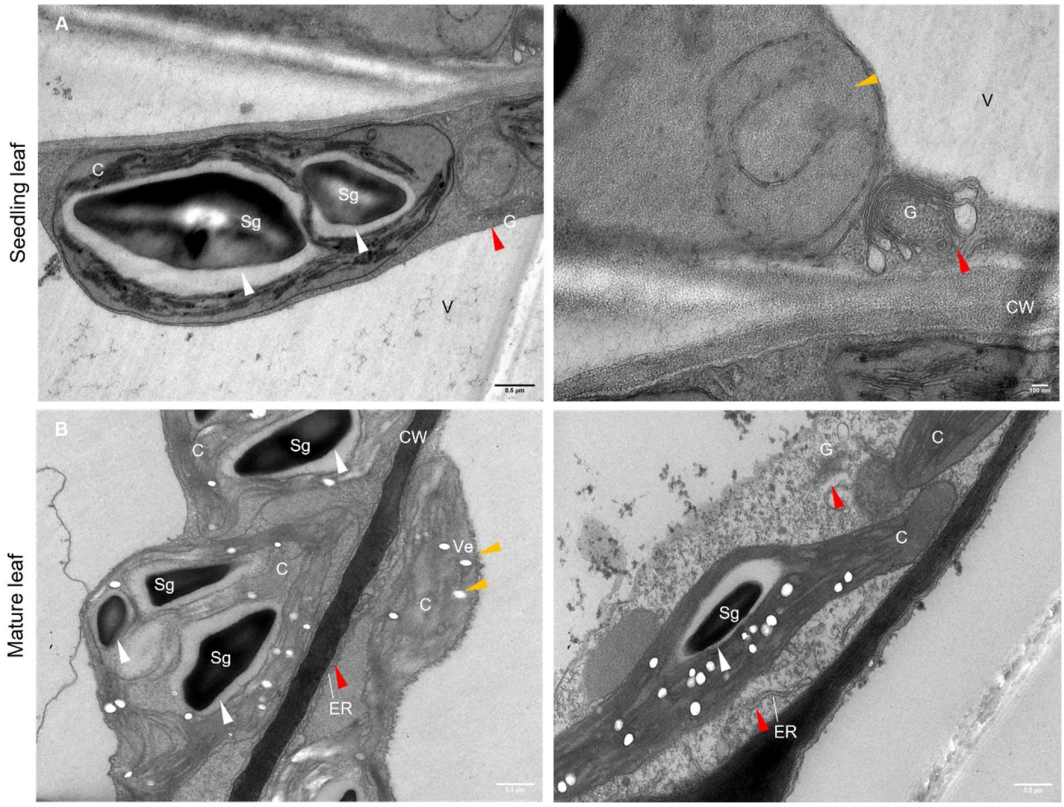


Figure 3.6 – Ultrastructure of cells from *Arabidopsis thaliana nai2-2* mutated line, in seedling leaf (A) and mature leaf (B). The most relevant organelles are evidenced and labelled. Red arrows indicate important organelles, white arrows indicate the starch granules and orange arrows indicate other relevant details of the cell's ultrastructure. Scale bars: 0.5 µm or 100 nm. Images were analyzed and processed using ImageJ/Fiji software. Abbreviations: C, chloroplasts; CW, cell wall; ER, endoplasmic reticulum; G, Golgi apparatus; M, mitochondria; Sg, starch granules; V, vacuole; Ve, vesicles.

Finally, in the *leb-2 GFP-h* mutated line, similarly to what was observed in the other mutants, huge well-defined starch granules were found present in the chloroplasts of both leaf tissues (Figure 3.7, white arrows), the Golgi apparatus also presented enlarged cisternae (Figure 3.7, red arrows) and numerous vesicles were observed in the cytoplasm. In the seedling leaves of this line, ER was found to have abnormal morphology, as it appeared to be enlarged (Figure 3.7-A, red arrow). In this mutant, thylakoid membranes appeared loosely packed into grana and it possessed more plastoglobuli (Figure 3.7, orange arrows).

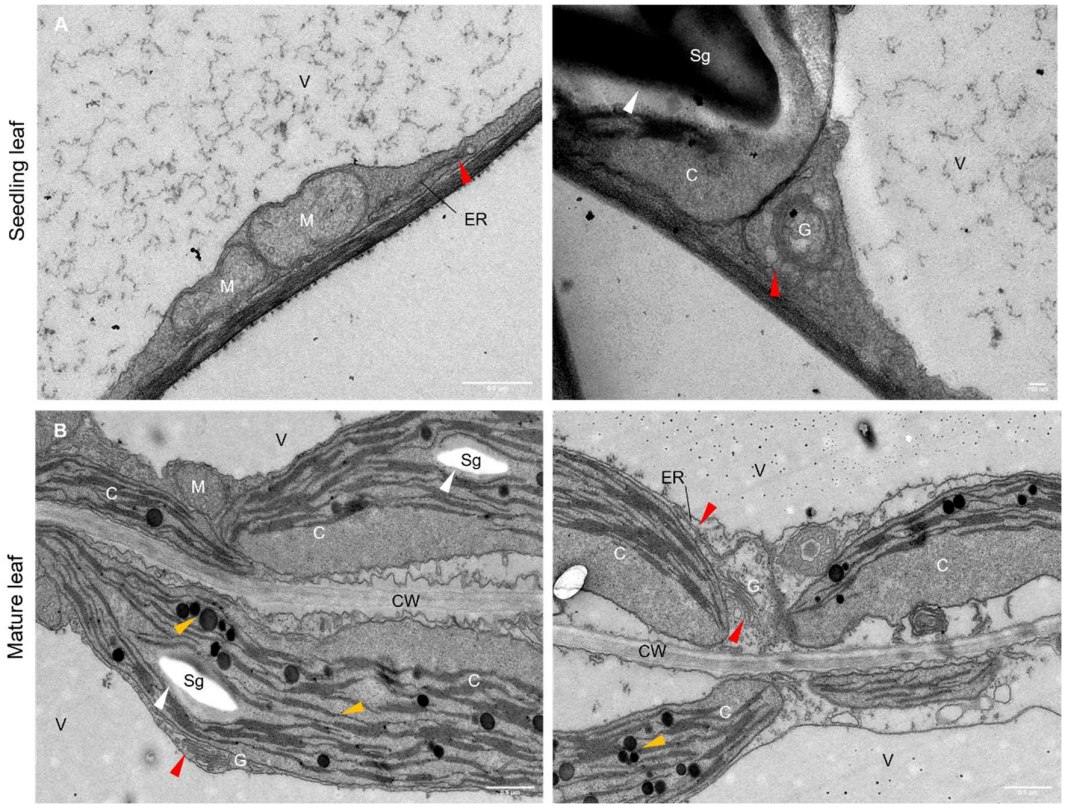


Figure 3.7 – Ultrastructure of cells from *Arabidopsis thaliana leb-2 GFP-h* mutated line, in seedling leaf (A) and mature leaf (B). The most relevant organelles are evidenced and labelled. Red arrows indicate important organelles, white arrows indicate the starch granules and orange arrows indicate other relevant details of the cell's ultrastructure. Scale bars: 0.5 µm or 100 nm. Images were analyzed and processed using ImageJ/Fiji software. Abbreviations: C, chloroplasts; CW, cell wall; ER, endoplasmic reticulum; G, Golgi apparatus; M, mitochondria; Sg, starch granules; V, vacuole.

To have a better understanding and a full perspective of all the characteristics of the ultrastructure of these ER-defective Arabidopsis plants, the following table (Table 3.1) condenses our observations.

Table 3.1 – Summary of the ultrastructural features of the *Arabidopsis thaliana* ER-defective plants.

Line	Tissue	Features
syp22-1 syp23	Seedling leaf	No starch granules, chloroplasts of disorganized grana, Golgi with enlarged cisternae
	Mature leaf	More organized grana in the chloroplasts, well-defined starch granules, Golgi with enlarged cisternae
sec24a-2	Seedling leaf	Well-defined starch granules, normal ER and Golgi morphology
	Mature leaf	Well-defined starch granules, normal ER and Golgi morphology
nai GFP-h	Seedling leaf	Well-defined starch granules, normal ER, numerous vesicles, Golgi with enlarged cisternae
	Mature leaf	No starch granules, normal ER, numerous vesicles, Golgi with enlarged cisternae

nai2-2	Seedling leaf	Well-defined starch granules, numerous vesicles, Golgi are more prominent and in higher amount, Golgi with enlarged cisternae
	Mature leaf	Well-defined starch granules, numerous vesicles, ER tubules are more prominent and in higher amount, Golgi with enlarged cisternae
leb-2 GFP-h	Seedling leaf	Well-defined starch granules, Golgi with enlarged cisternae, numerous vesicles, abnormal ER morphology
	Mature leaf	Well-defined starch granules, Golgi with enlarged cisternae, numerous vesicles

After looking at the mutant's ultrastructure, we noticed that chloroplasts were very different in size and different in the size and type of inclusions between lines and we decided to measure the starch granules and the chloroplasts in both evaluated tissues to be able to quantify these changes. All measurements are presented in Figure 3.8 and the parameter evaluated was the perimeter.

Regarding starch inclusions, as it may be observed, the *sec24a*-2, *nai GFP-h*, *nai2-2* and *leb-2 GFP-h* lines are significantly different from the WT line since these mutants have starch granules in seedlings, whereas the WT and the *syp22-1 syp23* mutant do not (Figure 3.8-A). In the case of the starch granules of mature leaves, the differences shift, as *nai GFP-h* line is the only mutant significantly different from the WT line since this mutant does not possess starch granules in the mature leaves (Figure 3.8). The differences observed in the perimeter of these inclusions between the WT and the rest of the mutants are not significant. Similar to what happens for the WT line, starch granules appear in the mature leaves of the *syp22-1 syp23* mutant.

Looking at the perimeter of chloroplasts, the significant differences between the WT line and all mutated lines in seedlings are evident, as the mutants present larger chloroplasts than the WT (Figure 3.8). On the other hand, the chloroplasts of the *nai GFP-h* line decrease in perimeter from seedling to mature leaves, with this line's results being significantly different from the WT line. In the WT line also may be observed an increase in the perimeter of chloroplasts from seedling to mature leaf.

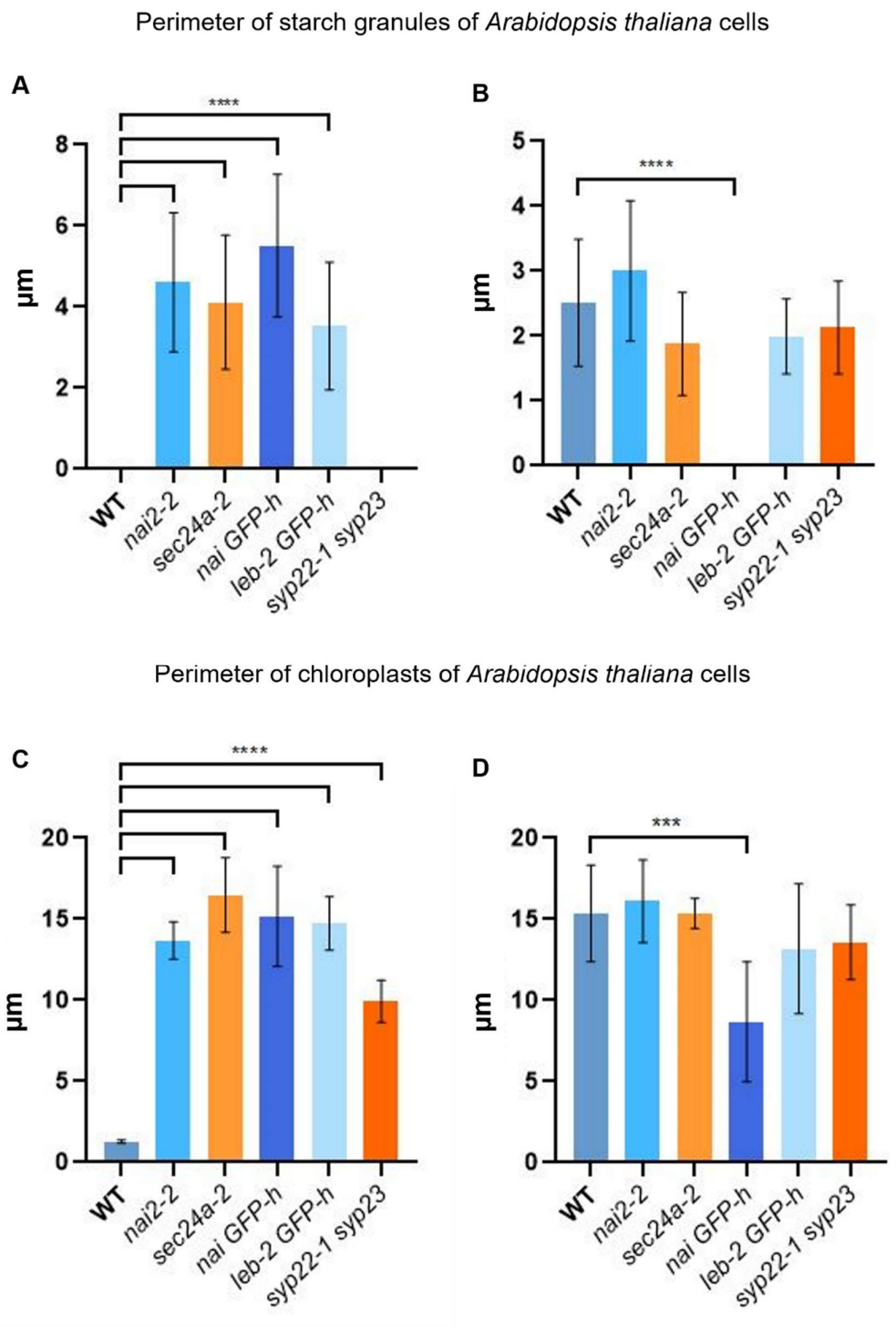


Figure 3.8 – Perimeter of starch granules in chloroplasts *of Arabidopsis thaliana* cells from seedling-leaves (A) and mature-leaves (B) and perimeter of chloroplasts *of Arabidopsis thaliana* cells from seedling-leaves (C) and mature-leaves (D). Measurements were obtained using ImageJ/Fiji software and data was analysed through a One-Way ANOVA test using GraphPad Prism8 software. The * indicates the existing significative differences: **** indicates a p value of <0.0001 and *** indicates a p value of 0.0008.

3.2. Definition of trafficking pathways in ER-defective plants

3.2.1. Selection of constructs for co-expression of PSIs and marker proteins

Taking into count what is proposed in this study and in order to observe how the PSIs' trafficking occurred in the Arabidopsis mutants, both PSI A and PSI B were fused with the photoconvertible fluorescent protein mEos 3.2. With specific primers especially designed, mEos 3.2 was fused with both PSIs in the pMDC83 plasmid. Following Gibson Assembly, transformed bacterial colonies were screened by enzymatic restriction of purified plasmids with EcoRI and these were finally sequenced (Figure 3.9 and Figure 3.10). One positive clone of each construct was thus selected and used for transient expression in Arabidopsis and *Nicotiana tabacum* plants.

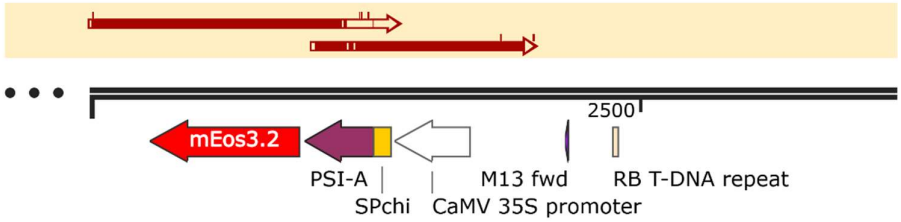


Figure 3.9 – Alignment of the sequencing results of pMDC83::SP::PSIA::mEos3.2. The sequencing results with M13rev primer and PSIA sequencing (Table 2.3) were aligned with the respective expected pMDC83::SP::PSIA::mEos3.2 sequence. The sequences alignment was performed resorting to SnapGene software (https://www.snapgene.com/). Red portions of the arrows represent sequence match and alignment, whereas white portions represent no alignment.

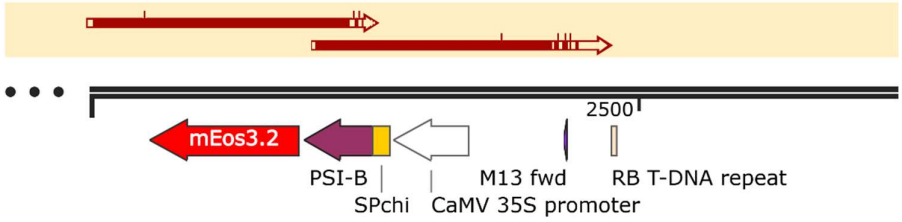


Figure 3.10 – Alignment of the sequencing results of pMDC83::SP::PSIB::mEos3.2. The sequencing results with M13 and PSIB sequencing (Table 2.3) were aligned with the respective expected pMDC83::SP::PSIB::mEos3.2 sequence. The sequences alignment was performed resorting to SnapGene software (https://www.snapgene.com/). Red portions of the arrows represent sequence match and alignment, whereas white portions represent no alignment.

Once the intended constructs were prepared, such constructs were tested in both *A. thaliana* and *N. tabacum* mature leaves, as described in section 2.5, before transforming the mutated lines. This allowed us to understand if the constructs would

work later for the vacuum infiltration of the mutated Arabidopsis seedlings. Visualization was done through Confocal Microscopy, and, with this test, we were able to determine that photoconversion of the mEos tag was not working properly. Thus, we were obligated to abandon this tag and switch back to mCherry. The constructs of the PSIs fused with mCherry were already prepared and ready to be used in our laboratory (Supplementary figure 7.4 and Supplementary figure 7.5).

3.2.2. Expression of PSIs in ER-defective plants

The heterologous expression of the PSIs fused with mCherry in Arabidopsis allowed us to assess the localization of these domains in the cell. Several images of each condition were captured and analysed and the most representative may be found in the following figures (Figure 3.11 and Figure 3.13). Moreover, a quantitative approach of the PSIs' localization is also presented (Figure 3.14), giving a more complete perception of our observations.

Firstly, we evaluated the localization of PSI A and PSI B in the ER-defective lines, and such results may be observed in Figure 3.11 and Figure 3.13 As it may be noted, PSI A was mainly found in the vacuolar compartments in the WT line, as well as in the *sec24a-2*, *nai2-2*, *nai GFP-h* and *leb-2 GFP-h* lines (Figure 3.11). However, this domain was also observed in other locations, like at the cell's periphery, in a less pronounced way (Figure 3.11, white arrows). In the wild-type line, besides the conspicuous vacuolar localization, the PSI A was also observed to be secreted (Figure 3.12-A). In the *sec24a-2*, *nai2-2,* and *leb-2 GFP-h* mutants some secretion was also observed (Figure 3.11 and Figure 3.12), whereas in the *nai GFP-h* mutant the PSI A was only found in the vacuole (Figure 3.11). In the *nai GFP-h* and *leb-2 GFP-h* lines, as they stably express GFP marked for ER retention, we may also observe the reticular network of such mutants (Figure 3.11-D and E). The quantitative evaluation of the PSI A localization confirmed these observations (Figure 3.14).

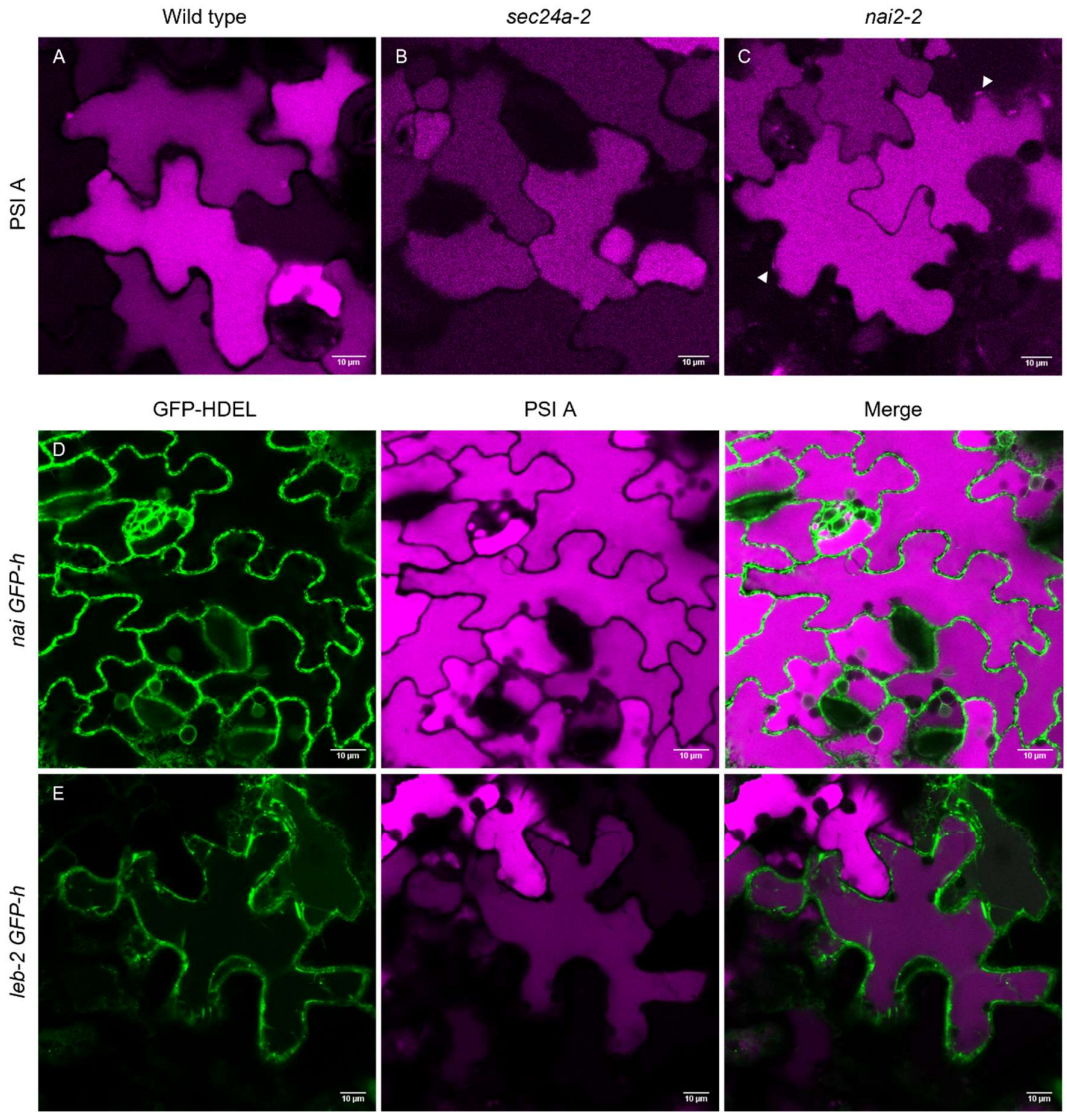


Figure 3.11 – Subcellular localization of Cardosin PSI A fused with mCherry in cotyledon leaves of *Arabidopsis thaliana* wild-type and ER-defective seedlings. (A, B and C) Expression of PSI A::mCherry in wild-type, *sec24a-2,* and *nai2-2* lines, respectively; (D and E) Expression of PSI A::mCherry in *nai GFP-h* and *leb-2 GFP-h*, respectively, which possess a GFP marked for ER retention. Note the evident vacuolar accumulation in the Arabidopsis lines (wild-type, *sec24a-2*, *nai2-2*, *nai GFP-h* and *leb-2 GFP-h*). The white arrows indicated other subcellular accumulation sites, such as secreted. All images were acquired 3 days post-infiltration and were analyzed and processed using ImageJ/Fiji software. Scale bar: 10 µm.

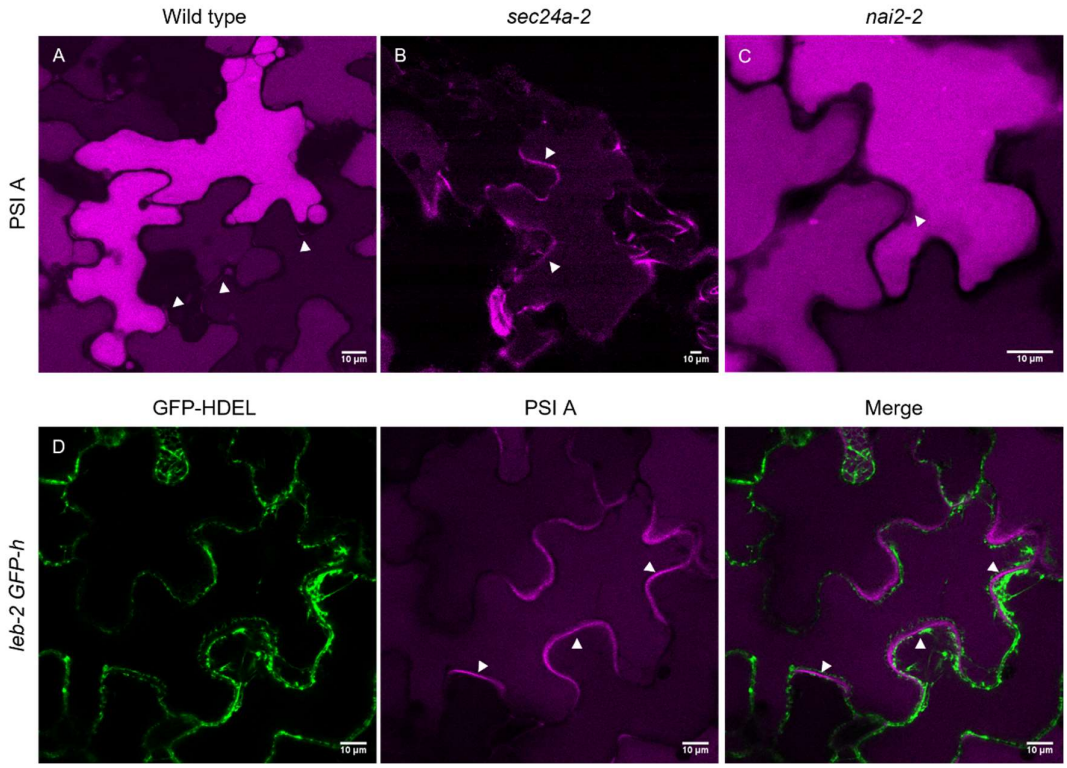


Figure 3.12 – Additional observed subcellular localizations of Cardosin PSI A fused with mCherry in cotyledon leaves of *Arabidopsis thaliana* wild-type and ER-defective seedlings. (A, B and C) Expression of PSI A::mCherry in wild-type, *sec24a-2* and *nai2-2* lines, respectively; (D) Expression of PSI A::mCherry in *leb-2 GFP-h*, which possesses a GFP marked for ER retention. Note the evident vacuolar accumulation in the Arabidopsis lines (wild-type, *sec24a-2*, *nai2-2* and *leb-2 GFP-h*). The white arrows indicated other subcellular accumulation sites, such as secreted. All images were acquired 3 days post-infiltration and were analyzed and processed using ImageJ/Fiji software. Scale bar: 10 µm.

Regarding PSI B localization, more differences between WT and mutant lines were observed. In the WT line, PSI B was mostly observed in the vacuole and secreted (Figure 3.13-A, white arrows), despite being also found exclusively in the vacuole in some cells. In *sec24a-2* and *leb-2 GFP-h* mutants, PSI B was found to be secreted, despite it mainly accumulated in the vacuole (Figure 3.13-B and E, white arrows). In the remaining mutated lines (*nai2-2* and *nai GFP-h*), PSI B was found to be mostly secreted, although some accumulation in the vacuole was still observed (Figure 3.13-C and D, white arrows). These patterns of accumulation of the PSI B were quantified and are illustrated in Figure 3.14.

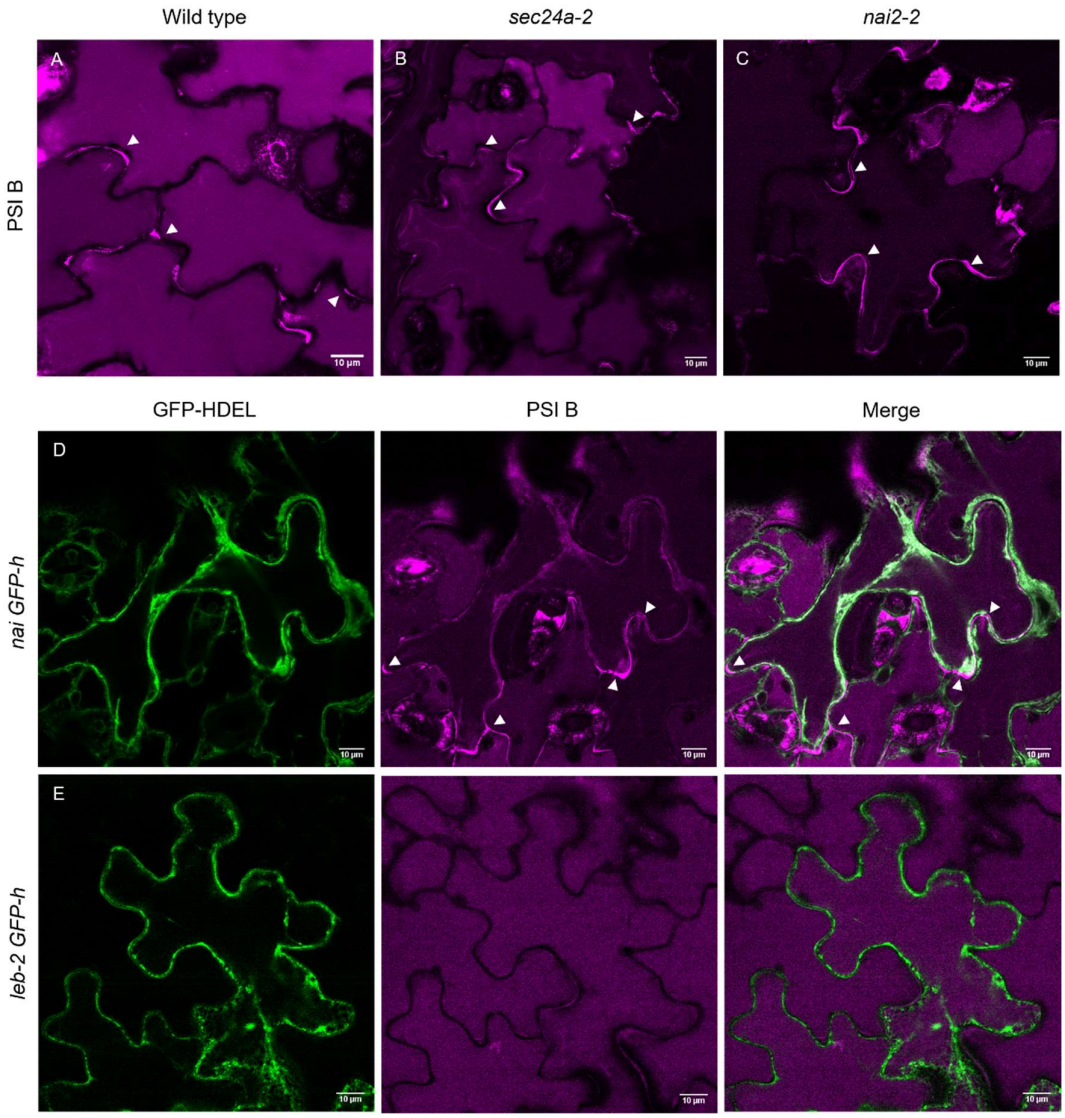


Figure 3.13 – Subcellular localization of Cardosin PSI B fused with mCherry in cotyledon leaves of *Arabidopsis thaliana* wild-type and ER-defective seedlings. (A, B and C) Expression of PSI B::mCherry in wild-type, *sec24a-2* and *nai2-2* lines, respectively; (D and E) Expression of PSI B::mCherry in *nai GFP-h* and *leb-2 GFP-h*, respectively, which possess a GFP marked for ER retention. Note the differences in accumulation patterns in the Arabidopsis lines (wild-type, *sec24a-2*, *nai2-2*, *nai GFP-h* and *leb-2 GFP-h*). The white arrows indicated other subcellular accumulation sites, such as secreted. All observations and images were acquired 3 days post-infiltration and images were analyzed and processed using ImageJ/Fiji software. Scale bar: 10 µm.

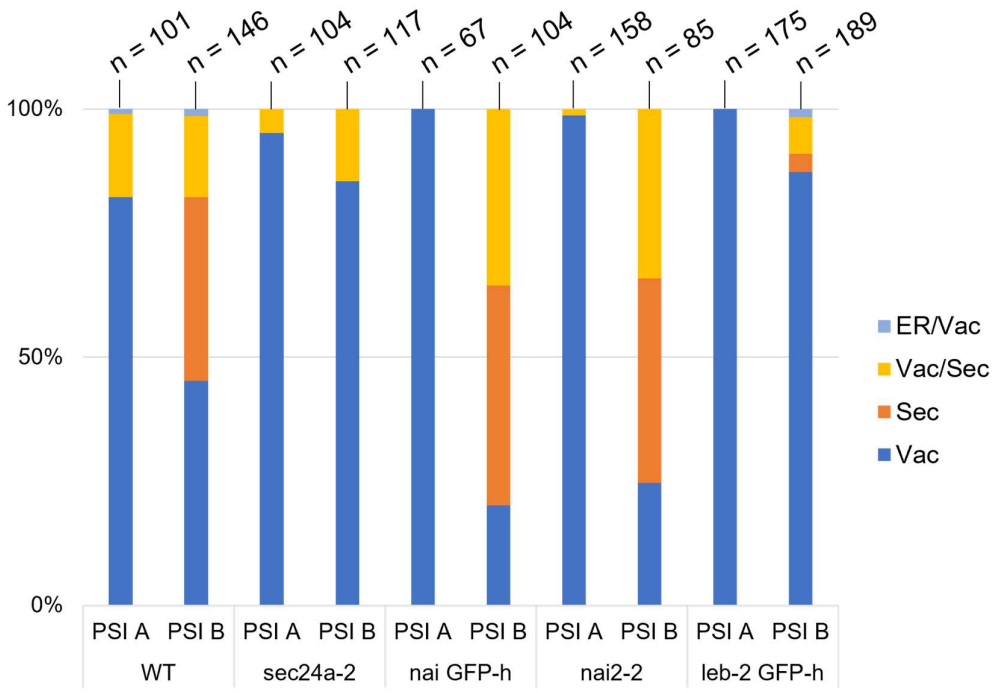


Figure 3.14 – Quantitative localization of Cardosin A and B PSI in cotyledon leaves of *Arabidopsis thaliana* wild-type and ER-defective seedlings. The *n* above the bars refers the number of cells counted. The PSIs were considered "secreted" when found at the cell periphery (cell wall) and/or extracellularly. For the analysis of the images to be as reliable as possible, cropped cells were not considered. Abbreviations: ER, endoplasmic reticulum; Sec, secreted; Vac, vacuole.

3.2.3. Expression of PSIs in ER-defective plants treated with BFA

After obtaining the results described in the previous section, we decided to assess if these patterns of accumulation were affected by Brefeldin A (BFA). BFA is a fungal macrocyclic lactone widely used as an inhibitor of vacuolar protein transport and secretion in plant cells, causing the formation of an ER-Golgi hybrid compartments (Nebenführ et al. 2002). As described in section 2.6.2., the WT and mutated lines were treated with BFA one day after being infiltrated with the PSIs constructs.

In the case of PSI A, its accumulation remained mostly in the vacuole, even if some secretion was still observed (Figure 3.15, white arrows). In the WT line, PSI A presented some residual labelling both in the ER and the vacuole, but overall, it was found in the vacuole (Figure 3.15-A). A similar pattern was observed in the *sec24a-2* and *leb-2 GFP-h* lines, where PSI A was mainly accumulated in the vacuole, however showing a little secretion (Figure 3.15-B and E). In the remaining lines (*nai2-2* and *nai GFP-h*), PSI A was found to be secreted in higher amounts when compared with the untreated condition, as it was found in the extracellular space while maintaining some accumulation in the vacuole (Figure 3.15-C and D, white arrows). These observations were corroborated with the quantitative analysis (Figure 3.17).

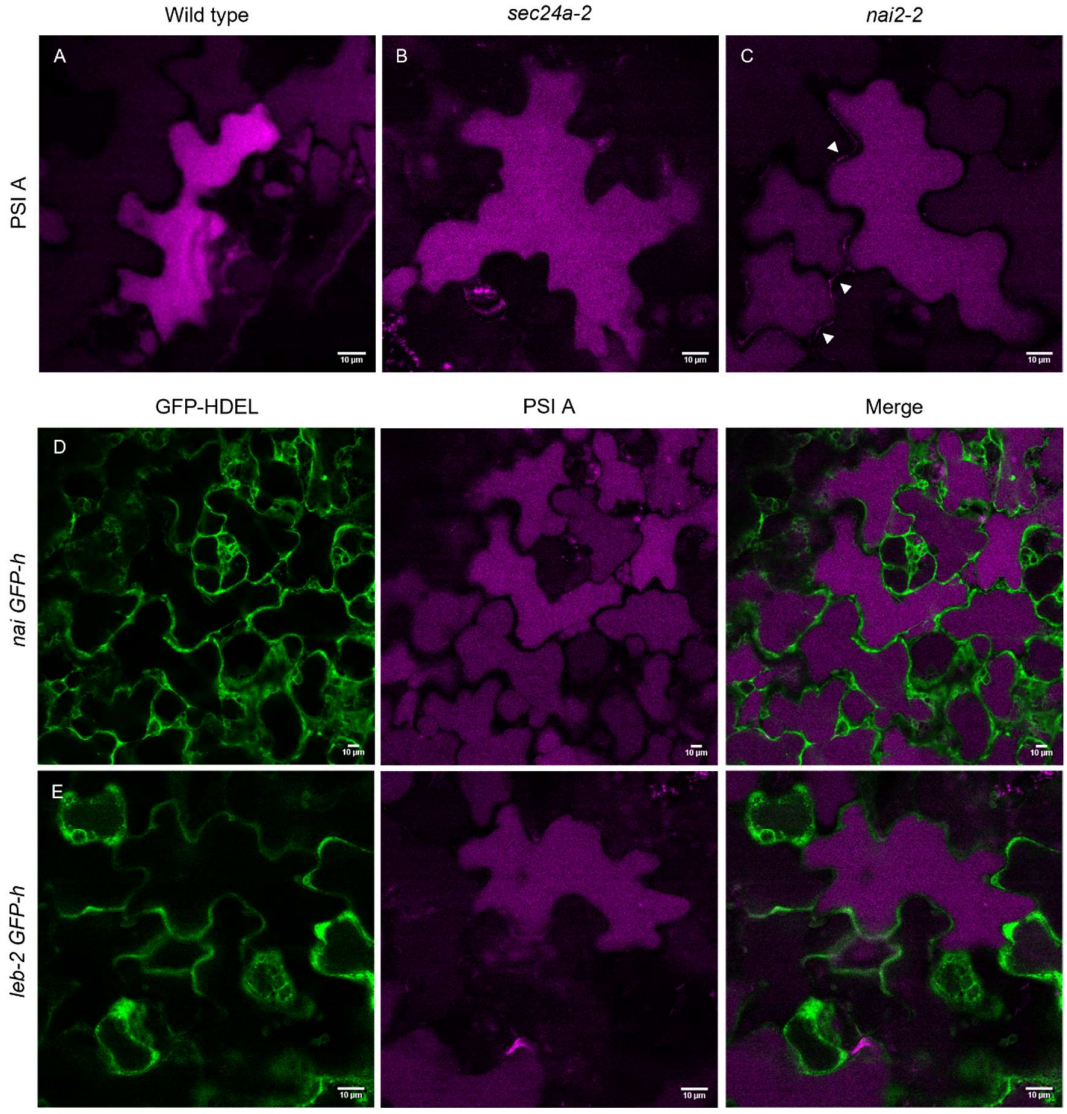


Figure 3.15 – Subcellular localization of Cardosin PSI A fused with mCherry in cotyledon leaves of *Arabidopsis thaliana* wild-type and ER-defective seedlings treated with BFA. (A, B and C) Expression of PSI A::mCherry in wild-type, *sec24a-2* and *nai2-2* lines, respectively; (D and E) Expression of PSI A::mCherry in *nai GFP-h* and *leb-2 GFP-h*, respectively, which possess a GFP marked for ER retention. Note the evident vacuolar accumulation in the Arabidopsis lines (wild-type, *sec24a-2*, *nai2-2*, *nai GFP-h* and *leb-2 GFP-h*). The white arrows indicated other subcellular accumulation sites, such as secreted. All observations and images were acquired 3 days post-infiltration and images were analyzed and processed using ImageJ/Fiji software. Scale bar: 10 µm.

Regarding PSI B, the general secretion observed in the untreated condition was decreased in the BFA treated plants, but still maintaining some accumulation in the extracellular space (Figure 3.16). Except for the *leb-2 GFP-h*, where PSI B was only located in the vacuole (Figure 3.16-E), the other lines presented the PSI B in the vacuole and secreted, as well as just secreted (Figure 3.16). In the WT and *sec24a-2* lines, this secretion was much less pronounced than in the *nai2-2* and *nai GFP-h* lines (Figure 3.16Figure 3.16), as it is in these lines where the PSI B is the most secreted, especially

nai GFP-h (Figure 3.16, white arrows). Like before, such observations were confirmed with the quantitative analysis (Figure 3.18).

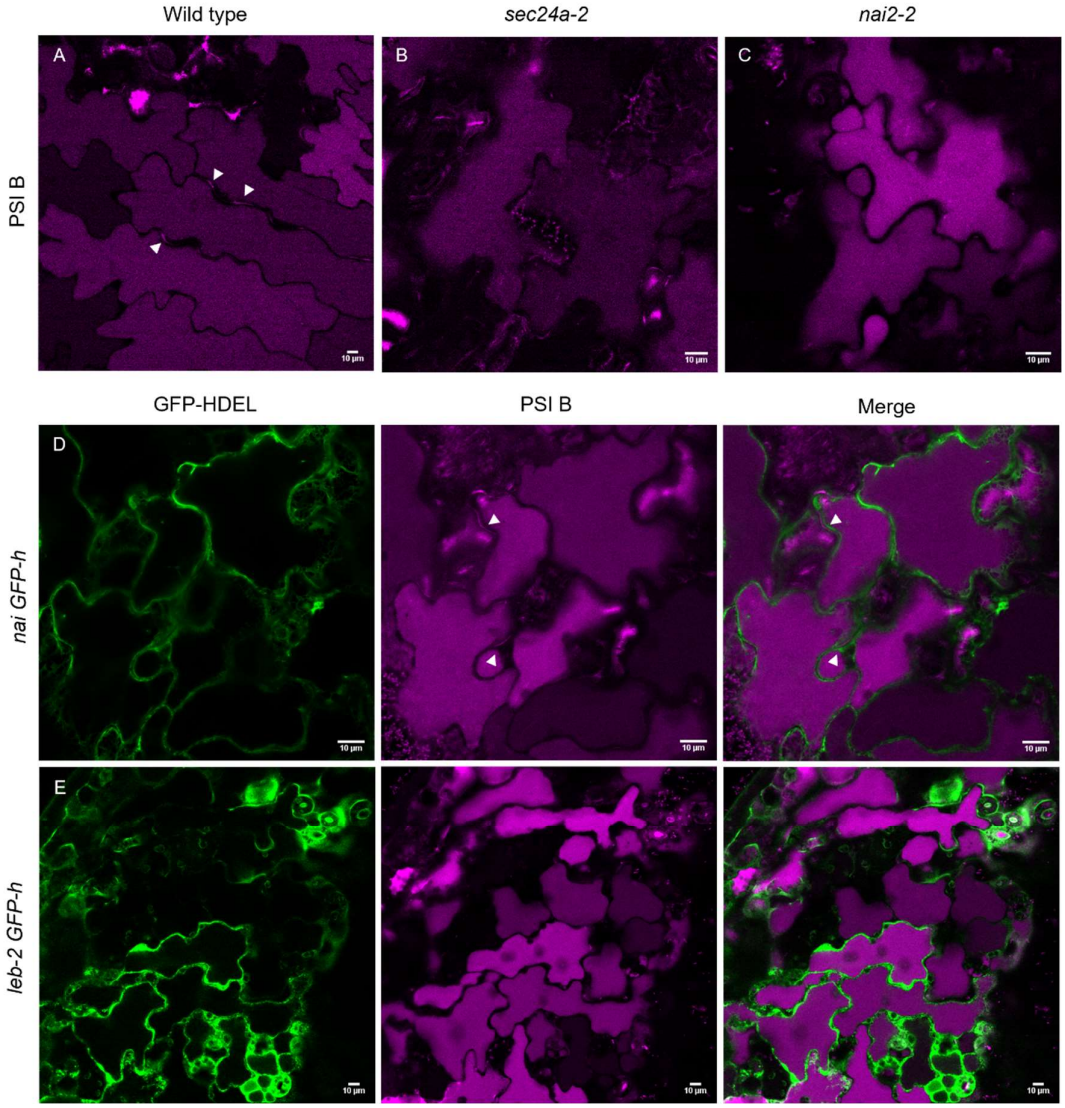


Figure 3.16 – Subcellular localization of Cardosin PSI B fused with mCherry in cotyledon leaves of *Arabidopsis thaliana* wild-type and ER-defective seedlings treated with BFA. (A, B and C) Expression of PSI B::mCherry in wild-type, *sec24a-2* and *nai2-2* lines, respectively; (D and E) Expression of PSI B::mCherry in *nai GFP-h* and *leb-2 GFP-h*, respectively, which possess a GFP marked for ER retention. Note the differences in accumulation patterns in the Arabidopsis lines (wild-type, *sec24a-2*, *nai2-2*, *nai GFP-h* and *leb-2 GFP-h*). The white arrows indicated other subcellular accumulation sites, such as secreted. All observations and images were acquired 3 days post-infiltration and images were analyzed and processed using ImageJ/Fiji software. Scale bar: 10 µm.

Additionally, the quantitative localization allowed the better visualization of the effect of BFA in the plants. As it may be observed, when comparing untreated with treated plants, a decrease in the secretion was verified for both PSIs in most of the Arabidopsis lines (Figure 3.17 and Figure 3.18). The exception to these observations is the residual

secretion of PSI A observed in the *nai2-2*, *nai GFP-h* and *leb-2 GFP-h* lines when treated with BFA, which is not observed in the untreated plants (Figure 3.17).

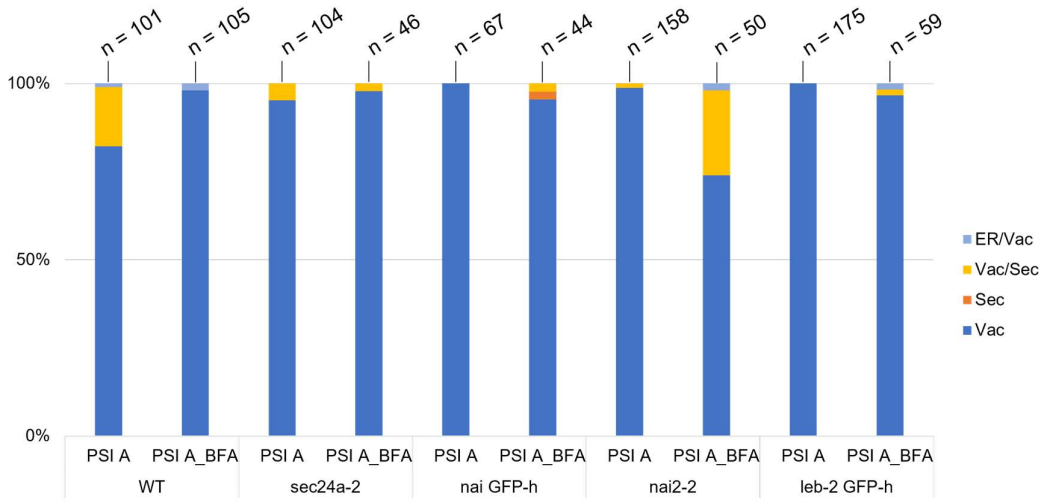


Figure 3.17 – Quantitative localization of Cardosin A PSI in cotyledonary leaves of *Arabidopsis thaliana* wild-type and ER-defective seedlings untreated and treated with BFA. The *n* above the bars refers the number of cells counted. The PSI was considered "secreted" when found at the cell periphery (cell wall) and/or extracellularly. For the analysis of the images to be as reliable as possible, cropped cells were not considered. Abbreviations: ER, endoplasmic reticulum; Sec, secreted; Vac, vacuole.

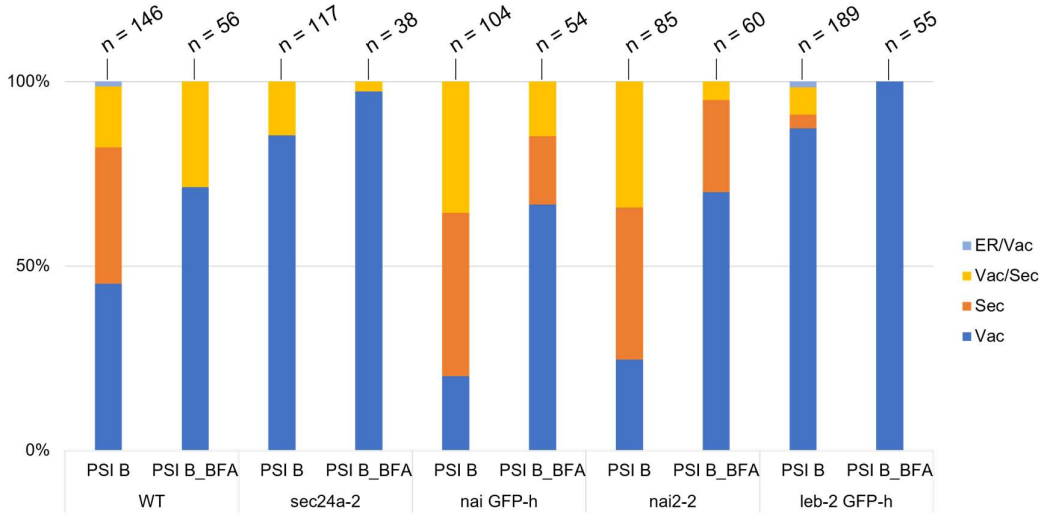


Figure 3.18 – Quantitative localization of Cardosin B PSI in cotyledonary leaves of *Arabidopsis thaliana* wild-type and ER-defective seedlings untreated and treated with BFA. The *n* above the bars refers the number of cells counted. The PSI was considered "secreted" when found at the cell periphery (cell wall) and/or extracellularly. For the analysis of the images to be as reliable as possible, cropped cells were not considered. Abbreviations: ER, endoplasmic reticulum; Sec, secreted; Vac, vacuole.

3.2.4. Co-localization with the endosomal marker FM2-10

To possibly identify one or more intermediate compartments common to the secretory and endocytic pathway, we infiltrated the Arabidopsis lines with the PSIs and, two days later, the infiltrated seedlings were stained with the endosomal marker FM2-10 for 2-3 h, before cell imaging. For the assay, two of our lines (*nai GFP-h* and *leb-2 GFP-h*) could not be used, since they are already marked with green fluorescence (*GPF-h*) that wouldn't permit distinguishing between said marking and the FM dye.

Regarding the PSI A, in the WT and *nai2-2* lines, co-localization was observed at the cell periphery (Figure 3.19-A and C, white arrows). In the *sec24a-2* line such co-localization between the PSI A and the FM dye was not observed (Figure 3.19-B). In this assay, the PSI A's localization corresponded to what had already been seen and it was mostly found in the vacuolar compartments, besides presenting some secretion (Figure 3.19). The FM dye was also easily observed at the cells' periphery.

In the case of the PSI B, co-localization of both markers (PSI and FM dye) was only observed in the *nai2-2* line, again at the periphery of the cell (Figure 3.20-C, white arrows). In the WT and *sec24a-2* lines, such co-localization was not observed (Figure 3.20-A and B). In this assay, and similarly to what was observed for the PSI A, PSI B was found in the same locations as before: in the vacuole and some secreted at the cell's periphery (Figure 3.20Figure 3.20). Again, the FM2-10 easily labelled the cell's periphery.

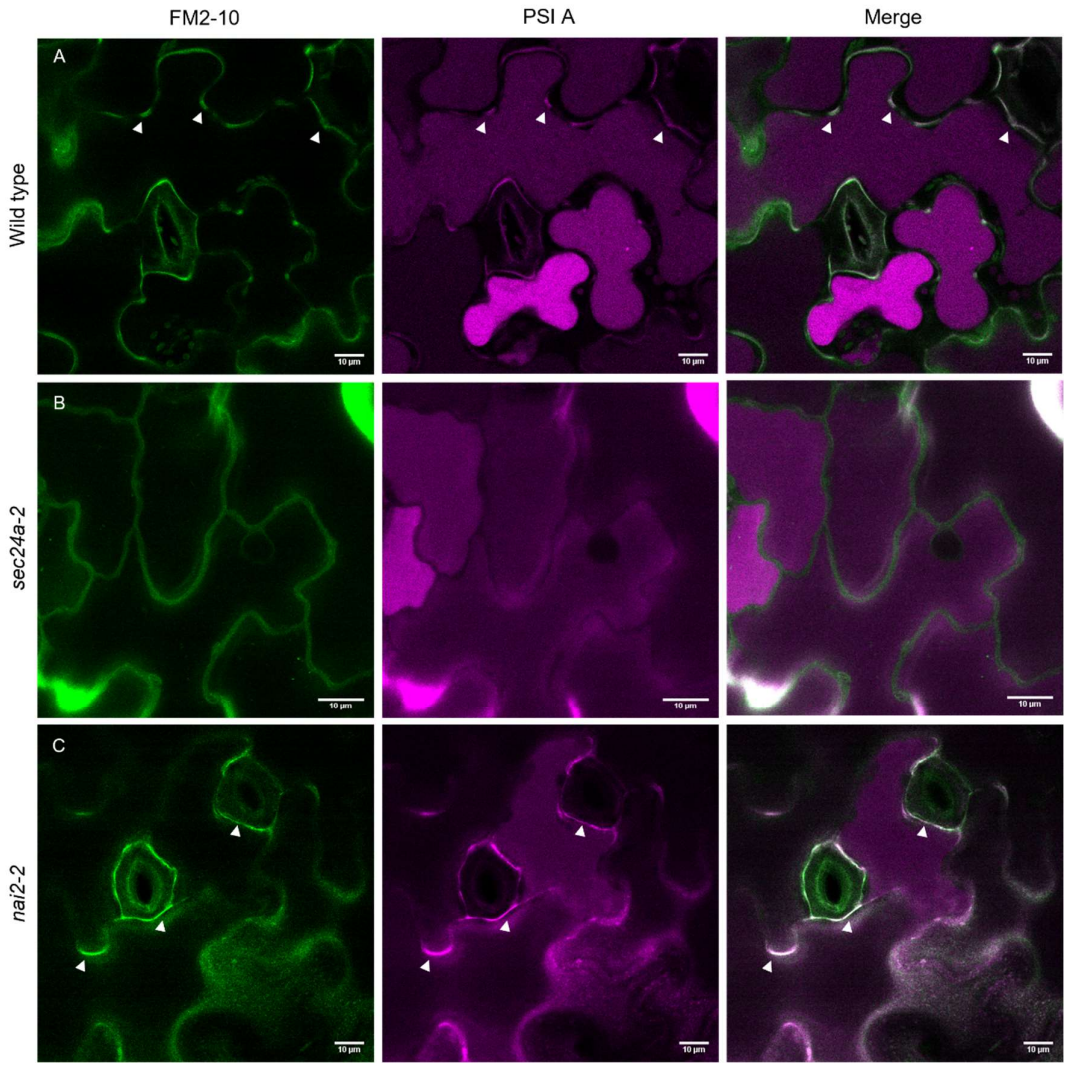


Figure 3.19 – Subcellular co-localization of Cardosin PSI A fused with mCherry, and FM2-10 dye in cotyledonary leaves of *Arabidopsis thaliana* wild-type and ER-defective seedlings. (A, B and C) Expression of PSI A::mCherry in wild-type, *sec24a-2* and *nai2-2* lines, respectively. Note the defined white marking, where PSI A and the FM dye co-localize. The white arrows evidence the co-localization. The seedlings were exposed to the dye 2 days after vacuum infiltration. All observations and images were acquired 2 days post-infiltration and images were analyzed and processed using ImageJ/Fiji software. Scale bar: 10 µm.

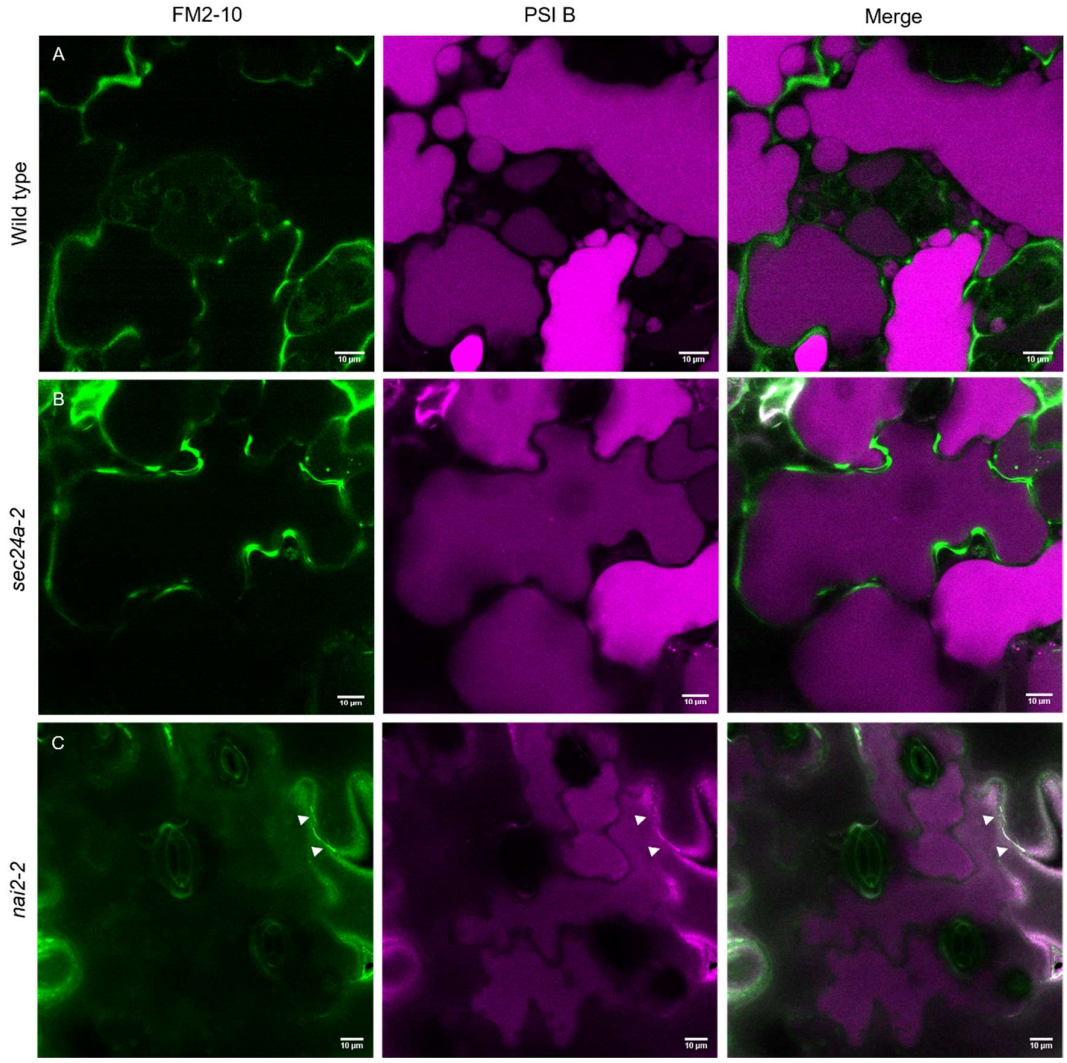


Figure 3.20 – Subcellular co-localization of Cardosin PSI B fused with mCherry, and FM2-10 dye in cotyledonary leaves of *Arabidopsis thaliana* wild-type and ER-defective seedlings. (A, B and C) Expression of PSI B::mCherry in wild-type, *sec24a-2* and *nai2-2* lines, respectively. Note the defined white marking, where PSI B and the FM dye co-localize. The white arrows evidence the co-localization. The seedlings were exposed to the dye 2 days after vacuum infiltration. All observations and images were acquired 2 days post-infiltration and images were analyzed and processed using ImageJ/Fiji software. Scale bar: 10 µm.

3.2.5. Analysis of secreted proteins

Finally, since our CLSM imaging revealed the secretion of PSI B in the Arabidopsis lines here studied, we decided to further confirm this secretion by isolating the extracellular protein content of seedlings of the WT and mutated lines infiltrated with PSI B fused with mCherry, as described in section 2.7. This allowed us to whether confirm or not the presence of the PSI domain in the extracellular space of our plants. In this assay, a double control system was used: the control sample was an extract of total protein content of seedlings that stably express the PSI B (a line developed in our

laboratory by a fellow researcher) and, to ensure the bands obtained were not from intracellular proteins, an antibody against the H3 histone, a protein exclusively found in the intracellular content (section 2.7.4.) was used. Indeed, the PSI B, with an expected size of 15 kDa, was detected in the extracellular protein content of the *nai GFP-h*, *nai2-2*, *sec24a-2,* and *leb-2 GPF-h* lines infiltrated with this domain (Figure 3.21), as observed through Confocal Microscopy (Figure 3.13 and Figure 3.16, white arrows). Moreover, the decrease in secretion observed in CLSM imaging in the BFA treatment was also confirmed by the western blot (Figure 3.21). However, regarding the WT line, the PSI B was not detected in the blot for both situations analysed (with and without BFA treatment). The PSI B domain was detected fused with mCherry, with a combined expected size of 35 kDa, as the expected size of mCherry was about 25 kDa. The faint detection of the histone H3, with an expected size of 17 kDa, shows there is no intracellular content. The other bands observed represent unspecific proteins of the extracellular content.

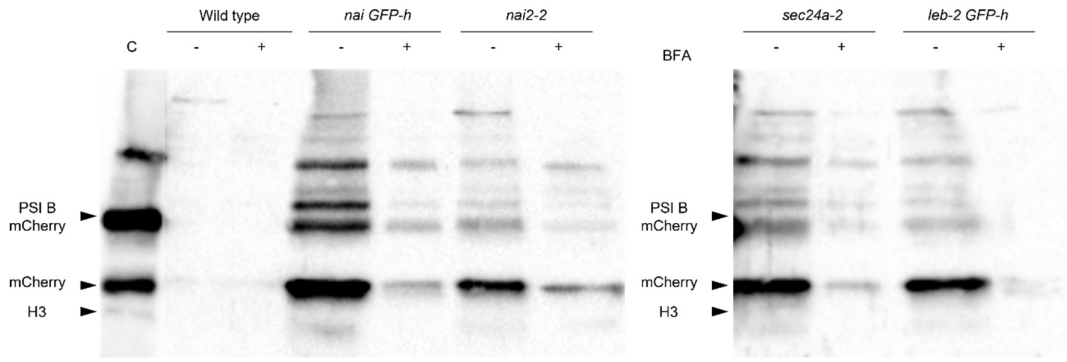


Figure 3.21 – pMDC83::SP::PSICardB::mCherry expression and secretion in *Arabidopsis thaliana* wild-type and mutated lines. Western blot of PSI B expression and secretion in Arabidopsis wild-type, *nai GFP-h*, *nai2-2*, *sec24a-2,* and *leb-2 GPF-h* lines. The arrows indicate the bands corresponding to the PSI B fused with mCherry, the mCherry and the histone H3. The minus sign indicates the absence of BFA treatment, and the plus sign indicates the presence of BFA treatment. Abbreviations: C, control sample.

4. DISCUSSION

4.1. Characterization of *Arabidopsis thaliana* ER-defective plants

As sessile organisms, plants' fast and creative adaptation to the environment they are in is essential for their survival. The driving activities of the endomembrane system along with the individual dynamics of its organelles provide the plant cells with a unique plasticity to deal with a multitude of environmental cues. The secretory pathway, a major pathway of the endomembrane system, has its starting point in the Endoplasmic Reticulum (ER), a highly versatile network of continuous tubules and cisterns contacting with several organelles in the cell that coordinates with membrane compartments along the secretory and endocytic pathways (Staehelin 1997; Stefan et al. 2013; Stefano et al. 2015). Moreover, it has been established that the ER is in close association with endosomes and the integrity of the reticular network is a requirement for the positioning and dynamics of the endosomes and for endocytosis (Stefano et al., 2015).

As it occurs at the plasma membrane, endocytosis is a fundamental process characterized by the uptake of extracellular materials and cell surface proteins (Fan et al. 2015), mediating the recycling of membranes, ion channels and surface cell receptors, thus contributing to the perception of extracellular cues (Dhonukshe et al. 2007; Taylor 2011; Stefano et al. 2015). Taking these features into account, this dissertation describes the work developed to explore the possibility that the ER may directly generate intermediate compartments that might be placed in both the secretory and endocytic trafficking routes, representing a link between the two pathways.

The strategy defined for this study involved the use of plants that exhibit defects at the ER level so that we could better understand the influence of the ER in the vacuolar and endocytic pathways. *Arabidopsis thaliana* plants were selected as a model organism because of all the advantages this organism presents and that were previously mentioned (section 1.4.). Benefiting from the available bioinformatics resources, five mutated lines were chosen from the Nottingham Arabidopsis Stock Centre (NASC) database. Those lines are as follows: 68719 - *syp22-1 syp23 or vam3-1 plp* (Shirakawa et al. 2010); 68909 - *sec24a-2* (Qu et al. 2014); 69075 - *nai GFP-h* (Matsushima et al. 2004); 69077 - *nai2-2* (Yamada et al. 2008); 69081 - *leb-2 GFP-h* (unpublished). i) The first line mentioned (*syp22-1 syp23 or vam3-1 plp*) was generated by Shirakawa et al. (2010) to thoroughly analyse vacuolar Qa-SNAREs (group Qa- of soluble N-ethylmaleimide-sensitive factor attachment protein receptor), thought to be involved in protein trafficking between pre-vacuolar compartments and vacuoles, by producing mutants of *SYP2* family genes. Shirakawa et al. (2010) suggested that SYP21, SYP22

and SYP23 function redundantly in vacuolar protein transport, vein patterning, myrosin cell differentiation and plant growth, although it was observed that a deficiency of either *SYP21/PEP12* or *SYP23/PLP* in the *syp22* background resulted in a defect in vacuolar protein sorting. ii) The second line mentioned (*sec24a-2*) is mutated on a gene encoding a cargo-binding subunit of the coat protein complex II (COPII) vesicle complex that is involved in ER-to-Golgi trafficking in the early secretory pathway. This mutant presented defects on both the ER and Golgi morphology, with abnormalities being consistent with what is previously described for other *sec24a* alleles (Faso et al. 2009; Nakano et al. 2009; Qu et al. 2014). iii) With a single base pair change at the intron splicing acceptor site of the At2g22770 gene, the *nai1* mutant (*nai GFP-h*) revealed that the *NAI1* gene is involved in the regulation of the development of ER bodies, a spindle-shaped ER-derived structure that specifically accumulates high levels of β-glucosidase PYK10/BGLU23 bearing an ER-retention signal (Matsushima et al. 2003b; Yamada et al. 2008), since the mutation on this gene suppresses the formation of such structures (Matsushima et al. 2004). iv) Similarly, the *nai2-2* mutant has also repercussions concerning the ER body. It was observed that *NAI2* is a key factor on ER body formation and the mutation on its gene (At3g15950), encoding a member of a unique protein family that is only found in the *Brassicaceae*, resulted in a reduction in expression of this gene that led to elongated and fewer in number ER bodies (Yamada et al. 2008). v) Finally, regarding the *leb-2 GFP-h* mutant, there is no publication describing it yet. However, it is known that this mutated line has a single nucleotide change (CCT→TCT) in the first exon of PYK10/BGLU23 gene, which causes an amino acid substitution (P41S) on the PYK10/BGLU23 protein.

Our work with these lines began by growing them and that was when we noticed differences in the development of these plants. This led us to perform a developmental assay, where we measured the time taken for each line to reach a determined developmental stage. Such stages of the chronological progression of the plants' growth (Cotyledons fully opened, Two rosette leaves, Three rosette leaves, Four rosette leaves, First flower buds visible, First flower open and Presence of first siliques) were defined based on the literature available (Boyes et al. 2001). The results obtained demonstrated that, except for the *syp22-1 syp23* line, the mutants' development was close to that of the wild-type line. The *syp22-1 syp23* line began to delay its development at the emergence of the first flower buds and this delay was maintained from this point forward, as it is the last line to present the first siliques. In fact, it had already been reported that *syp22* mutants exhibited semi-dwarfism and short midribs (Ohtomo et al. 2005; Ueda et al. 2006), and the mutation of *SYP21* and/or *SYP23* in *syp22* additively enhanced the

growth defects (Shirakawa et al. 2010). Also, Shirakawa et al. (2010) demonstrated a primary function for *SYP22* in plant growth, as of the single null mutants studied (*syp21*, *syp22* and *syp23*), only *syp22* showed dwarfism.

To further understand and characterize the effects of these mutations in these Arabidopsis lines, the ultrastructure of the cells from seedling and mature leaves was assessed through TEM. Here, the ER and associated vesicles, and the Golgi were given special attention so subtle phenotypes in these organelles could be detected, along with any other distinctive phenotypic trait, since the ultrastructure of the cells of these mutated lines was not included in the provided descriptions. Several features of these lines specially caught our eye. i) Starting with the *syp22-1 syp23* line, the chloroplasts of its seedlings were found to be more disorganized, comparing to the WT's and to those of the other mutated lines. All seedlings were of the same age (12-15 days old) when the tissue was prepared for TEM. This is consistent with the delay in growth we also observed for this line in the developmental assay and with what has been reported concerning the visual phenotype of this line (Shirakawa et al. 2010). ii) In the *sec24a-2* line, no major difference was observed from the WT, especially regarding ER and Golgi morphologies. This does not coincide with the abnormalities that have been described to both organelles' morphologies in this mutant (Qu et al. 2014). In fact, using the fluorescent Golgi marker ST-GFP, Qu et al. (2014) observed Golgi clumps that consisted of punctate and diffuse fluorescence and are highly similar to the abnormal globular structures described by (Faso et al. 2009). Similarly, morphological disruption of the ER as a consequence of mutations of *SEC24A* had already been described (Nakano et al. 2009) and this disorganized ER with globular structures was also reported for the *sec24a-2* line (Qu et al. 2014). iii) The *nai GFP-h* line shared many of its features with the other mutants and iv) the *nai2-2* line presented more pronounced and in higher amount Golgi bodies in the seedling leaf cells, while in the mature leaf this occurred for the ER. Moreover, not much is known about the cellular ultrastructure of these lines, aside from both *NAI* genes being linked to the formation and development of ER bodies (Matsushima et al. 2004; Yamada et al. 2008). The descriptions of these mutants refer the absence (Matsushima et al. 2004) and the reduction in number (Yamada et al. 2008) of ER bodies, and our observations are in line with this, since no structures of this kind were observed. v) Finally, in the *leb-2 GFP-h* line, we observed an intriguing structural anomaly in the ER. Although there is no published description for this line, there is another mutated line very similar to this, to which it is described the presence of significantly fewer and larger ER bodies than the wild-type line (Nagano et al. 2009). This mutant, *leb-1*, is characterized by an amino acid substitution of cysteine (Cys29) with

tyrosine (C29Y) on PYK10, a major component protein of ER bodies (Nagano et al. 2009), and we know the *leb-2 GFP-h* mutant to have a similar mutation (an amino acid substitution of proline (Pro41) with serine (P41S)). The structure we observed in the *leb-2 GFP-h* line could correspond to the long ER bodies observed by Nagano et al. (2009). Additionally, in our observations, some common features to the mutant lines were established: the presence of huge well-defined starch granules and the enlarged Golgi cisternae. Along with these features, also numerous vesicles were observed in the cell's cytoplasm, which may be indicative of high metabolic activity in the cell.

As we noticed that chloroplasts and starch granules were very different in size between all lines, we decided to measure them in both leaf tissues so we could have a quantitative perspective of these differences. The perimeter of chloroplasts and starch granules was measured in seedling and mature leaves. The size of the chloroplast is influenced by the presence of the starch granules, i.e., when starch granules are present, the chloroplast tends to be bigger. This is translated in our measurements. As it may be observed, for the wild-type line, in seedlings, no granules were found and the chloroplasts were the smallest, whereas, in mature leaves, the appearance of the granules increases the size of the chloroplast (Figure 3.8). A similar pattern is observed for the mutant lines (Figure 3.8). Along the development from seedling leaves to mature leaves in Arabidopsis wild-type plants, chloroplasts with the increase in the photosynthetic activity and starch storage, evident by the starch granules, are transformed in chloro-amyloplasts. However, in the Arabidopsis mutant lines, chloro-amyloplasts are seen from the early stages of development, since they occur in seedling leaves, and persist in mature leaves, except for *nai GFP-h* plantlets. The increase in the chloroplasts perimeter and, therefore, chloroplast volume is a result of the starch granules accumulation (Figure 3.8). Again, in mature leaves of *nai GFP-h* plants, chloroplasts, which do not accumulate starch granules, are smaller than the chloro-amyloplasts in the leaves of the other mutants. It is known that the starch accumulation or mobilization is not the main factor involved in the regulation of the photosynthesis; however, the starch dissipation from mature leaves of *nai GFP-h* plants could be the result of an impair in sucrose synthesis and starch accumulation or the result of an increase in sucrose translocation and distribution within the plant body. Considering that the development of *nai GFP-h* mutants was kept in path with that of control plants, this hypothesis of increased photo-assimilates translocation for growth and development deserves further research.

4.2. Definition of trafficking pathways in ER-defective plants

For the past years, our team has been specially interested in cardosin A and cardosin B PSIs-mediated sorting routes (Pereira et al. 2013; Vieira et al. 2019) and such studies have helped unveil novel unconventional vacuolar sorting routes. This was the case of PSI A, since it would still accumulate in the vacuole when co-expressed with the dominant negative mutant $SarI^{H74L}$ in *N. tabacum* leaves, indicating that this domain does not require the normal COPII vesicle machinery in order to traffic between the ER and the Golgi. As an alternative, the proteinase's sorting mediated by PSI A would lead it directly to the vacuole, bypassing the Golgi (Vieira et al. 2019). However, this was not the case of PSI B. By blocking the COPII vesicles, the proteins accumulated in the ER in *N. tabacum* leaves. Although they share high similarity, the existent differences function-wise do not go unnoticed. Additionally, the PSI A and PSI B domains' capacity to direct proteins to the vacuole led them to be classified as vacuolar sorting domains, since no match has been accounted for to any of the classic VSD types (Pereira et al. 2013; Vieira et al. 2019). Other influencing factors of the vacuolar routes may be the cell type and the stage of development, as in *Cynara cardunculus* cardosin A is mostly found in the PSVs of the stigmatic papillae, whereas cardosin B appears in the extracellular matrix of both stigma and style transmitting tissue (Ramalho-Santos et al. 1997; Vieira et al. 2001; Duarte et al. 2008). When expressing these enzymes in heterologous systems, like *Arabidopsis thaliana* and *Nicotiana tabacum*, cardosin A's accumulation is observed in different types of vacuoles (PSV and LV) (Duarte et al. 2008; Pereira et al. 2013), and cardosin B accumulates in the LVs (da Costa et al. 2010). These characteristics make cardosins puzzling and solidify the evidence for their advantage as reporters for the study of vacuolar trafficking and VSDs in plants.

4.2.1. Expression of the PSIs and the effect of BFA

To understand if the PSIs trafficking routes would be influenced by the ER morphological defects of the selected Arabidopsis lines, PSI A and PSI B fused with mCherry were expressed in such lines (section 2.4) and their localization was visualized through Confocal Microscopy, as described in section 2.6.1. Our initial approach involved the use of photoconvertible fluorescent tag mEos 3.2, allowing us to visualise the PSIs' accumulation site and where they were being produced *de novo*. However, after successfully obtaining these constructs, when they were tested in the plants (*A. thaliana* and *N. tabacum*), the photoconversion wouldn't work, so we decided to go back to the mCherry tag and use it instead. The localization of the PSIs was evaluated three days after the infiltration.

Starting with the PSI A and PSI B expression, we observed that PSI A was mostly localized in the vacuole in all lines and the PSI B was observed also in the vacuole, but it presented some secretion, as it was also localized in the periphery of the cell (cell wall and some in extracellular space). The vacuolar localization of the PSI A in our Arabidopsis mutant lines is consistent with what has been previously described in heterologous systems (Duarte et al. 2008; Pereira et al. 2013). To solidify these observations, a quantitative analysis was conducted, and the vacuolar accumulation of the PSI A was confirmed for all lines (WT, *sec24a-2*, *nai2-2*, *nai GFP-h* and *leb-2 GFP-h* lines). Such results strengthen the view of the PSI A as a vacuolar sorting domain, as it was efficient in leading the mCherry tag to the vacuole and, therefore, seems to be not affected by the ER morphological defects

The case of the PSI B presented some differences. Our results revealed that the PSI B was mainly accumulated in the vacuole, as expected, but had a very pronounced secretion to the extracellular space, especially in the *nai2-2* and *nai GFP-h* mutated lines. On the other hand, in *sec24a-2* and *leb-2 GFP-h* mutants, this secretion was much less pronounced. Despite more information is needed to fully understand how alterations in the ultrastructure influences how the proteins leave ER, the shift towards the vacuole or cell wall are an indication that indeed the ER integrity is crucial for signal recognition. The work by Soares da Costa and co-workers (2010) in our lab had shown cardosin B's accumulation in the LVs, but the authors also mention its detection at the cell wall. Given its location in the native system (*Cynara cardunculus*), cardosin B's secretion has been suggested to be tissue specific (Pissarra et al. 2007), with cardosin B being secreted in specialized organs, such as flowers and seeds and vacuolar in vegetative tissues, which are the case of fully expanded leaves. It is worth noting, that the images presented here correspond to the cotyledonary cells and we may argue that these cells constitute a transition stage with characteristics and cellular machinery of both seed tissue and vegetative tissue. Nevertheless, it seems an interesting stage to uncover in more detail the mechanisms of PSI B, and as consequence cardosin B mediated sorting.

To further scrutinize the protein trafficking mediated by the PSIs and evaluate if the localization patterns previously observed were maintained, we re-infiltrated plants transiently expressing these domains with Brefeldin A (BFA). This is a fungal macrocyclic lactone that has been widely used to inhibit secretion and vacuolar protein transport in plant cells, as it blocks the recruitment of COPI coat proteins onto Golgi membranes, which leads to the direct fusion of most Golgi cisternae to the ER, ultimately ending in the formation of an ER-Golgi hybrid compartment (Nebenführ et al. 2002). So, one day after the plants were infiltrated with the PSIs fused with the mCherry tag, such plants

were exposed for 16-18 h to BFA. Our observations revealed that the PSI A domain fused with the mCherry tag was mostly detected in the vacuole, although some residual secretion was observed. In the case of PSI B, it was detected both in the vacuole and secreted. The quantitative analysis, once again, solidified our observations and allowed us to better visualize the effect of BFA in the Arabidopsis mutants. In fact, and in accordance with the literature, the secretion observed for both PSIs without BFA was decreased in the presence of this drug. However, instead of being retained in the ER/Golgi, both PSIs were still detected in the vacuole. One explanation for this could be the timing of drug exposure not being the best for trafficking blockage, i.e., when the plants were exposed to BFA, PSI A and PSI B could already be close to the vacuole or the cell's periphery. However, this is a complex situation, because even though both PSIs have the ability to sort proteins to the vacuole, they do it in very different ways. It has been demonstrated that the PSI A-mediated route bypasses the Golgi, whereas the route mediated by PSI B is more conventional (ER-Golgi-Vacuole) (Pereira et al. 2013). Another difference concerns the vesicle carries involved in the transport from the ER to the Golgi: the PSI A-mediated sorting is COPII-independent, while the PSI B-mediated sorting is COPII-dependent (Vieira et al. 2019). So, considering this, our results of the PSI A localisation in plants treated with BFA correspond to what we expected, since the route mediated by this domain takes the protein from the ER to the vacuole, bypassing the Golgi. In the case of PSI B, our results may be indicative of an insufficient BFA sensitivity, since this domain was still secreted and detected in the vacuole, in spite of being retained in the ER.

4.2.2. Co-expression of the PSIs with FM2-10

To check for possible intermediate compartments shared between the secretory and endocytic pathways, our Arabidopsis mutants transiently expressing PSI A and PSI B were stained with the FM2-10 dye. Such dyes were originally advanced for *in vivo* staining of synaptic vesicles (Beta and Bewick 1992), later refined for following endo- and exocytosis in animal cells (Betz et al. 1996) and have proved to be immensely useful in studying endocytosis and recycling processes of the plasma membrane in other organisms (Bolte et al. 2004; Šamajová et al. 2012; Malínská et al. 2014). The styryl dye N-(3-triethylammoniumpropyl)-4-(6-(4-(diethylamino) phenyl) hexatrienyl) pyridinium dibromide (FM4-64) is the more commonly used in plants, but others similar to this may also be used, such as FM2-10. Given its amphiphilic nature, FM4-64 emits strong fluorescence in hydrophobic environments, like lipid rich membranes (Rigal et al. 2015). When applied exogenously, this dye will rapidly stain the plasma membrane and soon begins to be internalized (Malínská et al. 2014; Rigal et al. 2015). Once in endocytic

vesicles, FM4-64 may overtake numerous destinations in the cells, including early endosomes, intermediate membrane vesicles, TGN or late endosomal compartments, PVC/MVB, vacuoles and also exocytic vesicles recycled to the plasma membrane (Jürgens 2004; Šamaj et al. 2005; Hicks and Raikhel 2010; Reyes et al. 2011; Malínská et al. 2014; Rigal et al. 2015). Given these properties, we decided to use the FM2-10 dye, because its fluorescence wouldn't interfere with the mCherry dye, and both could be simultaneously observed. Moreover, the molecular structure of these two dyes is very similar (Meckel et al. 2004), so we expected that it would not affect the cell's machinery.

In plants transiently expressing PSI A, some co-localization was observed in the WT and *nai2-2* lines at the cell's periphery, while the *sec24a-2* mutant exhibited no co-localization. With PSI B, co-localization was only observed in the *nai2-2* line. The observed seedlings were stained with FM2-10 for 2-3 h, prior to cell imaging, and this was done two days after the infiltration with the PSIs. At this timing of expression, the PSIs could still be trafficking to their sorted destination, so an intersection with the incoming dye was a possibility. On the other hand, as the dye was mostly restrained to the cell's periphery, it is possible that the tissue was not stained enough timewise for the dye to be fully incorporated into endocytic vesicle and progress further into the endocytic pathway. Therefore, it is likely that this assay requires some optimization, so the endocytosis might be better analysed.

4.2.3. Western blotting analysis of PSI B secretion

Finally, to further confirm our observations of PSI B's secretion, the extracellular protein content of seedlings of the WT and mutated lines infiltrated with PSI B fused with mCherry was isolated and examined through Western blotting, as described in section 2.7. For this assay, to guarantee the veracity of the bands in the blot, two controls were used: an extract of total protein content of seedlings that stably express the PSI B (a line developed in our laboratory by a fellow researcher) was used as the control sample and, to ensure the extracellular protein content was not contaminated by intracellular proteins, an antibody against the H3 histone was also used. In fact, the expected band of 15 kDa for the PSI B was detected in the extracellular protein content of the *nai GFP-h*, *nai2-2*, *sec24a-2,* and *leb-2 GPF-h* lines infiltrated with this domain, with and without the BFA treatment. However, conversely to what had been observed through Confocal Microscopy, in the WT line no secretion was detected. This could be due to an inefficient infiltration and/or extraction of the extracellular proteins. Nevertheless, this assay should be repeated.

5. CONCLUSIONS

In a complex network as the endomembrane system, the coordination and control of sorting and trafficking events are extremely important for the cell's proper function. The secretory and endocytic pathways are two crucial routes of the endomembrane system that require a tight and precise mechanism of control. To better understand how such mechanisms operate and how a protein travels in the cell, we must look at the signals directing this traffic. The PSIs can be used to decipher this intricate protein sorting since these domains have been shown to be able to direct proteins to the vacuole through conventional (PSI B) and unconventional (PSI A) routes (Vieira et al. 2019). Moreover, considering that this sorting must be defined early in the pathway, the ER, being a central organelle of the secretory pathway, must also have some influence on the route a protein takes to its final destination. To complicate things further, given its role in membrane recycling, perception of external cues and in internalization of macromolecules, endocytosis must similarly be under tight regulation and coordinate with the membrane compartments inside the cell.

In this study, as we aimed to understand the ER's influence on protein sorting, we selected five *Arabidopsis thaliana* lines with alterations on the ER morphology (*syp22-1 syp23 or vam3-1 plp*, *sec24a-2*, *nai GFP-h*, *nai2-2* and *leb-2 GFP-h*), which we used as working organism in all our experiments. Regarding the expression of both PSIs in such mutants, we were able to successfully infiltrate the plants with the PSIs fused to the widely used mCherry tag. Also, this allowed us to optimize Arabidopsis as a transient system for the expression of such markers, as this plant enables the study of protein trafficking mediated by the PSIs in tissues with characteristics typical of both seed tissue and vegetative tissue.

Considering all the work here presented, this study provided useful information regarding the sorting of proteins in plants presenting defects at the ER level, adding interesting components to what is known about this domain. In fact, it is possible to conclude that alterations in the ER structure or components does effect at some extent vacuolar trafficking, or at least the way vacuolar proteins leave the ER. Despite we are still far from understanding the mechanisms behind the localization patterns observed, our results represent an interesting starting point to scrutinize the crosstalk between the secretory and endocytic pathways, as further analysis beyond what is here presented is necessary for the construction of the bigger picture that is the complexity of vacuolar sorting mechanisms.

6. REFERENCES

Afrin T, Diwan D, Sahawneh K, Pajerowska-Mukhtar K (2020) Multilevel regulation of endoplasmic reticulum stress responses in plants: Where old roads and new paths meet. Journal of Experimental Botany 71:1659–1667. https://doi.org/10.1093/jxb/erz487

Aguilar RC, Wendland B (2005) Endocytosis of membrane receptors: Two pathways are better than one. Proceedings of the National Academy of Sciences of the United States of America 102:2679 LP – 2680. https://doi.org/10.1073/pnas.0500213102

Alberts B, Johnson A, Lewis J, Raff M, Roberts K, Walter P (2002) Transport from the ER through the Golgi apparatus. In: Molecular Biology of the Cell. 4th edition. Garland Science

Alonso JM, Stepanova AN, Leisse TJ, Kim C, Chen H, Shinn P, Stevenson D, Zimmerman J, Barajas P, Cheuk R, Gadrinab C, Heller C, Jeske A, Koesema E, Meyers C, Parker H, Prednis L, Ansari Y, Choy N, Deen H, Geralt M, Hazari N, Hom E, Karnes M, Mulholland C, Ndubaku R, Schmidt I, Guzman P, Aguilar-Henonin L, Schmid M, Weigel D, Carter D, Marchand T, Risseeuw E, Brogden D, Zeko A, Crosby W, Berry C, Ecker J (2003) Genome-Wide Insertional Mutagenesis of Arabidopsis thaliana. Science 301:653–657. https://doi.org/10.1126/SCIENCE.1086391

Altan-Bonnet N, Phair RD, Polishchuk RS, Weigert R, Lippincott-Schwartz J (2003) A role for Arf1 in mitotic Golgi disassembly, chromosome segregation, and cytokinesis. Proceedings of the National Academy of Sciences 100:13314 LP – 13319. https://doi.org/10.1073/pnas.2234055100

Ang AL, Taguchi T, Francis S, Fölsch H, Murrells L, Pypaert M, Warren G, Mellman I (2004) Recycling endosomes can serve as intermediates during transport from the Golgi to the plasma membrane of MDCK cells. Journal of Cell Biology 167:531–543. https://doi.org/10.1083/jcb.200408165

Appenzeller-Herzog C, Hauri H-P (2006) The ER-Golgi intermediate compartment (ERGIC): in search of its identity and function. Journal of Cell Science 119:2173–2183. https://doi.org/10.1242/jcs.03019

Baerenfaller K, Grossmann J, Grobei MA, Hull R, Hirsch-Hoffmann M, Yalovsky S, Zimmermann P, Grossniklaus U, Gruissem W, Baginsky S (2008) Genome-Scale

Proteomics Reveals Arabidopsis thaliana Gene Models and Proteome Dynamics. Science 320:938–941. https://doi.org/10.1126/SCIENCE.1157956

Baluška F, Šamaj J, Hlavacka A, Kendrick-Jones J, Volkmann D (2004) Actin-dependent fluid-phase endocytosis in inner cortex cells of maize root apices. Journal of Experimental Botany 55:463–473. https://doi.org/10.1093/jxb/erh042

Bassham DC, Brandizzi F, Otegui MS, Sanderfoot AA (2008) The Secretory System of Arabidopsis. The Arabidopsis Book 6:e0116. https://doi.org/10.1199/TAB.0116

Becker B, Melkonian M (1996) The secretory pathway of protists: spatial and functional organization and evolution. Microbiological Reviews 60:697–721. https://doi.org/10.1128/mr.60.4.697-721.1996

Benning C (2009) Mechanisms of Lipid Transport Involved in Organelle Biogenesis in Plant Cells. Annual Review of Cell and Developmental Biology 25:71–91. https://doi.org/10.1146/annurev.cellbio.042308.113414

Bernales S, McDonald KL, Walter P (2006) Autophagy Counterbalances Endoplasmic Reticulum Expansion during the Unfolded Protein Response. PLOS Biology 4:e423. https://doi.org/10.1371/JOURNAL.PBIO.0040423

Bernat-Silvestre C, de Sousa Vieira V, Sánchez-Simarro J, Aniento F, Marcote M (2021) Transient Transformation of A. thaliana Seedlings by Vacuum Infiltration. In: Methods in Molecular Biology. Humana Press Inc., pp 147–155

Bethke PC, Jones RL (2000) Vacuoles and prevacuolar compartments. Current Opinion in Plant Biology 3:469–475. https://doi.org/10.1016/S1369-5266(00)00115-1

Betz WJ, Bewick GS (1992) Optical analysis of synaptic vesicle recycling at the frog neuromuscular junction. Science 255:200–203. https://doi.org/10.1126/science.1553547

Betz WJ, Mao F, Smith CB (1996) Imaging exocytosis and endocytosis. Current Opinion in Neurobiology 6:365–371. https://doi.org/10.1016/S0959-4388(96)80121-8

Boevink P, Oparka K, Cruz SS, Martin B, Betteridge A, Hawes C (1998) Stacks on tracks: the plant Golgi apparatus traffics on an actin/ER network†. The Plant Journal 15:441–447. https://doi.org/https://doi.org/10.1046/j.1365-313X.1998.00208.x

Bolte S, Talbot C, Boutte Y, Catrice O, Read N, Satiat-Jeunemaitre B (2004) FM-dyes as experimental probes for dissecting vesicle trafficking in living plant cells. In: Journal of Microscopy. Blackwell Publishing Ltd, pp 159–173

Boncompain G, Weigel A V. (2018) Transport and sorting in the Golgi complex: multiple mechanisms sort diverse cargo. Current Opinion in Cell Biology 50:94–101. https://doi.org/10.1016/J.CEB.2018.03.002

Bonfanti L, Mironov AA, Martínez-Menárguez JA, Martella O, Fusella A, Baldassarre M, Buccione R, Geuze H, Mironov A, Luini A (1998) Procollagen Traverses the Golgi Stack without Leaving the Lumen of Cisternae: Evidence for Cisternal Maturation. Cell 95:993–1003. https://doi.org/10.1016/S0092-8674(00)81723-7

Bonifacino JS, Traub LM (2003) Signals for Sorting of Transmembrane Proteins to Endosomes and Lysosomes. Annual Review of Biochemistry 72:395–447. https://doi.org/10.1146/annurev.biochem.72.121801.161800

Boyes DC, Zayed AM, Ascenzi R, McCaskill A, Hoffman N, Davis K, Görlach J (2001) Growth Stage–Based Phenotypic Analysis of Arabidopsis: A Model for High Throughput Functional Genomics in Plants. The Plant Cell 13:1499–1510. https://doi.org/10.1105/TPC.010011

Braulke T, Bonifacino JS (2009) Sorting of lysosomal proteins. Biochimica et Biophysica Acta (BBA) - Molecular Cell Research 1793:605–614. https://doi.org/10.1016/J.BBAMCR.2008.10.016

Cacas JL, Buré C, Grosjean K, Gerbeau-Pissot P, Lherminier J, Rombouts Y, Maes E, Bossard C, Gronnier J, Furt F, Fouillen L, Germain V, Bayer E, Cluzet S, Robert F, Schmitter J, Deleu M, Lins L, Simon-Plas F, Mongrand S (2016) Revisiting plant plasma membrane lipids in tobacco: A focus on sphingolipids. Plant Physiology 170:367–384. https://doi.org/10.1104/pp.15.00564

Carrasco S, Meyer T (2011) STIM Proteins and the Endoplasmic Reticulum-Plasma Membrane Junctions. Annual Review of Biochemistry 80:973–1000. https://doi.org/10.1146/annurev-biochem-061609-165311

Carter C, Pan S, Zouhar J, Avila E, Girke T, Raikhel N (2004) The Vegetative Vacuole Proteome of Arabidopsis thaliana Reveals Predicted and Unexpected Proteins. The Plant Cell 16:3285–3303. https://doi.org/10.1105/tpc.104.027078

Cassim AM, Gouguet P, Gronnier J, Laurent N, Germain V, Grison M, Boutté Y, Gerbeau-Pissot P, Simon-Plas F, Mongrand S (2019) Plant lipids: Key players of plasma membrane organization and function. Progress in Lipid Research 73:1–27

Cevher-Keskin B (2020) Endomembrane Trafficking in Plants. Electrodialysis 1–22. https://doi.org/10.5772/intechopen.91642

Chen M, Markham JE, Dietrich CR, Jaworski J, Cahoon E (2008) Sphingolipid Long-Chain Base Hydroxylation Is Important for Growth and Regulation of Sphingolipid Content and Composition in Arabidopsis. The Plant Cell 20:1862–1878. https://doi.org/10.1105/tpc.107.057851

Chen X, Irani NG, Friml J (2011) Clathrin-mediated endocytosis: The gateway into plant cells. Current Opinion in Plant Biology 14:674–682. https://doi.org/10.1016/j.pbi.2011.08.006

Chen Y-F, Randlett MD, Findell JL, Schaller GE (2002) Localization of the Ethylene Receptor ETR1 to the Endoplasmic Reticulum of Arabidopsis*. Journal of Biological Chemistry 277:19861–19866. https://doi.org/10.1074/jbc.M201286200

Chen YN, Slabaugh E, Brandizzi F (2008) Membrane-tethered transcription factors in Arabidopsis thaliana: novel regulators in stress response and development. Current Opinion in Plant Biology 11:695–701. https://doi.org/10.1016/J.PBI.2008.10.005

Cheng C-Y, Krishnakumar V, Chan AP, Thibaud-Nissen F, Schobel S, Town C (2017) Araport11: a complete reannotation of the Arabidopsis thaliana reference genome. The Plant Journal 89:789–804. https://doi.org/https://doi.org/10.1111/tpj.13415

Chrispeels MJ (1983) The Golgi apparatus mediates the transport of phytohemagglutinin to the protein bodies in bean cotyledons. Planta 158:140–151. https://doi.org/10.1007/BF00397707

Costa DS da, Pereira S, Pissarra J (2011) The heterologous systems in the study of cardosin b trafficking pathways. Plant Signaling and Behavior 6:895–897. https://doi.org/10.4161/psb.6.6.15321

Costaguta G, Stefan CJ, Bensen ES, Emr S, Payne G (2001) Yeast Gga Coat Proteins Function with Clathrin in Golgi to Endosome Transport. Molecular Biology of the Cell 12:1885–1896. https://doi.org/10.1091/mbc.12.6.1885

Curtis MD, Grossniklaus U (2003) A Gateway Cloning Vector Set for High-Throughput Functional Analysis of Genes in Planta. Plant Physiology 133:462–469. https://doi.org/10.1104/pp.103.027979

Curto P, Lufrano D, Pinto C, Custódio V, Gomes A, Trejo S, Bakás L, Vairo-Cavalli S, Faro C, Simões I (2014) Establishing the Yeast Kluyveromyces lactis as an Expression Host for Production of the Saposin-Like Domain of the Aspartic Protease Cirsin. Applied and Environmental Microbiology 80:86–96. https://doi.org/10.1128/AEM.03151-13

da Costa DS, Pereira S, Moore I, Pissarra J (2010) Dissecting cardosin B trafficking pathways in heterologous systems. Planta 232:1517–1530. https://doi.org/10.1007/s00425-010-1276-9

de Caroli M, Lenucci MS, di Sansebastiano G-P, Dalessandro G, De Lorenzo G, Piro G (2011) Protein trafficking to the cell wall occurs through mechanisms distinguishable from default sorting in tobacco. The Plant Journal 65:295–308. https://doi.org/https://doi.org/10.1111/j.1365-313X.2010.04421.x

De Marchis F, Bellucci M, Pompa A (2013) Unconventional pathways of secretory plant proteins from the endoplasmic reticulum to the vacuole bypassing the Golgi complex. Plant Signaling & Behavior 8:e25129. https://doi.org/10.4161/psb.25129

De Moura DC, Bryksa BC, Yada RY (2014) In Silico Insights into Protein-Protein Interactions and Folding Dynamics of the Saposin-Like Domain of Solanum tuberosum Aspartic Protease. PLOS ONE 9:e104315

Deloche O, Yeung BG, Payne GS, Schekman R (2001) Vps10p Transport from the trans-Golgi Network to the Endosome Is Mediated by Clathrin-coated Vesicles. Molecular Biology of the Cell 12:475–485. https://doi.org/10.1091/mbc.12.2.475

Dhonukshe P, Aniento F, Hwang I, Robinson D, Mravec J, Stierhof Y, Friml J (2007) Clathrin-Mediated Constitutive Endocytosis of PIN Auxin Efflux Carriers in Arabidopsis. Current Biology 17:520–527. https://doi.org/10.1016/j.cub.2007.01.052

di Sansebastiano G Pietro, Barozzi F, Piro G, Denecke J, de Marcos Lousa C (2018) Trafficking routes to the plant vacuole: connecting alternative and classical pathways. Journal of Experimental Botany 69:79–90. https://doi.org/10.1093/jxb/erx376

Diaz M (2019) Arabidopsis Thaliana: From Weed to Model Organism. Current Protocols in Essential Laboratory Techniques 19:1–14. https://doi.org/10.1002/cpet.38

Doignon F, Laquel P, Testet E, Tuphile K, Fouillen L, Bessoule J (2016) Requirement of Phosphoinositides Containing Stearic Acid To Control Cell Polarity. Molecular and Cellular Biology 36:765–780. https://doi.org/10.1128/MCB.00843-15

Donaldson JG, Lippincott-Schwartz J (2000) Sorting and Signaling at the Golgi Complex. Cell 101:693–696. https://doi.org/10.1016/S0092-8674(00)80881-8

Doray B, Ghosh P, Griffith J, Geuze H, Kornfeld S (2002) Cooperation of GGAs and AP-1 in Packaging MPRs at the Trans-Golgi Network. Science 297:1700–1703. https://doi.org/10.1126/science.1075327

Du Y, Tejos R, Beck M, Himschoot E, Li H, Robatzek S, Vanneste S, Friml J (2013) Salicylic acid interferes with clathrin-mediated endocytic protein trafficking. Proceedings of the National Academy of Sciences 110:7946 LP – 7951. https://doi.org/10.1073/pnas.1220205110

Duarte P, Pissarra J, Moore I (2008) Processing and trafficking of a single isoform of the aspartic proteinase cardosin a on the vacuolar pathway. Planta 227:1255–1268. https://doi.org/10.1007/s00425-008-0697-1

Dunphy WG, Rothman JE (1985) Compartmental organization of the golgi stack. Cell 42:13–21. https://doi.org/10.1016/S0092-8674(85)80097-0

Dupree P, Sherrier DJ (1998) The plant Golgi apparatus. Biochimica et Biophysica Acta - Molecular Cell Research 1404:259–270. https://doi.org/10.1016/S0167-4889(98)00061-5

Earley KW, Haag JR, Pontes O, Opper K, Juehne T, Song K, Pikaard C (2006) Gateway-compatible vectors for plant functional genomics and proteomics. The Plant Journal 45:616–629. https://doi.org/https://doi.org/10.1111/j.1365-313X.2005.02617.x

Echeverría E (2000) Vesicle-Mediated Solute Transport between the Vacuole and the Plasma Membrane1. Plant Physiology 123:1217–1226. https://doi.org/10.1104/pp.123.4.1217

Egas C, Lavoura N, Resende R, Brito R, Pires E, Pedroso De Lima M, Faro C (2000) The saposin-like domain of the plant aspartic proteinase precursor is a potent inducer of vesicle leakage. Journal of Biological Chemistry 275:38190–38196. https://doi.org/10.1074/jbc.M006093200

Eisenach C, Francisco R, Martinoia E (2015) Plant vacuoles. Current Biology 25:R136–R137

English AR, Voeltz GK (2013) Endoplasmic reticulum structure and interconnections with other organelles. Cold Spring Harbor perspectives in biology 5:a013227

Etxeberria E, Gonzalez P, Pozueta J (2009) Evidence for two endocytic transport pathways in plant cells. Plant Science 177:341–348. https://doi.org/10.1016/j.plantsci.2009.06.014

Fan L, Li R, Pan J, Ding Z, Lin J (2015) Endocytosis and its regulation in plants. Trends in Plant Science 20:388–397. https://doi.org/10.1016/j.tplants.2015.03.014

Farquhar MG (1985) Progress in Unraveling Pathways of Golgi Traffic. Annual Review of Cell Biology 1:447–488. https://doi.org/10.1146/annurev.cb.01.110185.002311

Faso C, Chen Y-NN, Tamura K, Held M, Zemelis S, Marti L, Saravanan R, Hummel E, Kung L, Miller E, Hawes C, Brandizzia F, Brandizzi F (2009) A Missense Mutation in the Arabidopsis COPII Coat Protein Sec24A Induces the Formation of Clusters of the Endoplasmic Reticulum and Golgi Apparatus. The Plant Cell 21:3655–3671. https://doi.org/10.1105/tpc.109.068262

Feraru E, Paciorek T, Feraru MI, Zwiewka M, De Groodt R, De Rycke R, Kleine-Vehn J, Friml J (2010) The AP-3 β Adaptin Mediates the Biogenesis and Function of Lytic Vacuoles in Arabidopsis. The Plant Cell 22:2812–2824. https://doi.org/10.1105/tpc.110.075424

Frey ME, D'Ippolito S, Pepe A, Daleo G, Guevara M (2018) Transgenic expression of plant-specific insert of potato aspartic proteases (StAP-PSI) confers enhanced resistance to Botrytis cinerea in Arabidopsis thaliana. Phytochemistry 149:1–11. https://doi.org/10.1016/j.phytochem.2018.02.004

Frigerio L, Hawes C (2008) The endomembrane system: A green perspective. Traffic 9:1563. https://doi.org/10.1111/J.1600-0854.2008.00795.X

Frigerio L, Hinz G, Robinson DG (2008) Multiple vacuoles in plant cells: Rule or exception? Traffic 9:1564–1570. https://doi.org/10.1111/j.1600-0854.2008.00776.x

Fuji K, Shimada T, Takahashi H, Tamura K, Koumoto Y, Utsumi S, Nishizawa K, Maruyama N, Hara-Nishimura I (2007) Arabidopsis Vacuolar Sorting Mutants (green fluorescent seed) Can Be Identified Efficiently by Secretion of Vacuole-Targeted Green Fluorescent Protein in Their Seeds. The Plant Cell 19:597–609. https://doi.org/10.1105/tpc.106.045997

Furt F, König S, Bessoule J-J, Sargueil F, Zallot R, Stanislas T, Noirot E, Lherminier J, Simon-Plas F, Heilmann I, Mongrand S (2010) Polyphosphoinositides Are Enriched in Plant Membrane Rafts and Form Microdomains in the Plasma Membrane. Plant Physiology 152:2173–2187. https://doi.org/10.1104/pp.109.149823

Furt F, Simon-Plas F, Mongrand S (2011) Lipids of the Plant Plasma Membrane. Plant Cell Monographs 19:3–30. https://doi.org/10.1007/978-3-642-13431-9_1

Galili G (2004) ER-Derived Compartments Are Formed by Highly Regulated Processes and Have Special Functions in Plants. Plant Physiology 136:3411–3413. https://doi.org/10.1104/PP.104.900125

Gerbeau-Pissot P, Der C, Thomas D, Anca I, Grosjean K, Roche Y, Perrier-Cornet J, Mongrand S, Simon-Plas F (2014) Modification of Plasma Membrane Organization in Tobacco Cells Elicited by Cryptogein . Plant Physiology 164:273–286. https://doi.org/10.1104/pp.113.225755

Ghedin E, Debrabant A, Engel JC, Dwyer DM (2001) Secretory and Endocytic Pathways Converge in a Dynamic Endosomal System in a Primitive Protozoan. Traffic 2:175–188. https://doi.org/https://doi.org/10.1034/j.1600-0854.2001.020304.x

Ghosh P, Dahms NM, Kornfeld S (2003) Mannose 6-phosphate receptors: new twists in the tale. Nature Reviews Molecular Cell Biology 4:202–213. https://doi.org/10.1038/nrm1050

Gibson DG, Young L, Chuang R-YY, Venter J, Hutchison C, Smith H (2009) Enzymatic assembly of DNA molecules up to several hundred kilobas1. In: Nature Methods. http://www.nature.com/articles/nmeth.1318. Accessed 8 Apr 2019

Glick BS, Malhotra V (1998) The Curious Status of the Golgi Apparatus. Cell 95:883–889. https://doi.org/10.1016/S0092-8674(00)81713-4

Glick BS, Nakano A (2009) Membrane traffic within the Golgi apparatus. Annual Review of Cell and Developmental Biology 25:113–132. https://doi.org/10.1146/annurev.cellbio.24.110707.175421

Grison MS, Brocard L, Fouillen L, Nicolas W, Wewer V, Dörmann P, Nacir H, Benitez-Alfonso Y, Claverol S, Germain V, Boutté Y, Mongrand S, Bayer E (2015) Specific Membrane Lipid Composition Is Important for Plasmodesmata Function in Arabidopsis. The Plant Cell 27:1228–1250. https://doi.org/10.1105/tpc.114.135731

Gronnier J, Gerbeau-Pissot P, Germain V, Mongrand S, Simon-Plas F (2018) Divide and Rule: Plant Plasma Membrane Organization. Trends in Plant Science 23:899–917. https://doi.org/10.1016/J.TPLANTS.2018.07.007

Grosjean K, Mongrand S, Beney L, Simon-Plas F, Gerbeau-Pissot P (2015) Differential Effect of Plant Lipids on Membrane Organization: SPECIFICITIES OF PHYTOSPHINGOLIPIDS AND PHYTOSTEROLS *. Journal of Biological Chemistry 290:5810–5825. https://doi.org/10.1074/jbc.M114.598805

Gupton SL, Collings DA, Allen NS (2006) Endoplasmic reticulum targeted GFP reveals ER organization in tobacco NT-1 cells during cell division. Plant Physiology and Biochemistry 44:95–105. https://doi.org/10.1016/J.PLAPHY.2006.03.003

Happel N, Höning S, Neuhaus J-M, Paris N, Robinson D, Holstein S (2004) ArabidopsisμA-adaptin interacts with the tyrosine motif of the vacuolar sorting receptor VSR-PS1. The Plant Journal 37:678–693. https://doi.org/https://doi.org/10.1111/j.1365-313X.2003.01995.x

Hara-Nishimura I, Hatsugai N (2011) The role of vacuole in plant cell death. Cell Death & Differentiation 18:1298–1304. https://doi.org/10.1038/cdd.2011.70

Hara-Nishimura I, Matsushima R, Shimada T, Nishimura M (2004) Diversity and Formation of Endoplasmic Reticulum-Derived Compartments in Plants. Are These Compartments Specific to Plant Cells? Plant Physiology 136:3435–3439. https://doi.org/10.1104/pp.104.053876

Hara-Nishimura I, Shimada T, Hatano K, Takeuchi Y, Nishimura M (1998) Transport of Storage Proteins to Protein Storage Vacuoles Is Mediated by Large Precursor-Accumulating Vesicles. The Plant Cell 10:825–836. https://doi.org/10.1105/tpc.10.5.825

Hatsugai N, Kuroyanagi M, Yamada K, Meshi T, Tsuda S, Kondo M, Nishimura M, Hara-Nishimura I (2004) A plant vacuolar protease, VPE, mediates, virus-induced hypersensitive cell death. Science 305:855–858. https://doi.org/10.1126/SCIENCE.1099859

Hawes C (2012) The ER/Golgi Interface – Is There Anything in-between? . Frontiers in Plant Science 3:73

Hayashi Y, Yamada K, Shimada T, Matsushima R, Nishizawa N, Nishimura M, Hara-Nishimura I (2001) A Proteinase-Storing Body that Prepares for Cell Death or Stresses in the Epidermal Cells of Arabidopsis. Plant and Cell Physiology 42:894–899. https://doi.org/10.1093/pcp/pce144

Heiland I, Erdmann R (2005) Biogenesis of peroxisomes. The FEBS Journal 272:2362–2372. https://doi.org/https://doi.org/10.1111/j.1742-4658.2005.04690.x

Henkel AW, Lübke J, Betz WJ (1996) FM1-43 dye ultrastructural localization in and release from frog motor nerve terminals. Proceedings of the National Academy of Sciences 93:1918 LP – 1923. https://doi.org/10.1073/pnas.93.5.1918

Herman E, Schmidt M (2004) Endoplasmic Reticulum to Vacuole Trafficking of Endoplasmic Reticulum Bodies Provides an Alternate Pathway for Protein Transfer to the Vacuole. Plant Physiology 136:3440–3446. https://doi.org/10.1104/pp.104.051722

Herman EM (2008) Endoplasmic reticulum bodies: solving the insoluble. Current Opinion in Plant Biology 11:672–679. https://doi.org/10.1016/J.PBI.2008.08.004

Hernandez LE, Perotto S, Brewin NJ, DrØbak BK (1995) A novel inositol-lipid in plant-bacteria symbiosis. Biochemical Society Transactions 23:582S-582S. https://doi.org/10.1042/bst023582s

Hetzer MW (2010) The nuclear envelope. Cold Spring Harbor perspectives in biology 2:a000539

Hicks GR, Raikhel N V. (2010) Advances in dissecting endomembrane trafficking with small molecules. Current Opinion in Plant Biology 13:706–713

Hinz G, Colanesi S, Hillmer S, Rogers J, Robinson D 2007) Localization of Vacuolar Transport Receptors and Cargo Proteins in the Golgi Apparatus of Developing Arabidopsis Embryos. Traffic 8:1452–1464. https://doi.org/https://doi.org/10.1111/j.1600-0854.2007.00625.x

Hinz G, Hillmer S, Bäumer M, Hohl I (1999) Vacuolar Storage Proteins and the Putative Vacuolar Sorting Receptor BP-80 Exit the Golgi Apparatus of Developing Pea Cotyledons in Different Transport Vesicles. The Plant Cell 11:1509–1524. https://doi.org/10.1105/tpc.11.8.1509

Hinz G, Menze A, Hohl I, Vaux D (1997) Isolation of prolegumin from developing pea seeds: its binding to endomembranes and assembly into prolegumin hexamers in the protein storage vacuole. Journal of Experimental Botany 48:139–149. https://doi.org/10.1093/jxb/48.1.139

Hoffmann MH (2002) Biogeography of Arabidopsis thaliana (L.) Heynh. (Brassicaceae). Journal of Biogeography 29:125–134. https://doi.org/10.1046/J.1365-2699.2002.00647.X

Hohl I, Robinson DG, Chrispeels MJ, Hinz G (1996) Transport of storage proteins to the vacuole is mediated by vesicles without a clathrin coat. Journal of Cell Science 109:2539–2550. https://doi.org/10.1242/jcs.109.10.2539

Hooper CM, Castleden IR, Tanz SK, Aryamanesh N, Millar A (2017) SUBA4: the interactive data analysis centre for Arabidopsis subcellular protein locations. Nucleic Acids Research 45:D1064–D1074. https://doi.org/10.1093/nar/gkw1041

Hwang I (2008) Sorting and Anterograde Trafficking at the Golgi Apparatus. Plant Physiology 148:673–683. https://doi.org/10.1104/pp.108.124925

Ibl V, Stoger E (2012) The formation, function and fate of protein storage compartments in seeds. Protoplasma 249:379–392. https://doi.org/10.1007/s00709-011-0288-z

Inada N, Ueda T (2014) Membrane trafficking pathways and their roles in plant-microbe interactions. Plant and Cell Physiology 55:672–686. https://doi.org/10.1093/pcp/pcu046

Iwaki T, Hosomi A, Tokudomi S, Kusunoki Y, Fujita Y, Giga-Hama Y, Tanaka N, Takegawa K (2006) Vacuolar protein sorting receptor in Schizosaccharomyces pombe. Microbiology 152:1523–1532. https://doi.org/10.1099/MIC.0.28627-0

Jiang L, Phillips TE, Hamm CA, Drozdowicz Y, Rea P, Maeshima M, Rogers S, Rogers J (2001) The protein storage vacuole: a unique compound organelle. Journal of Cell Biology 155:991–1002. https://doi.org/10.1083/jcb.200107012

Jiang L, Phillips TE, Rogers SW, Rogers JC (2000) Biogenesis of the Protein Storage Vacuole Crystalloid. Journal of Cell Biology 150:755–770. https://doi.org/10.1083/jcb.150.4.755

Jolliffe NA, Craddock CP, Frigerio L (2005) Pathways for protein transport to seed storage vacuoles. Biochemical Society Transactions 33:1016–1018. https://doi.org/10.1042/BST0331016

Jürgens G (2004) Membrane trafficking in plants. Annual Review of Cell and Developmental Biology 20:481–504. https://doi.org/10.1146/annurev.cellbio.20.082503.103057

Kaul S, Koo HL, Jenkins J, Rizzo M, Rooney T, Tallon L, Feldblyum T, Nierman W, Benito M, Lin X, Town C, Venter J, Fraser C, Tabata S, Nakamura Y, Kaneko T, Sato S, Asamizu E, Kato T, Kotani H, Sasamoto S, Ecker J, Theologis A, Federspiel N, Palm C, Osborne B, Shinn P, Dewar K, Kim C, Buehler E, Dunn P, Chao Q, Chen H, Theologis A, Osborne B, Vysotskaia V, Lenz C, Kim C, Hansen N, Liu S, Buehler E, Alta H, Sakano H, Dunn P, Lam B, Pham P, Chao Q, Nguyen M, Yu G, Chen H, Southwick A, Lee J, Miranda M, Toriumi M, Davis R, Federspiel N, Palm C, Conway A, Conn L, Hansen N, Hootan A, Lam B, Wambutt R, Murphy G, Düsterhöft A,

Stiekema W, Pohl T, Entian K, Terryn N, Volckaert G, Salanoubat M, Choisne N, Artiguenave F, Weissenbach J, Quetier F, Rieger M, Ansorge W, Unseld M, Fartmann B, Valle G, Wilson R, Sekhon M, Pepin K, Murray J, Johnson D, Hillier L, de la Bastide M, Huang E, Spiegel L, Gnoj L, Habermann K, Dedhia N, Parnell L, Preston R, Marra M, McCombie W, Chen E, Martienssen R, Mayer K, Lemcke K, Haas B, Haase D, Rudd S, Schoof H, Frishman D, Morgenstern B, Zaccaria P, Mewes H, White O, Creasy T, Bielke C, Maiti R, Peterson J, Ermolaeva M, Pertea M, Quackenbush J, Volfovsky N, Wu D, Salzberg S, Bevan M, Lowe T, Rounsley S, Bush D, Subramaniam S, Levin I, Norris S, Schmidt R, Acarkan A, Bancroft I, Brennicke A, Eisen J, Bureau T, Legault B, Le Q, Agrawal N, Yu Z, Copenhaver G, Luo S, Preuss D, Pikaard C, Paulsen I, Sussman M, Britt A, Selinger D, Pandey R, Chandler V, Jorgensen R, Mount D, Pikaard C, Juergens G, Meyerowitz E, Dangl J, Jones J, Chen M, Chory J, Somerville C (2000) Analysis of the genome sequence of the flowering plant Arabidopsis thaliana. Nature 408:796–815. https://doi.org/10.1038/35048692

Kilian J, Whitehead D, Horak J, Wanke D, Weinl S, Batistic O, D'Angelo C, Bornberg-Bauer E, Kudla J, Harter K (2007) The AtGenExpress global stress expression data set: protocols, evaluation and model data analysis of UV-B light, drought and cold stress responses. The Plant Journal 50:347–363. https://doi.org/https://doi.org/10.1111/j.1365-313X.2007.03052.x

Kim D-Y, Scalf M, Smith LM, Vierstra RD (2013) Advanced Proteomic Analyses Yield a Deep Catalog of Ubiquitylation Targets in Arabidopsis . The Plant Cell 25:1523–1540. https://doi.org/10.1105/tpc.112.108613

Kim WT, Franceschi VR, Krishnan HB, Okita TW (1988) Formation of wheat protein bodies: Involvement of the Golgi apparatus in gliadin transport. Planta 176:173–182. https://doi.org/10.1007/BF00392442

Kirchhausen T (2000) Clathrin. Annual Review of Biochemistry 69:699–727. https://doi.org/10.1146/annurev.biochem.69.1.699

Kleene R, Berger EG (1993) The molecular and cell biology of glycosyltransferases. Biochimica et Biophysica Acta (BBA) - Reviews on Biomembranes 1154:283–325. https://doi.org/10.1016/0304-4157(93)90003-7

Kohorn BD (2000) Plasma Membrane-Cell Wall Contacts1. Plant Physiology 124:31–38. https://doi.org/10.1104/pp.124.1.31

Lam SK, Tse YC, Robinson DG, Jiang L (2007) Tracking down the elusive early endosome. Trends in Plant Science 12:497–505. https://doi.org/10.1016/J.TPLANTS.2007.09.001

Lev S (2010) Non-vesicular lipid transport by lipid-transfer proteins and beyond. Nature Reviews Molecular Cell Biology 11:739–750. https://doi.org/10.1038/nrm2971

Li L, Shimada T, Takahashi H, Ueda H, Fukao Y, Kondo M, Nishimura M, Hara-Nishimura I (2006) MAIGO2 Is Involved in Exit of Seed Storage Proteins from the Endoplasmic Reticulum in Arabidopsis thaliana. The Plant Cell 18:3535–3547. https://doi.org/10.1105/tpc.106.046151

Li R, Liu P, Wan Y, Chen T, Wang Q, Mettbach U, Baluška F, Šamaj J, Fang X, Lucas W, Lin J (2012) A Membrane Microdomain-Associated Protein, Arabidopsis Flot1, Is Involved in a Clathrin-Independent Endocytic Pathway and Is Required for Seedling Development. The Plant Cell 24:2105–2122. https://doi.org/10.1105/tpc.112.095695

Liu Y, Burgos JS, Deng Y, Srivastava R, Howell S, Bassham D (2012) Degradation of the endoplasmic reticulum by autophagy during endoplasmic reticulum stress in Arabidopsis. Plant Cell 24:4635–4651. https://doi.org/10.1105/tpc.112.101535

Lowe M (2011) Structural organization of the Golgi apparatus. Current Opinion in Cell Biology 23:85–93. https://doi.org/10.1016/j.ceb.2010.10.004

MacGurn JA, Hsu P-C, Emr SD (2012) Ubiquitin and Membrane Protein Turnover: From Cradle to Grave. Annual Review of Biochemistry 81:231–259. https://doi.org/10.1146/annurev-biochem-060210-093619

Malínská K, Jelínková A, Petrášek J (2014) The use of FM dyes to analyze plant endocytosis. Methods in Molecular Biology 1209:1–11. https://doi.org/10.1007/978-1-4939-1420-3_1

Malinsky J, Opekarová M, Grossmann G, Tanner W (2013) Membrane Microdomains, Rafts, and Detergent-Resistant Membranes in Plants and Fungi. Annual Review of Plant Biology 64:501–529. https://doi.org/10.1146/annurev-arplant-050312-120103

Marcos Lousa C, Gershlick DC, Denecke J (2012) Mechanisms and Concepts Paving the Way towards a Complete Transport Cycle of Plant Vacuolar Sorting Receptors. The Plant Cell 24:1714–1732. https://doi.org/10.1105/tpc.112.095679

Markham JE, Jaworski JG (2007) Rapid measurement of sphingolipids from Arabidopsis thaliana by reversed-phase high-performance liquid chromatography coupled to

electrospray ionization tandem mass spectrometry. Rapid Communications in Mass Spectrometry 21:1304–1314. https://doi.org/https://doi.org/10.1002/rcm.2962

Markham JE, Li J, Cahoon EB, Jaworski JG (2006) Separation and Identification of Major Plant Sphingolipid Classes from Leaves *. Journal of Biological Chemistry 281:22684–22694. https://doi.org/10.1074/jbc.M604050200

Martinière A, Lavagi I, Nageswaran G, Rolfe D, Maneta-Peyret L, Luu D, Botchway S, Webb S, Mongrand S, Maurel C, Martin-Fernandez M, Kleine-Vehn J, Friml J, Moreau P, Runions J (2012) Cell wall constrains lateral diffusion of plant plasma-membrane proteins. Proceedings of the National Academy of Sciences 109:12805 LP – 12810. https://doi.org/10.1073/pnas.1202040109

Martinoia E, Maeshima M, Neuhaus HE (2007) Vacuolar transporters and their essential role in plant metabolism. Journal of Experimental Botany 58:83–102. https://doi.org/10.1093/jxb/erl183

Martinoia E, Massonneau A, Frangne N (2000) Transport Processes of Solutes across the Vacuolar Membrane of Higher Plants. Plant and Cell Physiology 41:1175–1186. https://doi.org/10.1093/pcp/pcd059

Marty F (1999) Plant Vacuoles. The Plant Cell 11:587–599. https://doi.org/10.1105/tpc.11.4.587

Maruyama N, Mun LC, Tatsuhara M, Sawada M, Ishimoto M, Utsumi S (2006) Multiple Vacuolar Sorting Determinants Exist in Soybean 11S Globulin. The Plant Cell 18:1253–1273. https://doi.org/10.1105/tpc.105.036376

Matheson LA, Hanton SL, Brandizzi F (2006) Traffic between the plant endoplasmic reticulum and Golgi apparatus: to the Golgi and beyond. Current Opinion in Plant Biology 9:601–609. https://doi.org/10.1016/J.PBI.2006.09.016

Matsuoka K, Neuhaus J-M (1999) Cis-elements of protein transport to the plant vacuoles. Journal of Experimental Botany 50:165–174. https://doi.org/10.1093/jxb/50.331.165

Matsushima R, Fukao Y, Nishimura M, Hara-Nishimura I (2004) NAI1 gene encodes a basic-helix-loop-helix-type putative transcription factor that regulates the formation of an endoplasmic reticulum-derived structure, the ER body. Plant Cell 16:1536–1549. https://doi.org/10.1105/tpc.021154

Matsushima R, Hayashi Y, Yamada K, Shimada T, Nishimura M, Hara-Nishimura I (2003a) The ER Body, a Novel Endoplasmic Reticulum-Derived Structure in

Arabidopsis. Plant and Cell Physiology 44:661–666. https://doi.org/10.1093/pcp/pcg089

Matsushima R, Kondo M, Nishimura M, Hara-Nishimura I (2003b) A novel ER-derived compartment, the ER body, selectively accumulates a β-glucosidase with an ER-retention signal in Arabidopsis. Plant Journal 33:493–502. https://doi.org/10.1046/J.1365-313X.2003.01636.X

Matteis MA de, Morrow JS (2000) Spectrin tethers and mesh in the biosynthetic pathway. Journal of Cell Science 113:2331–2343. https://doi.org/10.1242/jcs.113.13.2331

Maxfield FR, McGraw TE (2004) Endocytic recycling. Nature Reviews Molecular Cell Biology 5:121–132. https://doi.org/10.1038/nrm1315

McGough IJ, Cullen PJ (2011) Recent Advances in Retromer Biology. Traffic 12:963–971. https://doi.org/https://doi.org/10.1111/j.1600-0854.2011.01201.x

Meckel T, Hurst AC, Thiel G, Homann U (2004) Endocytosis against high turgor: intact guard cells of Vicia faba constitutively endocytose fluorescently labelled plasma membrane and GFP-tagged K+-channel KAT1. The Plant Journal 39:182–193. https://doi.org/https://doi.org/10.1111/j.1365-313X.2004.02119.x

Mellman I, Simons K (1992) The Golgi complex: In vitro veritas? Cell 68:829–840. https://doi.org/10.1016/0092-8674(92)90027-A

Meusser B, Hirsch C, Jarosch E, Sommer T (2005) ERAD: the long road to destruction. Nature Cell Biology 7:766–772. https://doi.org/10.1038/ncb0805-766

Mitsuhashi N, Hayashi Y, Koumoto Y, Shimada T, Fukasawa-Akada T, Nishimura M, Hara-Nishimura I (2001) A Novel Membrane Protein That Is Transported to Protein Storage Vacuoles via Precursor-Accumulating Vesicles. The Plant Cell 13:2361–2372. https://doi.org/10.1105/tpc.010171

Molina MI, Otegui M, Petruccelli S (2006) Sunflower storage proteins are transported in dense vesicles that contain proteins homologous to the pumpkin vacuolar sorting receptor PV 72. Electronic Journal of Biotechnology 9:326–330. https://doi.org/10.2225/vol9-issue3-21

Mongrand S, Stanislas T, Bayer E, Lherminier J, Simon-Plas F (2010) Membrane rafts in plant cells. Trends in Plant Science 15:656–663. https://doi.org/10.1016/J.TPLANTS.2010.09.003

Mori T, Maruyama N, Nishizawa K, Higasa T, Yagasaki K, Ishimoto M, Utsumi S (2004) The composition of newly synthesized proteins in the endoplasmic reticulum determines the transport pathways of soybean seed storage proteins. The Plant Journal 40:238–249. https://doi.org/https://doi.org/10.1111/j.1365-313X.2004.02204.x

Morita MT, Shimada T (2014) The Plant Endomembrane System—A Complex Network Supporting Plant Development and Physiology. Plant and Cell Physiology 55:667–671. https://doi.org/10.1093/pcp/pcu049

Mortimer JC, Yu X, Albrecht S, Sicilia F, Huichalaf M, Ampuero D, Michaelson L, Murphy A, Matsunaga T, Kurz S, Stephens E, Baldwin T, Ishii T, Napier J, Weber A, Handford M, Dupree P (2013) Abnormal Glycosphingolipid Mannosylation Triggers Salicylic Acid–Mediated Responses in Arabidopsis. The Plant Cell 25:1881–1894. https://doi.org/10.1105/tpc.113.111500

Muñoz F, Mendieta JR, Pagano MR, Paggi R, Daleo G, Guevara M (2010) The swaposin-like domain of potato aspartic protease (StAsp-PSI) exerts antimicrobial activity on plant and human pathogens. Peptides 31:777–785. https://doi.org/https://doi.org/10.1016/j.peptides.2010.02.001

Muñoz F, Palomares-Jerez MF, Daleo G, Villalaín J, Guevara M (2014) Possible mechanism of structural transformations induced by StAsp-PSI in lipid membranes. Biochimica et Biophysica Acta (BBA) - Biomembranes 1838:339–347. https://doi.org/https://doi.org/10.1016/j.bbamem.2013.08.004

Müntz K (1998) Deposition of storage proteins. Plant Molecular Biology 38:77–99. https://doi.org/10.1023/A:1006020208380

Nagano AJ, Maekawa A, Nakano RT, Miyahara M, Higaki T, Kutsuna N, Hasezawa S, Hara-Nishimura I (2009) Quantitative analysis of ER body morphology in an arabidopsis mutant. Plant and Cell Physiology 50:2015–2022. https://doi.org/10.1093/pcp/pcp157

Nakano RT, Matsushima R, Ueda H, Tamura K, Shimada T, Li L, Hayashi Y, Kondo M, Nishimura M, Hara-Nishimura I (2009) GNOM-LIKE1/ERMO1 and SEC24a/ERMO2 Are Required for Maintenance of Endoplasmic Reticulum Morphology in Arabidopsis thaliana. The Plant Cell 21:3672–3685. https://doi.org/10.1105/tpc.109.068270

Nebenführ A, Ritzenthaler C, Robinson DG (2002) Brefeldin A: Deciphering an enigmatic inhibitor of secretion. Plant Physiology 130:1102–1108. https://doi.org/10.1104/pp.011569

Neuhaus J-M, Pietrzak M, Boller T (1994) Mutation analysis of the C-terminal vacuolar targeting peptide of tobacco chitinase: low specificity of the sorting system, and gradual transition between intracellular retention and secretion into the extracellular space. The Plant Journal 5:45–54. https://doi.org/https://doi.org/10.1046/j.1365-313X.1994.5010045.x

Niemes S, Langhans M, Viotti C, Scheuring D, San Wan Yan M, Jiang L, Hillmer S, Robinson D, Pimpl P (2010) Retromer recycles vacuolar sorting receptors from the trans-Golgi network. The Plant Journal 61:107–121. https://doi.org/https://doi.org/10.1111/j.1365-313X.2009.04034.x

Niihama M, Takemoto N, Hashiguchi Y, Tasaka M, Morita M (2009) ZIP Genes Encode Proteins Involved in Membrane Trafficking of the TGN–PVC/Vacuoles. Plant and Cell Physiology 50:2057–2068. https://doi.org/10.1093/pcp/pcp137

Occhialini A, Gouzerh G, Di Sansebastiano G-P, Neuhaus J-M (2016) Dimerization of the Vacuolar Receptors AtRMR1 and -2 from Arabidopsis thaliana Contributes to Their Localization in the trans-Golgi Network. International Journal of Molecular Sciences 17

Ohtomo I, Ueda H, Shimada T, Nishiyama C, Komoto Y, Hara-Nishimura I, Takahashi T (2005) Identification of an Allele of VAM3/SYP22 that Confers a Semi-dwarf Phenotype in Arabidopsis thaliana. Plant and Cell Physiology 46:1358–1365. https://doi.org/10.1093/pcp/pci146

Olbrich A, Hillmer S, Hinz G, Oliviusson P, Robinson D (2007) Newly formed vacuoles in root meristems of barley and pea seedlings have characteristics of both protein storage and lytic vacuoles. Plant Physiology 145:1383–1394. https://doi.org/10.1104/pp.107.108985

Oliveira A, Pereira C, da Costa DS, Teixeira J, Fidalgo F, Pereira S, Pissarra J (2010) Characterization of aspartic proteinases in C. cardunculus L. callus tissue for its prospective transformation. Plant Science 178:140–146. https://doi.org/10.1016/j.plantsci.2009.11.008

O'Malley RC, Ecker JR (2010) Linking genotype to phenotype using the Arabidopsis unimutant collection. The Plant Journal 61:928–940. https://doi.org/https://doi.org/10.1111/j.1365-313X.2010.04119.x

Onelli E, Prescianotto-Baschong C, Caccianiga M, Moscatelli A (2008) Clathrin-dependent and independent endocytic pathways in tobacco protoplasts revealed by labelling with charged nanogold. Journal of Experimental Botany 59:3051–3068. https://doi.org/10.1093/jxb/ern154

Orci L, Glick BS, Rothman JE (1986) A new type of coated vesicular carrier that appears not to contain clathrin: Its possible role in protein transport within the Golgi stack. Cell 46:171–184. https://doi.org/10.1016/0092-8674(86)90734-8

Ott T (2017) Membrane nanodomains and microdomains in plant–microbe interactions. Current Opinion in Plant Biology 40:82–88. https://doi.org/10.1016/J.PBI.2017.08.008

Paczkowski JE, Richardson BC, Fromme JC (2015) Cargo adaptors: structures illuminate mechanisms regulating vesicle biogenesis. Trends in Cell Biology 25:408–416. https://doi.org/10.1016/J.TCB.2015.02.005

Paez Valencia J, Goodman K, Otegui MS (2016) Endocytosis and Endosomal Trafficking in Plants. Annual Review of Plant Biology 67:309–335. https://doi.org/10.1146/annurev-arplant-043015-112242

Paris N, Neuhaus J-M (2002) BP-80 as a vacuolar sorting receptor. Plant Molecular Biology 50:903–914. https://doi.org/10.1023/A:1021205715324

Paris N, Stanley CM, Jones RL, Rogers JC (1996) Plant Cells Contain Two Functionally Distinct Vacuolar Compartments. Cell 85:563–572. https://doi.org/10.1016/S0092-8674(00)81256-8

Patterson GH, Hirschberg K, Polishchuk RS, Gerlich D, Phair R, Lippincott-Schwartz J (2008) Transport through the Golgi Apparatus by Rapid Partitioning within a Two-Phase Membrane System. Cell 133:1055–1067. https://doi.org/10.1016/J.CELL.2008.04.044

Peixoto B, Pereira S, Pereira C, Pissarra J (2018) Vacuolar sorting determinants: Isolation and study. In: Methods in Molecular Biology. Humana Press, New York, NY, pp 21–31

Pereira C, da Costa DS, Pereira S, De Moura Nogueira F, Albuquerque P, Teixeira J, Faro C, Pissarra J (2008) Cardosins in postembryonic development of cardoon:

Towards an elucidation of the biological function of plant aspartic proteinases. Protoplasma 232:203–213. https://doi.org/10.1007/s00709-008-0288-9

Pereira C, Pereira S, Pissarra J (2014) Delivering of Proteins to the Plant Vacuole—An Update. International Journal of Molecular Sciences 15:7611–7623. https://doi.org/10.3390/ijms15057611

Pereira C, Pereira S, Satiat-Jeunemaitre B, Pissarra J (2013) Cardosin A contains two vacuolar sorting signals using different vacuolar routes in tobacco epidermal cells. The Plant Journal 76:n/a-n/a. https://doi.org/10.1111/tpj.12274

Pissarra J, Pereira C, da Costa DS, Figueiredo R, Duarte P, Teixeira J, Pereira S (2007) From Flower to Seed Germination in Cynara cardunculus: A Role for Aspartic Proteinases. Internation Journal of Plant Developmental Biology 274–281

Pompa A, de Marchis F, Pallotta MT, Benitez-Alfonso Y, Jones A, Schipper K, Moreau K, Žárský V, Di Sansebastiano G, Bellucci M (2017) Unconventional transport routes of soluble and membrane proteins and their role in developmental biology. International Journal of Molecular Sciences 18:. https://doi.org/10.3390/ijms18040703

Preuss D, Mulholland J, Franzusoff A, Segev N, Botstein D (1992) Characterization of the Saccharomyces Golgi complex through the cell cycle by immunoelectron microscopy. Molecular Biology of the Cell 3:789–803. https://doi.org/10.1091/mbc.3.7.789

Provart NJ, Alonso J, Assmann SM, Bergmann D, Brady S, Brkljacic J, Browse J, Chapple C, Colot V, Cutler S, Dangl J, Ehrhardt D, Friesner J, Frommer W, Grotewold E, Meyerowitz E, Nemhauser J, Nordborg M, Pikaard C, Shanklin J, Somerville C, Stitt M, Torii K, Waese J, Wagner D, Mccourt P (2016) 50 years of Arabidopsis research: Highlights and future directions. New Phytologist 209:921–944. https://doi.org/10.1111/nph.13687

Puhka M, Joensuu M, Vihinen H, Belevich I, Jokitalo E (2012) Progressive sheet-to-tubule transformation is a general mechanism for endoplasmic reticulum partitioning in dividing mammalian cells. Molecular Biology of the Cell 23:2424–2432. https://doi.org/10.1091/mbc.e10-12-0950

Puhka M, Vihinen H, Joensuu M, Jokitalo E (2007) Endoplasmic reticulum remains continuous and undergoes sheet-to-tubule transformation during cell division in

mammalian cells. Journal of Cell Biology 179:895–909. https://doi.org/10.1083/jcb.200705112

Qu X, Chatty PR, Roeder AHK (2014) Endomembrane trafficking protein SEC24A regulates cell size patterning in arabidopsis. Plant Physiology 166:1877–1890. https://doi.org/10.1104/pp.114.246033

Quader H, Schnepf E (1986) Endoplasmic reticulum and cytoplasmic streaming: Fluorescence microscopical observations in adaxial epidermis cells of onion bulb scales. Protoplasma 131:250–252. https://doi.org/10.1007/BF01282989

Rabouille C, Klumperman J (2005) The maturing role of COPI vesicles in intra-Golgi transport. Nature Reviews Molecular Cell Biology 6:812–817. https://doi.org/10.1038/nrm1735

Raffaele S, Bayer E, Lafarge D, Cluzet S, German Retana S, Boubekeur T, Leborgne-Castel N, Carde J, Lherminier J, Noirot E, Satiat-Jeunemaître B, Laroche-Traineau J, Moreau P, Ott T, Maule A, Reymond P, Simon-Plas F, Farmer E, Bessoule J, Mongrand S (2009) Remorin, a Solanaceae Protein Resident in Membrane Rafts and Plasmodesmata, Impairs Potato virus X Movement. The Plant Cell 21:1541–1555. https://doi.org/10.1105/tpc.108.064279

Raiborg C, Rusten TE, Stenmark H (2003) Protein sorting into multivesicular endosomes. Current Opinion in Cell Biology 15:446–455. https://doi.org/10.1016/S0955-0674(03)00080-2

Ramalho-Santos M, Pissarra J, Veríssimo P, Pereira S, Salema R, Pires E, Faro C (1997) Cardosin A, an abundant aspartic proteinase, accumulates in protein storage vacuoles in the stigmatic papillae of Cynara cardunculus L. Planta 203:204–212. https://doi.org/10.1007/s004250050183

Ramalho-Santos M, Verissimo P, Cortes L, Samyn B, Van Beeumen J, Pires E, Faro C (1998) Identification and proteolytic processing of procardosin A. European Journal of Biochemistry 255:133–138. https://doi.org/10.1046/j.1432-1327.1998.2550133.x

Rambourg A, Clermont Y (1990) Three-dimensional electron microscopy: structure of the Golgi apparatus. European journal of cell biology 51:189–200

Reczek D, Schwake M, Schröder J, Hughes H, Blanz J, Jin X, Brondyk W, Van Patten S, Edmunds T, Saftig P (2007) LIMP-2 Is a Receptor for Lysosomal Mannose-6-Phosphate-Independent Targeting of β-Glucocerebrosidase. Cell 131:770–783. https://doi.org/10.1016/J.CELL.2007.10.018

Reyes FC, Buono R, Otegui MS (2011) Plant endosomal trafficking pathways. Current Opinion in Plant Biology 14:666–673. https://doi.org/10.1016/j.pbi.2011.07.009

Rigal A, Doyle SM, Robert S (2015) Live cell imaging of FM4-64, a tool for tracing the endocytic pathways in Arabidopsis root cells. Methods in Molecular Biology 1242:93–103. https://doi.org/10.1007/978-1-4939-1902-4_9

Robinson DG (2020) Plant Golgi ultrastructure. Journal of Microscopy 280:111–121. https://doi.org/10.1111/jmi.12899

Robinson DG, Hinz G, Holstein SEH (1998) The molecular characterization of transport vesicles. Plant Molecular Biology 38:49–76. https://doi.org/10.1007/978-94-011-5298-3_3

Robinson DG, Hoh B, Hinz G, Jeong BK (1995) One Vacuole or two Vacuoles: Do Protein Storage Vacuoles Arise de novo during Pea Cotyledon Development? Journal of Plant Physiology 145:654–664. https://doi.org/10.1016/S0176-1617(11)81278-2

Robinson DG, Jiang L, Schumacher K (2008) The endosomal system of plants: Charting new and familiar territories. Plant Physiology 147:1482–1492. https://doi.org/10.1104/pp.108.120105

Robinson DG, Oliviusson P, Hinz G (2005) Protein Sorting to the Storage Vacuoles of Plants: A Critical Appraisal. Traffic 6:615–625. https://doi.org/https://doi.org/10.1111/j.1600-0854.2005.00303.x

Roche Y, Gerbeau-Pissot P, Buhot B, Thomas D, Bonneau L, Gresti J, Mongrand S, Perrier-Cornet J, Simon-Plas F (2008) Depletion of phytosterols from the plant plasma membrane provides evidence for disruption of lipid rafts. The FASEB Journal 22:3980–3991. https://doi.org/https://doi.org/10.1096/fj.08-111070

Roche Y, Klymchenko AS, Gerbeau-Pissot P, Gervais P, Mély Y, Simon-Plas F, Perrier-Cornet J (2010) Behavior of plant plasma membranes under hydrostatic pressure as monitored by fluorescent environment-sensitive probes. Biochimica et Biophysica Acta (BBA) - Biomembranes 1798:1601–1607. https://doi.org/10.1016/J.BBAMEM.2010.03.024

Rogers JC (2008) Multiple Vacuoles in Plant Cells. Plant Physiology 146:1024–1025. https://doi.org/10.1104/pp.107.900248

Rojo E, Denecke J (2008) What Is Moving in the Secretory Pathway of Plants? Plant Physiology 147:1493–1503. https://doi.org/10.1104/pp.108.124552

Rothman JE, Wieland FT (1996) Protein sorting by transport vesicles. Science 272:227–234. https://doi.org/10.1126/SCIENCE.272.5259.227

Rouillé Y, Rohn W, Hoflack B (2000) Targeting of lysosomal proteins. Seminars in Cell & Developmental Biology 11:165–171. https://doi.org/10.1006/SCDB.2000.0168

Russinova E, Borst J-W, Kwaaitaal M, Caño-Delgado A, Yin Y, Chory J, de Vries S (2004) Heterodimerization and Endocytosis of Arabidopsis Brassinosteroid Receptors BRI1 and AtSERK3 (BAK1). The Plant Cell 16:3216–3229. https://doi.org/10.1105/tpc.104.025387

Šamaj J, Müller J, Beck M, Böhm N, Menzel D (2006) Vesicular trafficking, cytoskeleton and signalling in root hairs and pollen tubes. Trends in Plant Science 11:594–600. https://doi.org/10.1016/J.TPLANTS.2006.10.002

Šamaj J, Read ND, Volkmann D, Menzel D, Baluška F (2005) The endocytic network in plants. Trends in Cell Biology 15:425–433. https://doi.org/10.1016/j.tcb.2005.06.006

Šamajová O, Takáč T, von Wangenheim D, Stelzer E, Šamaj J (2012) Update on methods and techniques to study endocytosis in plants. In: Endocytosis in Plants. Springer-Verlag Berlin Heidelberg, pp 1–36

Samarakoon T, Shiva S, Lowe K, Tamura P, Roth M, Welti R (2012) Arabidopsis thaliana Membrane Lipid Molecular Species and Their Mass Spectral Analysis. Methods in Molecular Biology 918:179–268. https://doi.org/10.1007/978-1-61779-995-2_13

Schmid M, Davison TS, Henz SR, Pape U, Demar M, Vingron M, Schölkopf B, Weigel D, Lohmann J (2005) A gene expression map of Arabidopsis thaliana development. Nature Genetics 37:501–506. https://doi.org/10.1038/ng1543

Schrick K, Shiva S, Arpin JC, Delimont N, Isaac G, Tamura P, Welti R (2012) Steryl Glucoside and Acyl Steryl Glucoside Analysis of Arabidopsis Seeds by Electrospray Ionization Tandem Mass Spectrometry. Lipids 47:185–193. https://doi.org/https://doi.org/10.1007/s11745-011-3602-9

Schröder M (2008) Endoplasmic reticulum stress responses. Cellular and Molecular Life Sciences 65:862–894. https://doi.org/10.1007/s00018-007-7383-5

Schwacke R, Schneider A, van der Graaff E, Fischer K, Catoni E, Desimone M, Frommer W, Flügge U, Kunze R (2003) ARAMEMNON, a Novel Database for Arabidopsis Integral Membrane Proteins. Plant Physiology 131:16–26. https://doi.org/10.1104/pp.011577

Seaman MNJ (2005) Recycle your receptors with retromer. Trends in Cell Biology 15:68–75. https://doi.org/10.1016/J.TCB.2004.12.004

Shevchenko A, Simons K (2010) Lipidomics: coming to grips with lipid diversity. Nature Reviews Molecular Cell Biology 11:593–598. https://doi.org/10.1038/nrm2934

Shibata Y, Shemesh T, Prinz WA, Palazzo A, Kozlov M, Rapoport T (2010) Mechanisms Determining the Morphology of the Peripheral ER. Cell 143:774–788. https://doi.org/10.1016/J.CELL.2010.11.007

Shimada T, Koumoto Y, Li L, Yamazaki M, Kondo M, Nishimura M, Hara-Nishimura I (2006) AtVPS29, a Putative Component of a Retromer Complex, is Required for the Efficient Sorting of Seed Storage Proteins. Plant and Cell Physiology 47:1187–1194. https://doi.org/10.1093/pcp/pcj103

Shimada T, Nishimura M, Hara-Nishimura I (1994) Small GTP-Binding Proteins are Associated with the Vesicles That are Targeted to Vacuoles in Developing Pumpkin Cotyledons. Plant and Cell Physiology 35:995–1001. https://doi.org/10.1093/oxfordjournals.pcp.a078702

Shimada T, Takagi J, Ichino T, Shirakawa M, Hara-Nishimura I (2018) Plant Vacuoles. Annual Review of Plant Biology 69:123–145. https://doi.org/10.1146/annurev-arplant-042817-040508

Shirakawa M, Ueda H, Shimada T, Koumoto Y, Shimada T, Kondo M, Takahashi T, Okuyama Y, Nishimura M, Hara-Nishimura I (2010) Arabidopsis Qa-SNARE SYP2 proteins localized to different subcellular regions function redundantly in vacuolar protein sorting and plant development. Plant Journal 64:924–935. https://doi.org/10.1111/j.1365-313X.2010.04394.x

Simões I, Faro C (2004) Structure and function of plant aspartic proteinases. European Journal of Biochemistry 271:2067–2075. https://doi.org/10.1111/j.1432-1033.2004.04136.x

Soares A, Ribeiro Carlton SM, Simões I (2019) Atypical and nucellin-like aspartic proteases: emerging players in plant developmental processes and stress responses. Journal of Experimental Botany 70:2059–2076. https://doi.org/10.1093/jxb/erz034

Son O, Yang HS, Lee HJ, Lee M, Shin K, Jeon S, Lee M, Choi S, Chun J, Kim H, An C, Hong S, Kim N, Koh S, Cho M, Kim S, Verma D, Cheon C (2003) Expression of

srab7 and SCaM genes required for endocytosis of Rhizobium in root nodules. Plant Science 165:1239–1244. https://doi.org/10.1016/S0168-9452(03)00331-5

Staehelin LA (1997) The plant ER: a dynamic organelle composed of a large number of discrete functional domains. The Plant Journal 11:1151–1165. https://doi.org/10.1046/j.1365-313X.1997.11061151.x

Staehelin LA, Moore I (1995) The Plant Golgi Apparatus: Structure, Functional Organization and Trafficking Mechanisms. Annual Review of Plant Physiology and Plant Molecular Biology 46:261–288. https://doi.org/10.1146/annurev.pp.46.060195.001401

Stefan CJ, Manford AG, Emr SD (2013) ER-PM connections: Sites of information transfer and inter-organelle communication. Current Opinion in Cell Biology 25:434–442. https://doi.org/10.1016/j.ceb.2013.02.020

Stefano G, Hawes C, Brandizzi F (2014a) ER - the key to the highway. Current Opinion in Plant Biology 22:30–38. https://doi.org/10.1016/j.pbi.2014.09.001

Stefano G, Renna L, Brandizzi F (2014b) The endoplasmic reticulum exerts control over organelle streaming during cell expansion. Journal of Cell Science 127:947–953. https://doi.org/10.1242/jcs.139907

Stefano G, Renna L, Lai Y, Slabaugh E, Mannino N, Buono R, Otegui M, Brandizzi F (2015) ER network homeostasis is critical for plant endosome streaming and endocytosis. Cell Discovery 1:1–16. https://doi.org/10.1038/celldisc.2015.33

Stigliano E, Faraco M, Neuhaus J-M, Montefusco A, Dalessandro G, Piro G, Di Sansebastiano G (2013) Two glycosylated vacuolar GFPs are new markers for ER-to-vacuole sorting. Plant Physiology and Biochemistry 73:337–343. https://doi.org/https://doi.org/10.1016/j.plaphy.2013.10.010

Surpin M, Raikhel N (2004) Traffic jams affect plant development and signal transduction. Nature Reviews Molecular Cell Biology 5:100–109. https://doi.org/10.1038/nrm1311

Takahashi H, Saito Y, Kitagawa T, Morita S, Masumura T, Tanaka K (2005) A Novel Vesicle Derived Directly from Endoplasmic Reticulum is Involved in the Transport of Vacuolar Storage Proteins in Rice Endosperm. Plant and Cell Physiology 46:245–249. https://doi.org/10.1093/pcp/pci019

Taylor NG (2011) A role for Arabidopsis dynamin related proteins DRP2A/B in endocytosis; DRP2 function is essential for plant growth. Plant Molecular Biology 76:117–129. https://doi.org/10.1007/s11103-011-9773-1

Teckman JH, Perlmutter DH (2000) Retention of mutant α1-antitrypsin Z in endoplasmic reticulum is associated with an autophagic response. American Journal of Physiology-Gastrointestinal and Liver Physiology 279:G961–G974. https://doi.org/10.1152/ajpgi.2000.279.5.G961

Terasaki M, Chen LB, Fujiwara K (1986) Microtubules and the endoplasmic reticulum are highly interdependent structures. Journal of Cell Biology 103:1557–1568. https://doi.org/10.1083/jcb.103.4.1557

Terauchi K, Asakura T, Ueda H, Tamura T, Tamura K, Matsumoto I, Misaka T, Hara-Nishimura I, Abe K (2006) Plant-specific insertions in the soybean aspartic proteinases, soyAP1 and soyAP2, perform different functions of vacuolar targeting. Journal of Plant Physiology 163:856–862. https://doi.org/10.1016/j.jplph.2005.08.007

Törmäkangas K, Hadlington JL, Pimpl P, Hillmer S, Brandizzi F, Teeri T, Denecke J (2001) A vacuolar sorting domain may also influence the way in which proteins leave the endoplasmic reticulum. Plant Cell 13:2021–2032. https://doi.org/10.1105/tpc.13.9.2021

Toulmay A, Prinz WA (2011) Lipid transfer and signaling at organelle contact sites: the tip of the iceberg. Current Opinion in Cell Biology 23:458–463. https://doi.org/https://doi.org/10.1016/j.ceb.2011.04.006

Toyooka K, Okamoto T, Minamikawa T (2000) Mass Transport of Proform of a Kdel-Tailed Cysteine Proteinase (Sh-EP) to Protein Storage Vacuoles by Endoplasmic Reticulum–Derived Vesicle Is Involved in Protein Mobilization in Germinating Seeds. Journal of Cell Biology 148:453–464. https://doi.org/10.1083/jcb.148.3.453

Traub LM, Bonifacino JS (2013) Cargo Recognition in Clathrin-Mediated Endocytosis. Cold Spring Harbor Perspectives in Biology 5:a016790. https://doi.org/10.1101/CSHPERSPECT.A016790

Trigg SA, Garza RM, MacWilliams A, Nery J, Bartlett A, Castanon R, Goubil A, Feeney J, O'Malley R, Huang S, Zhang Z, Galli M, Ecker J (2017) CrY2H-seq: a massively multiplexed assay for deep-coverage interactome mapping. Nature Methods 14:819–825. https://doi.org/10.1038/nmeth.4343

Tse YC, Mo B, Hillmer S, Zhao M, Lo S, Robinson D, Jiang L (2004) Identification of Multivesicular Bodies as Prevacuolar Compartments in Nicotiana tabacum BY-2 Cells[W]. The Plant Cell 16:672–693. https://doi.org/10.1105/tpc.019703

Ueda H, Nishiyama C, Shimada T, Koumoto Y, Hayashi Y, Kondo M, Takahashi T, Ohtomo I, Nishimura M, Hara-Nishimura I (2006) AtVAM3 is Required for Normal Specification of Idioblasts, Myrosin Cells. Plant and Cell Physiology 47:164–175. https://doi.org/10.1093/pcp/pci232

Van der Wilden W, Herman EM, Chrispeels MJ (1980) Protein bodies of mung bean cotyledons as autophagic organelles. Proceedings of the National Academy of Sciences 77:428 LP – 432. https://doi.org/10.1073/pnas.77.1.428

Vieira M, Pissarra J, Veríssimo P, Castanheira P, Costa Y, Pires E, Faro C (2001) Molecular cloning and characterization of cDNA encoding cardosin B, an aspartic proteinase accumulating extracellularly in the transmitting tissue of Cynara cardunculus L. Plant Molecular Biology 45:529–539. https://doi.org/10.1023/A:1010675015318

Vieira V, Pain C, Wojcik S, Spatola Rossi T, Denecke J, Osterrieder A, Hawes C, Kriechbaumer V (2020) Living on the edge: the role of Atgolgin-84A at the plant ER–Golgi interface. Journal of Microscopy 280:158–173. https://doi.org/https://doi.org/10.1111/jmi.12946

Vieira V, Peixoto B, Costa M, Pereira S, Pissarra J, Pereira C (2019) N-linked glycosylation modulates Golgi-independent vacuolar sorting mediated by the plant specific insert. Plants 8:1–21. https://doi.org/10.3390/plants8090312

Viotti C (2014) ER and vacuoles: Never been closer. Frontiers in Plant Science 5:. https://doi.org/10.3389/fpls.2014.00020

Viotti C, Bubeck J, Stierhof YD, Krebs M, Langhans M, van den Berg W, van Dongen W, Richter S, Geldner N, Takano J, Jürgens G, de Vries S, Robinson D, Schumacher K (2010) Endocytic and secretory traffic in Arabidopsis merge in the trans-golgi network/early endosome, an independent and highly dynamic organelle. Plant Cell 22:1344–1357. https://doi.org/10.1105/tpc.109.072637

Viotti C, Krüger F, Krebs M, Neubert C, Fink F, Lupanga U, Scheuring D, Boutté Y, Frescatada-Rosa M, Wolfenstetter S, Sauer N, Hillmer S, Grebe M, Schumacher K (2013) The Endoplasmic Reticulum Is the Main Membrane Source for Biogenesis

of the Lytic Vacuole in Arabidopsis. The Plant Cell 25:3434–3449. https://doi.org/10.1105/tpc.113.114827

Vitale A, Chrispeels MJ (1992) Sorting of proteins to the vacuoles of plant cells. BioEssays 14:151–160. https://doi.org/https://doi.org/10.1002/bies.950140303

Vitale A, Denecke J (1999) The Endoplasmic Reticulum—Gateway of the Secretory Pathway. The Plant Cell 11:615–628. https://doi.org/10.1105/tpc.11.4.615

Vitale A, Hinz G (2005) Sorting of proteins to storage vacuoles: how many mechanisms? Trends in Plant Science 10:316–323. https://doi.org/10.1016/J.TPLANTS.2005.05.001

Waese J, Fan J, Pasha A, Yu H, Fucile G, Shi R, Cumming M, Kelley L, Sternberg M, Krishnakumar V, Ferlanti E, Miller J, Town C, Stuerzlinger W, Provart N (2017) ePlant: Visualizing and Exploring Multiple Levels of Data for Hypothesis Generation in Plant Biology. The Plant Cell 29:1806–1821. https://doi.org/10.1105/tpc.17.00073

Wang X, Chung KP, Lin W, Jiang L (2017) Protein secretion in plants: Conventional and unconventional pathways and new techniques. Journal of Experimental Botany 69:21–37. https://doi.org/10.1093/jxb/erx262

Wang X, Xu M, Gao C, Zeng Y, Cui Y, Shen W, Jiang L (2020) The roles of endomembrane trafficking in plant abiotic stress responses. Journal of Integrative Plant Biology 62:55–69. https://doi.org/10.1111/jipb.12895

Wenzel D, Schauermann G, Lüpke A von, Hinz G (2005) The Cargo in Vacuolar Storage Protein Transport Vesicles is Stratified. Traffic 6:45–55. https://doi.org/https://doi.org/10.1111/j.1600-0854.2004.00243.x

West M, Zurek N, Hoenger A, Voeltz GK (2011) A 3D analysis of yeast ER structure reveals how ER domains are organized by membrane curvature. Journal of Cell Biology 193:333–346. https://doi.org/10.1083/jcb.201011039

Wewer V, Dombrink I, vom Dorp K, Dörmann P (2011) Quantification of sterol lipids in plants by quadrupole time-of-flight mass spectrometry. Journal of Lipid Research 52:1039–1054. https://doi.org/10.1194/jlr.D013987

Wiedenmann J, Ivanchenko S, Oswald F, Schmitt F, Röcker C, Salih A, Spindler K, Nienhaus G (2004) EosFP, a fluorescent marker protein with UV-inducible green-to-red fluorescence conversion. Proceedings of the National Academy of Sciences

of the United States of America 101:15905–15910. https://doi.org/10.1073/pnas.0403668101

Winter D, Vinegar B, Nahal H, Ammar R, Wilson G, Provart N (2007) An “Electronic Fluorescent Pictograph” Browser for Exploring and Analyzing Large-Scale Biological Data Sets. PLOS ONE 2:e718

Wolfenstetter S, Wirsching P, Dotzauer D, Schneider S, Sauer N (2012) Routes to the Tonoplast: The Sorting of Tonoplast Transporters in Arabidopsis Mesophyll Protoplasts. The Plant Cell 24:215–232. https://doi.org/10.1105/tpc.111.090415

Woodward AW, Bartel B (2018) Biology in Bloom: A Primer on the Arabidopsis thaliana Model System. Genetics 208:1337–1349. https://doi.org/10.1534/genetics.118.300755

Worrall D, Ng CKY, Hetherington AM (2003) Sphingolipids, new players in plant signaling. Trends in Plant Science 8:317–320. https://doi.org/10.1016/S1360-1385(03)00128-6

Xiang L, Etxeberria E, Van den Ende W (2013) Vacuolar protein sorting mechanisms in plants. The FEBS Journal 280:979–993. https://doi.org/https://doi.org/10.1111/febs.12092

Yamada K, Hara-Nishimura I, Nishimura M (2011) Unique Defense Strategy by the Endoplasmic Reticulum Body in Plants. Plant and Cell Physiology 52:2039–2049. https://doi.org/10.1093/pcp/pcr156

Yamada K, Lim J, Dale JM, Chen H, Shinn P, Palm C, Southwick A, Wu H, Kim C, Nguyen M, Pham P, Cheuk R, Karlin-Newmann G, Liu S, Lam B, Sakano H, Wu T, Yu G, Miranda M, Quach H, Tripp M, Chang C, Lee J, Toriumi M, Chan M, Tang C,Onodera C, Deng J, Akiyama K, Ansari Y, Arakawa T, Banh J, Banno F, Bowser L, Brooks S, Carninci P, Chao Q, Choy N, Enju A, Goldsmith A, Gurjal M, Hansen N, Hayashizaki Y, Johnson-Hopson C, Hsuan V, Iida K, Karnes M, Khan S, Koesema E, Ishida J, Jiang P, Jones T, Kawai J, Kamiya A, Meyers C, Nakajima M, Narusaka M, Seki M, Sakurai T, Satou M, Tamse R, Vaysberg M, Wallender E, Wong C, Yamamura Y, Yuan S, Shinozaki K, Davis R, Theologis A, Ecker J (2003) Empirical Analysis of Transcriptional Activity in the Arabidopsis Genome. Science 302:842 LP – 846. https://doi.org/10.1126/science.1088305

Yamada K, Nagano AJ, Nishina M, Hara-Nishimura I, Nishimura M (2008) NAI2 Is an Endoplasmic Reticulum Body Component That Enables ER Body Formation in

Arabidopsis thaliana. The Plant Cell 20:2529–2540. https://doi.org/10.1105/tpc.108.059345

Yamazaki M, Shimada T, Takahashi H, Tamura K, Kondo M, Nishimura M, Hara-Nishimura I (2008) Arabidopsis VPS35, a Retromer Component, is Required for Vacuolar Protein Sorting and Involved in Plant Growth and Leaf Senescence. Plant and Cell Physiology 49:142–156. https://doi.org/10.1093/pcp/pcn006

Yetukuri L, Ekroos K, Vidal-Puig A, Orešič M (2008) Informatics and computational strategies for the study of lipids. Molecular BioSystems 4:121–127. https://doi.org/10.1039/B715468B

Yu D, Rupasinghe TWT, Boughton BA, Natera S, Hill C, Tarazona P, Feussner I, Roessner U (2018) A high-resolution HPLC-QqTOF platform using parallel reaction monitoring for in-depth lipid discovery and rapid profiling. Analytica Chimica Acta 1026:87–100. https://doi.org/10.1016/J.ACA.2018.03.062

Zhang L, Xing J, Lin J (2019) At the intersection of exocytosis and endocytosis in plants. New Phytologist 224:1479–1489. https://doi.org/10.1111/nph.16018

Zhang M, Chang H, Zhang Y, Yu J, Wu L, Ji W, Chen J, Liu B, Lu J, Liu Y, Zhang J, Xu P, Xu T (2012) Rational design of true monomeric and bright photoactivatable fluorescent proteins. Nature Methods 9:727–729. https://doi.org/10.1038/nmeth.2021

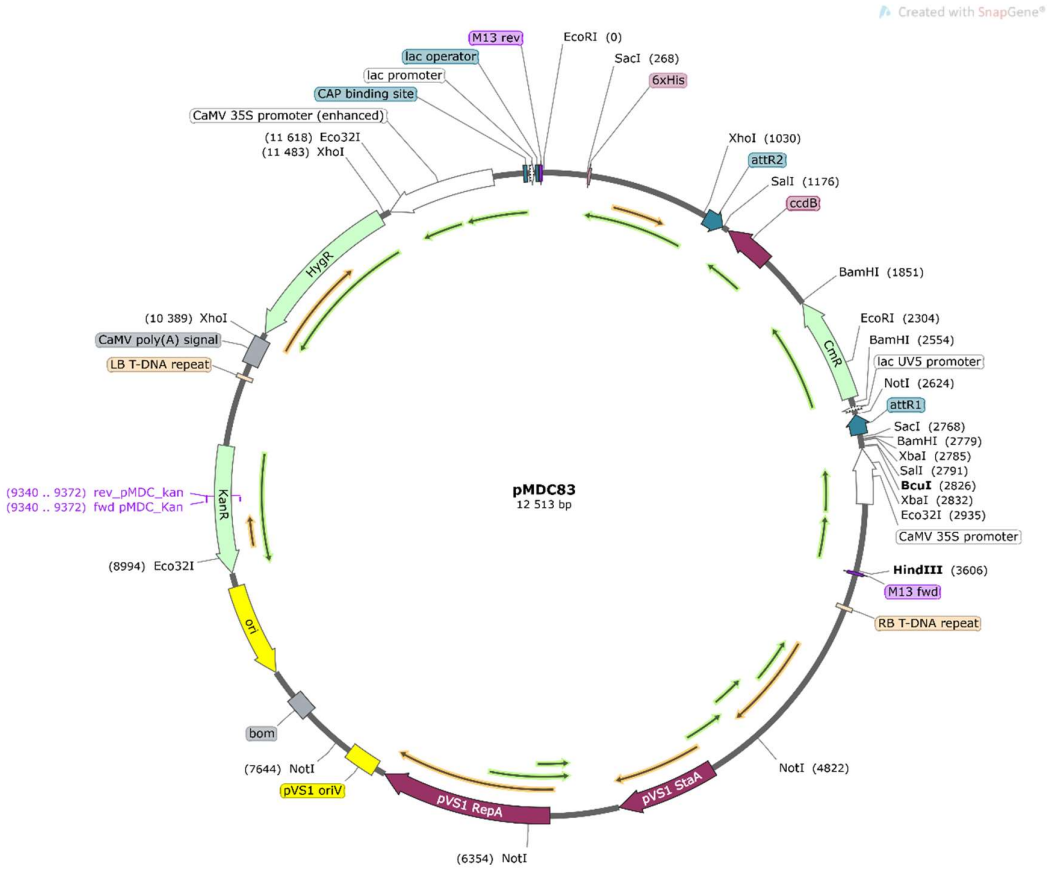
Zhao Z, Andersen SU, Ljung K, Dolezal K, Miotk A, Schultheiss S, Lohmann J (2010) Hormonal control of the shoot stem-cell niche. Nature 465:1089–1092. https://doi.org/10.1038/nature09126

Zouhar J, Muñoz A, Rojo E (2010) Functional specialization within the vacuolar sorting receptor family: VSR1, VSR3 and VSR4 sort vacuolar storage cargo in seeds and vegetative tissues. Plant Journal 64:577–588. https://doi.org/10.1111/j.1365-313X.2010.04349.x

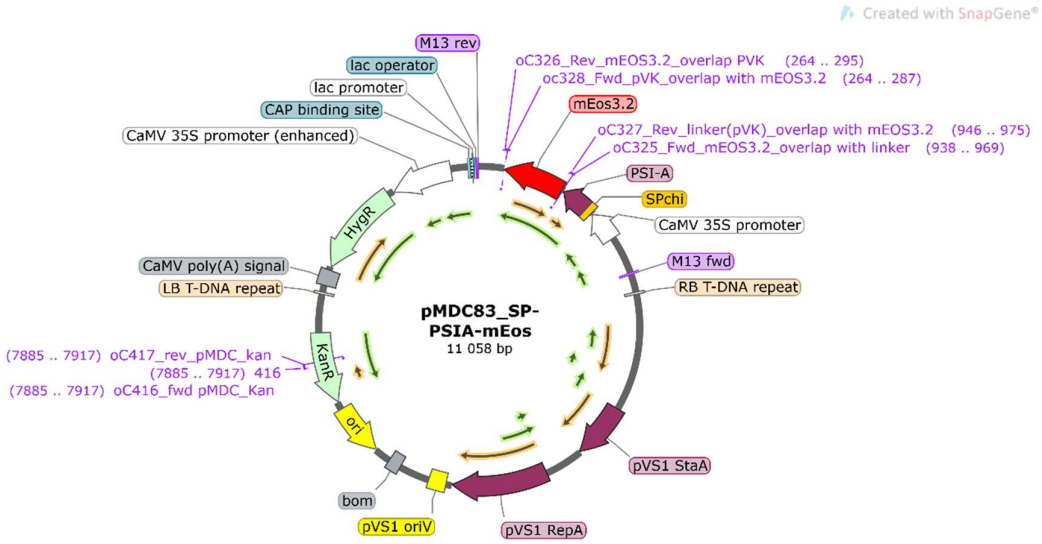
Zwiewka M, Feraru E, Möller B, Hwang I, Feraru M, Kleine-Vehn J, Weijers D, Friml J (2011) The AP-3 adaptor complex is required for vacuolar function in Arabidopsis. Cell Research 21:1711–1722. https://doi.org/10.1038/cr.2011.99

Zwiewka M, Nodzyński T, Robert S, Vanneste S, Friml J (2015) Osmotic Stress Modulates the Balance between Exocytosis and Clathrin-Mediated Endocytosis in Arabidopsis thaliana. Molecular Plant 8:1175–1187. https://doi.org/10.1016/j.molp.2015.03.007

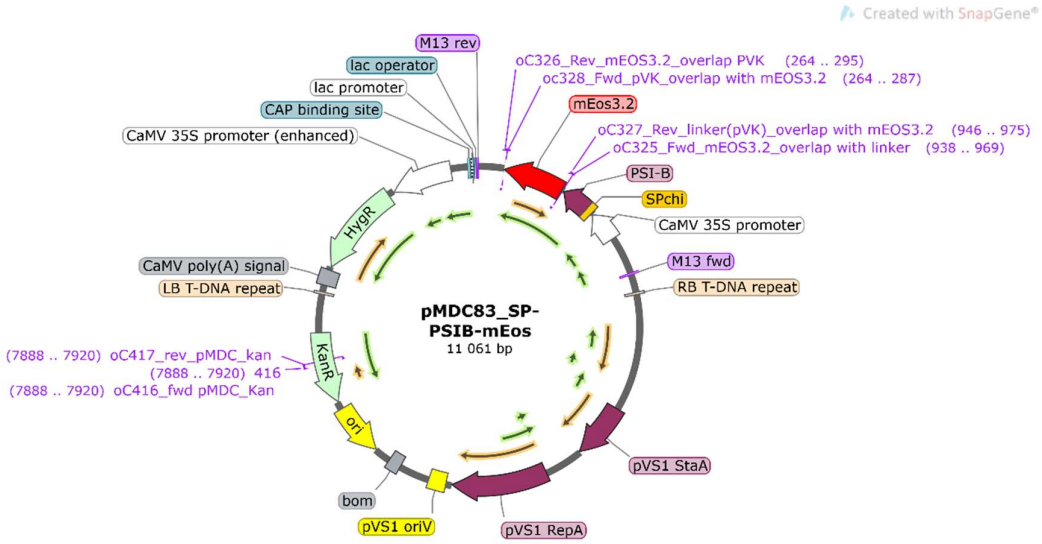
7. APPENDIX



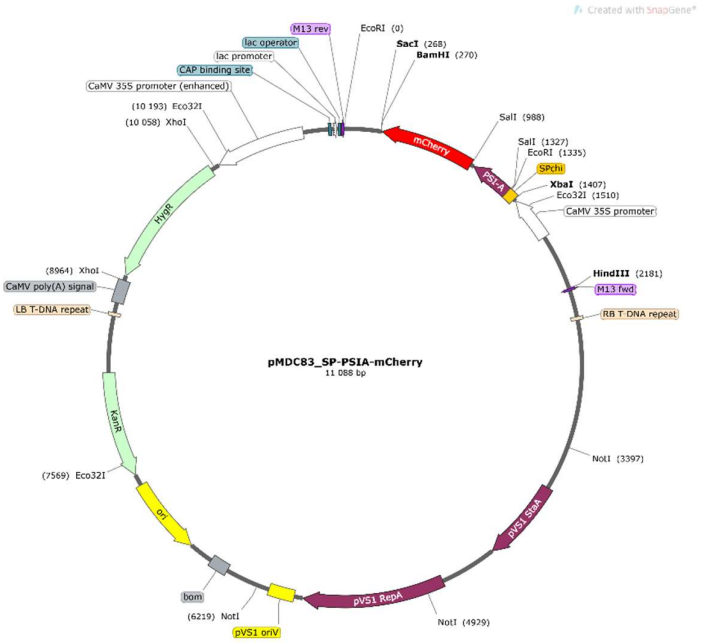
Supplementary figure 7.1 – pMDC83 empty plasmid map.



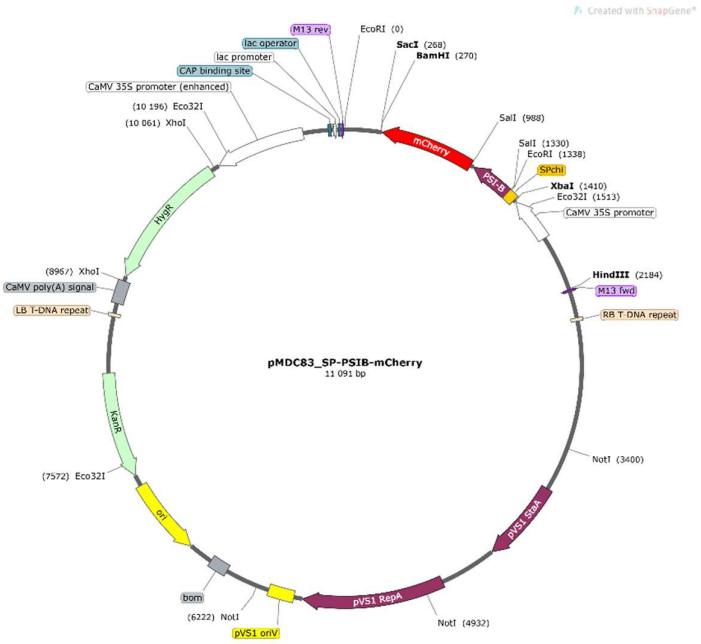
Supplementary figure 7.2 – pMDC83 construct containing PSI A fused with mEos 3.2.



Supplementary figure 7.3 – pMDC83 construct containing PSI B fused with mEos 3.2.



Supplementary figure 7.4 – pMDC83 construct containing PSI A fused with mCherry.



Supplementary figure 7.5 – pMDC83 construct containing PSI B fused with mCherry.